



الجمهورية الجزائرية الديمقراطية الشعبية

République Algérienne Démocratique et Populaire
Ministère de l'Enseignement Supérieur et de la Recherche Scientifique



UNIVERSITÉ HADJ LAKHDAR BATNA

Faculté des Sciences de L'Ingénieur
Département d'Electronique

THESE

En vue de l'obtention du diplôme de

DOCTORAT ES-SCIENCES
Option : Electronique

Présentée par :

Mohamed BAHAZ
Magister en électronique

Thème

PROPRIÉTÉS NON LINÉAIRES DES TISSUS APPLIQUÉES À L'IMAGERIE ULTRASONORE

NONLINEAR TISSUS PROPERTIES APPLIED TO ULTRASOUND IMAGING

Soutenue le : 15 juillet 2010
Devant le Jury composé de :

M. Benslama

Prof., Université de Constantine

Président

K. Benmahammed

Prof., Université de Sétif et Umm Alqura University, Makkah

Rapporteur

A. Bouakaz

Directeur de Recherche, Inserm, Tours, France

Co-Rapporteur

H. Djelouah

Prof., Université USTHB, Alger

Examinateur

D. Benatia

Prof., Université de Batna

Examinateur

N. Benoudjit

Dr. MC. Université de Batna

Examinateur

ANNEE UNIVERSITAIRE : 2009/2010

Avec le support de l'Inserm/DPGRF/2007-08 & LEA

Acknowledgements

Acknowledgements

First of all, I would like to express my sincere appreciation and thanks to my thesis Advisors, Professor Kier Benmohammed from the University of Setif, Algeria, and Umm Alqura University of Mekkah (KSA), and Ayache Bouakaz, Inserm research director from the University François Rabelais of Tours, France. They were fountains of knowledge and it was truly a pleasure to able to perform research under them and to have them as my advisors.

My thanks are extended to the examining committee members for their interest in my work:

- Doctor Malek Benslama, professor at the department of electronics of the University of Constantine.
- Doctor Hakim Djelouah, professor at the USTHB, University of Algiers.
- Doctor Djamel Benatia, professor at the department of electronics of the University of Batna.
- Doctor Nabil Benoudjite, MC at the department of electronics of the University of Batna.

I am very grateful to all my colleagues in the department of electronics of the University of Batna for their support and encouragements.

The work in this thesis is supported in part by Inserm/DPGRF, 2007-08 (a cooperation project between the Inserm France and DPGRF Algeria), and the Advanced Electronics Laboratory of the University of Batna, so I would like Acknowledge them.

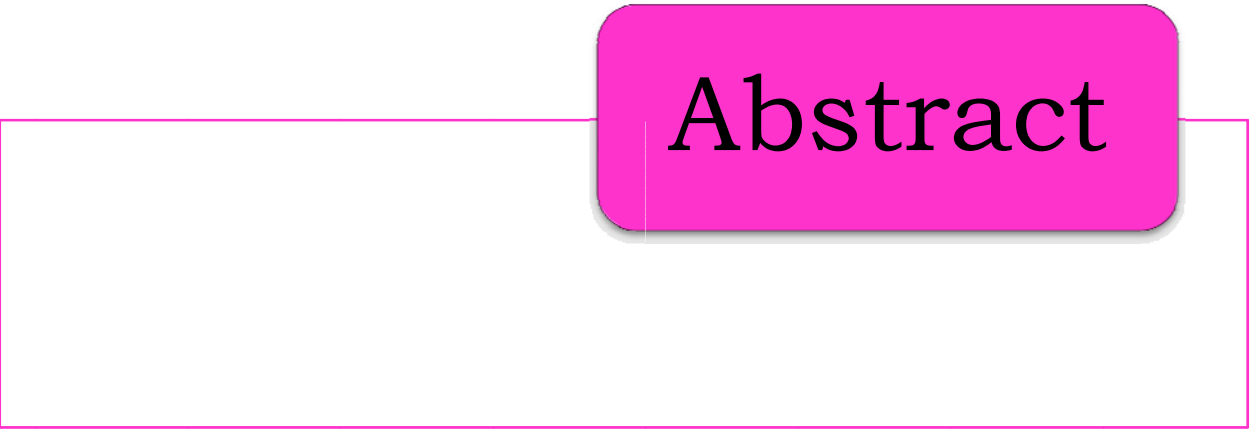
NONLINEAR TISSUS PROPERTIES
APPLIED
TO ULTRASOUND IMAGING

Thesis presented by

Mohamed BAHAZ

Magister in Electronics

to my mother.
to the memory of my father.



Abstract

Abstract

The main aim of the work in this thesis is to exploit nonlinear tissues properties for improving in medical ultrasound image quality.

Ultrasound imaging techniques have been widely used in modern hospitals for clinical ultrasound diagnosis because they can provide important information on the diseased state of the tissues in a human body non-invasively and non-destructively.

Ultrasound imaging is based on the generation, detection and processing of acoustic waves. The waves are transmitted into the human body, and on encountering variations in the properties of the medium, the waves are scattered and reflected. These reflections therefore contain information on the structures and shapes inside the body. When they are intercepted, the backscattered acoustic echoes are then beamformed and processed to form an image.

The standard approach for ultrasound imaging is to use the fundamental frequency from the reflected signal to form images. Tissue harmonic imaging is a new gray-scale imaging technique, which use harmonic information from nonlinear ultrasound propagation to form an image. It creates images that are derived solely from the higher frequency.

The properties of tissue cause the primary ultrasound signal to distort in the body. The distortion of this signal causes harmonics to be generated in tissue and these harmonics can then be used to generate an ultrasound image. The properties of these harmonic signals that can offer several advantages including improved contrast resolution, reduced noise and clutter, improved lateral resolution, reduced artefacts (side lobes, reverberations).

In this thesis, second harmonic component generation has been used to create images offering improvements over conventional B-mode images in penetration, spatial resolution and, more significantly, in the suppression of acoustic clutter and side-lobe artefacts.

In ultrasound harmonic imaging, an ongoing problem is that undesired signals are contained in the reflected waves, and that corrupt the image data, which leads to the contamination of the obtained image. Harmonic received frequency band must not contain components from transmit band, and its components must sufficiently be separable from fundamental spectral component. Thus, to effectively employ the information contained in the second harmonic of the received signal, this information should be properly extracted. In this thesis, a new technique for acquiring the proper second harmonic signal is presented; an optimization of the transmitted bandwidth is recommended to receive the purely second harmonic signal for harmonic imaging. Given a certain available bandwidth for the transducer, it must be decide in what band the transmitted pulse may be send at, and what band the second harmonic signal should be received at.

Contents

Contents

CHAPTER I GENERAL INTRODUCTION.....	1
I.1 Introduction and motivation.....	1
I.2 Medical ultrasound imaging.....	3
I.3 Tissue harmonic imaging and nonlinear propagation.....	5
I.4 Modeling of nonlinear ultrasound propagation in tissue.....	6
I.5 Thesis Objective.....	7
I.6 Thesis outline.....	8
CHAPTER II THEORETICAL BACKGROUND.....	9
II.1 HISTORY.....	9
II.2 NATURE OF ULTRASOUND.....	10
II.3 GENERATION AND DETECTION OF ULTRASOUND WAVES.....	11
II.3.1 Piezoelectric effect.....	12
II.3.2 Piezoelectric materials.....	13
II.4 ULTRASOUND WAVE PROPAGATION.....	14
II.4.1 Ultrasound waves.....	14
II.4.2 Plane wave of small amplitude, equation of propagation.....	14
II.4.3 Nonlinear propagation of sound beams.....	16
II.5 PROPERTIES OF ULTRASOUND WAVES.....	17
II.5.1 Speed.....	17
II.5.2 Frequency.....	19
II.5.3 Acoustic impedance.....	19
II.5.4 Reflection.....	20
II.5.5 Attenuation.....	20
II.6 ULTRASOUND TRANSDUCERS.....	22
II.6.1 Radiation and reception.....	22
II.6.2 Important transducer performance parameters.....	25
II.6.3 Transducer in medical imaging.....	26
II.6.3.1 Beam profile.....	28
II.6.3.2 Focusing.....	28
II.7 RADIATED BEAM DESCRIPTION.....	29
II.7.1 Beam regions.....	29
II.7.1.1 Nearfield or Fresnel region.....	29
II.7.1.2 Farfield or Fraunhofer region.....	30
II.7.1.3 Transition region.....	30
II.7.2 Energy distribution.....	31
II.7.2.1 Main lobe.....	31
II.7.2.2 Secondary lobes.....	31

II.7.2.3 Grating lobes.....	31
II.8 MEDICAL ULTRASOUND IMAGING.....	31
II.8.1 Principle.....	31
II.8.2 Image displaying modes.....	33
II.8.2.1 A-mode.....	33
II.8.2.2 B-mode.....	33
II.8.2.3 C-mode.....	34
II.8.2.4 M-mode.....	34
II.9 BEAMFORMING FOR IMAGING.....	35
II.10 RESOLUTION AND IMAGE QUALITY.....	36
 CHAPTER III FUNDAMENTAL ULTRASOUND IMAGING.....	37
III.1 INTRODUCTION.....	37
III.2 FUNDAMENTAL ULTRASOUND IMAGING.....	38
III.3 LINEAR PROPAGATION AND SMALL SIGNAL APPROXIMATION.....	38
III.4 LINEAR ULTRASOUND SYSTEM.....	40
III.4.1 Field in linear ultrasound systems.....	41
III.4.2 Spatial impulse response.....	43
III.4.3 Calculation of spatial impulse response.....	43
III.5 NUMERICAL SIMULATION.....	46
III.5.1 <u>FIELD</u> : Program description.....	47
III.6 ARRAY TRANSDUCER.....	48
III.7 FOCUSING.....	50
III.9 SINGLE ELEMENT CIRCULAR TRANSDUCER.....	51
III.10 APODIZATION.....	52
III.11 SIMULATION RESULTS.....	53
III.11.1 Unfocused Circular Transducer.....	53
III.11.2 Focused Circular Transducer.....	55
III.12 EXAMPLE OF B-MODE IMAGE.....	57
 CHAPTER IV HARMONIC ULTRASOUND IMAGING.....	58
IV.1 INTRODUCTION.....	58
IV.2 HARMONIC ULTRASOUND IMAGING.....	59
IV.3 BENEFITS OF HARMONIC IMAGING.....	60
IV.4 NONLINEARITY IN WAVE PROPAGATION.....	61
IV.5 THEORY OF HARMONIC GENERATION.....	62
IV.5.1 Variation of wave speed in a wave.....	64
IV.5.2 Parameter B/A.....	65
IV.5.3 Amount of wave distortion.....	66
IV.5.4 Goldberg's number.....	67
IV.5.5 Mechanical index.....	68
IV.6 EQUATION OF PROPAGATION.....	68
IV.6.1 Lossless Burgers equation.....	69
IV.6.2 Burgers equation.....	69
IV.6.3 Sound beams and KZK equation.....	70
IV.7 MODELING OF NONLINEAR MEDICAL ULTRASOUND.....	71
IV.7.1 Medium under consideration.....	72
IV.7.2 Nonlinear numerical methods.....	73
IV.7.3 Finite difference analysis for ultrasound modeling.....	74
IV.8 NUMERICAL SOLUTION OF KZK EQUATION.....	75

IV.8.1 Boundary conditions.....	77
IV.9 SIMULATION RESULTS USING CIRCULAR TRANSDUCER.....	79
IV.9.1 Low excitation intensity.....	80
IV.9.2 High excitation intensity.....	82
IV.10 GRATING LOBES.....	86
IV.11 PENETRATION.....	87
IV.12 EXAMPLE OF COMPARATIVE IMAGES.....	88
CHAPTER V OPTIMIZATION OF HARMONIC IMAGING.....	90
V.1 INTRODUCTION.....	90
V.2 IMAGE FORMATION IN TISSUE HARMONICS.....	91
V.3 SECOND HARMONIC EXTRACTION TECHNIQUES.....	92
V.3.1 Filtration technique.....	92
V.3.2 Pulse encoding technique.....	94
V.3.3 Pulse inversion technique.....	94
V.3.4 Side-by-side phase cancellation technique.....	98
V.3.5 Power modulation technique.....	98
V.4 OPTIMIZATION OF HARMONIC IMAGING.....	101
V.4.1 Bandwidth.....	102
V.4.2 Overlap.....	105
CHAPTER VI CONCLUSION & FUTURE WORKS.....	109
REFERENCES	

Chapter I

General Introduction

General Introduction

I.1 INTRODUCTION AND MOTIVATION

Ultrasound or acoustic waves are used in wide number of fields as means to test and view the inner structure of a medium without having to open it up. It may be possible to discover the motions of the internal parts of bodies, whether animal, vegetable, or mineral, by the sound they make, (Robert Hooke, 1635-1703) [1].

Ultrasound is a term used to describe sound waves that have frequencies above the audible range. As the name implies, ultrasound is high-frequency sound. Sound is the rapid oscillatory motion of atoms or molecules and is produced when a body vibrates. Sound propagates in waves. A wave is a disturbance whose position in space changes with time. Unlike electromagnetic waves, which can travel in vacuum, the propagation of sound waves requires some physical elastic medium, such as gas, liquid or solid. Sound waves are of an elastic or mechanical nature. They travel through a medium by causing local displacement of particles within the medium, but there is no overall movement of this last. If a particle of the medium is displaced from its equilibrium position by any external applied stress, internal forces tend to restore the system to its original equilibrium. Particles making up the medium are not propagating away from the disturbance source but are only vibrating back and forth about their equilibrium positions. Mechanical vibrations become vibrating pressure waves, transferring energy to the medium and to objects that the wave contacts by intimate contact between masses of the medium. In term of energy, sound is mechanical energy that propagates through a continuous, elastic medium by the compression and rarefaction of particles that compose it. Compression is caused by a mechanical deformation induced by an external force, with a resultant increase in the pressure of the medium. Rarefaction occurs following the compression event; as the backward motion of the piston reverses the force, the compressed particles transfer their energy to adjacent particles, with a

subsequent reduction in the local pressure amplitude. The mechanical energy moves progressively from particle to particle when a sound wave propagates in a medium [2].

Many animals in the natural world, such as bats and dolphins, use sound echo-location, which is the key principle of diagnostic ultrasound imaging. The connection between echo-location and the medical application of sound, however, was not made until the science of underwater exploration matured. Sound echo-location is the use of reflections of sound to locate objects. The applications range from geophysical exploration and customs inspection to medical diagnostics and therapy.

In medical field, acoustic waves are used with a frequency that is generally between 1 and 50MHz, which is in ultrasound domain. The waves are transmitted into the human body, and on encountering variations in the properties of the medium the waves are scattered and reflected. These reflections therefore contain information on the structures and shapes inside the body, and when they are intercepted by a transducer, an image can be formed of the organs within the human body.

The discovery of piezoelectricity (the property by which electrical charge is created by the mechanical deformation of a crystal) by the Curie brothers in 1880 and the invention of the triode amplifier tube by Lee De Forest in 1907 set the stage for further advances in pulse-echo range measurement. The Curie brothers also showed that the reverse piezoelectric effect (voltages applied to certain crystals cause them to deform) could be used to transform piezoelectric materials into resonating transducers [5].

The potential of ultrasound as an imaging modality was realized as early as the late 1940s when, utilizing sonar and radar technology developed during World War II. After this, with sonar and radar as models, a few medical practitioners saw the possibilities of using pulse-echo techniques to probe the human body for medical purposes. When commercialized versions of the reflectoscope were applied to the human body in Japan, the United States, and Sweden in the late 1940s and early 1950s (Goldberg and Kimmelman, 1988), a new world of possibility for medical diagnosis was born, and several groups of investigators around the world started exploring diagnostic capabilities of ultrasound.

In medical domain, ultrasound not only complements the more traditional imaging approaches such as x-ray, but also possesses unique characteristics that are advantageous in comparison to other competing modalities such as x-ray computed tomography, radionuclide emission tomography, and magnetic resonance imaging. More specifically:

1. Ultrasound is a form of no ionizing radiation.
2. It is less expensive than imaging modalities of similar capabilities.
3. It produces images in real time, unattainable by any other methods.
4. It is portable and thus can be easily transported to the bedside of a patient.
5. It has a resolution in the millimeter range for the frequencies being clinically used today.

In ultrasound imaging, some limitations compared to other modalities include inferior resolution and poor penetration depth, are observed in the case of the fundamental imaging (the standard approach for ultrasound imaging is to use the fundamental frequency from the reflected signal to form images). Then, harmonic generation properties have been used to create improved images.

Because ultrasound attenuation is more severe for higher frequencies, there is typically an implicit tradeoff between resolution and penetration depth. Moreover, artifacts due to clutter, beam defocusing due to tissue path inhomogeneities, and multiple reflections can distort the image and cause erroneous interpretation. Many techniques are used in the aim to reinforce the ultrasound pressure field, and to increase the signal-to-noise ratio (SNR) of harmonic component, and consequently to improve the ultrasound image quality.

I.2 MEDICAL ULTRASOUND IMAGING

The history of medical ultrasound goes back more than 50 years, when tests were started using modified sonar equipment. It was seen that the principles of sonar and radar could be used to image human tissue, whose consistency is not that different from water. The first ultrasound systems having diagnostic value displayed what came to be known as A-mode images (A stands for amplitude). The A-mode technology had no focusing, and simply displayed a one-dimensional signal giving the echo strength. In the 1950s and 1960s the B-mode technology was developed (B standing for brightness), giving the first two-dimensional views of the

body. The B-mode technology forms the basis of the technology which today permeates most modern medical facilities. In a B-mode display the brightness in the image is proportional to the echo strength. In the beginning the B-mode images were generated using mechanically moving transducers, so that scans in various directions could be synthesized into an image. However, in the mid 1960s the first electronically steered array transducers were introduced, and this is the technology which has transformed into an advanced real-time scanners [11].

Today, ultrasound imaging techniques have been widely used in modern hospitals for clinical ultrasound diagnosis because they can provide important information on the diseased state of the tissues in a human body non-invasively and non-destructively.

Ultrasound imaging is based on the generation, detection and processing of acoustic signals. An ultrasound transducer converts electrical voltage pulses into mechanical pulses that propagate outwards as acoustic waves into the human body. Echo signals are produced when the ultrasound waves encounter the interfaces between human tissues with different acoustic impedances. These echo signals, which can have the same or multiple frequency of the original excitation wave, are generally detected by the same transducer. The electrical signals generated from the backscattered acoustic echoes are then beamformed and processed to form an ultrasound image.

Ultrasound instruments for medical imaging purposes have a significantly smaller size and lower cost compared with instruments in other medical imaging modalities such as Magnetic Resonance Imaging and Computed Tomography. In addition there are no special building requirements as for X-ray, and Nuclear imaging. One ultrasound scanner can be equipped with multiple ultrasound probes to meet various needs for imaging different regions of the human body, and it can form 2D, or 3D, images in real-time.

Finally, it is worth mentioning one of the great leaps taken in medical ultrasound imaging, namely harmonic imaging. It was seen that a clearer image could be synthesized by processing the second harmonic frequency instead of the frequency of the emitted pulse.

I.3 TISSUE HARMONIC IMAGING AND NONLINEAR PROPAGATION

The last few years has seen the emergence a new ultrasound technology called Tissue Harmonic Imaging, or Finite Amplitude Distortion-Based Harmonic Imaging, which overcomes some of the problems of phase aberration, clutter artifacts, reverberation artifacts, and offers improved spatial resolution. Tissue harmonic imaging is a new grayscale imaging technique, which use harmonic information from nonlinear ultrasound propagation to form an image. It creates images that are derived solely from the higher frequency.

The properties of tissue cause the primary ultrasound signal to distort in the body. The distortion of this signal causes harmonics to be generated in tissue and these harmonics can then be used to generate an ultrasound image. When these harmonics are not present in the transmitted pulse, they are mostly caused either by nonlinear propagation of the sound wave in the tissue or by the presence of a medium that is capable of reflecting the transmitted energy in nonlinear manner.

All finite amplitude ultrasonic waves undergo a degree of nonlinear distortion when traveling through real media. The distortion is due to slight nonlinearities in sound propagation that gradually deform the shape of the propagating wave, and result in the development of additional harmonic frequencies that were not present in the initial transmitted wave. More precisely, the reason of the distortion of the wave shape is that the tissue is not a completely incompressible medium. At the positives cycles of the acoustic pressure wave (compression) the temperature increases and, the density will increase proportionally while during the negatives cycles of the acoustic pressure wave (expansion) the temperature decreases and also the density of the medium. This change in medium density influences the local propagation speed of sound. Indeed, the positive part of the wave propagates a bit faster than the negative part, leading to a slight deformation in the shape of the wave [51]. This deformation accumulates in depth with propagation distance and is more significant for high acoustic pressure intensities. The distortion manifests itself in the frequency domain by the appearance of additional harmonic signals at integer multiples of the original excitation frequency. Distortion will be more severe for higher pressure amplitudes and another additional number of harmonics will be generated. The properties of these harmonic signals that can offer several advantages including improved contrast resolution, reduced noise and clutter,

improved lateral resolution, reduced artifacts (side lobes, reverberations). These improvements are especially in the region of interest in which the acoustic energy is sufficiently high to cause the harmonics to be generated.

Tissue harmonics uses various techniques to eliminate the echoes arising from the main transmitted ultrasound beam (the fundamental frequency), from which conventional images are made. Once the fundamental frequencies are eliminated, only the harmonic frequencies are left for image formation. Indeed, the quality of the harmonic image is primarily dependent on the complete elimination of all echoes derived from the transmitted frequencies.

I.4 MODELING OF NONLINEAR ULTRASOUND PROPAGATION IN TISSUE

An important aspect of modern engineering design is the use of computer models to simulate a technology before manufacturing. Often modeling not only saves money by allowing virtual research and development, but it also helps foster an understanding of principles needed for an optimal design. However, like in many engineering cases, either the structure geometry is complicated or some critical medium properties and behaviors are not uniform. Thus, an analytical solution cannot be found, or involves too many simplifying assumptions, which degrade the accuracy of the resulting solutions. In these situations, numerical analysis technique obtains piecewise approximate solutions for many engineering problems.

Modeling of nonlinear ultrasound propagation in tissue, like the other fields, for the design and engineering of new technologies and techniques that exploit the nonlinear propagation properties, it is primordial to be able to model the physical process with sufficient accuracy. Doing this, we can predict the consequences of certain design choices before we try to implement them.

In the present thesis, the model of nonlinear ultrasound propagation based on the KZK (Khokhlov-Zabolotskaya-Kuznetsov) equation is used. KZK equation is usually used to describe nonlinear wave propagation. It is based on a parabolic approximation, and describes the combined effects of diffraction, losses and nonlinearity. A numerical algorithm solves the equation in time domain and is based on finite differences method with a stepping in the axis of propagation direction. This algorithm follows similar lines as the algorithm described by Lee and Hamilton.

Numerical solutions have been investigated in the time domain, and the frequency domain.

I.5 THESIS OBJECTIVE

The objective of this thesis is firstly to develop a computationally efficient model of nonlinear ultrasound propagation, which may be used as a simulation tool for use in design of a harmonic imaging system. The model should enable simulation of nonlinear propagation in arbitrary media, and specifically, should accurately model propagation in tissue, and secondly exploiting the properties of the nonlinear propagation in tissue in the aim to searching improvements in ultrasound image quality.

In ultrasound imaging, some limitations compared to other modalities include inferior resolution and poor penetration depth, are observed in the case of fundamental imaging. In the work of this thesis, nonlinear tissues properties are exploited for the purpose of improving in medical ultrasound image quality. With this technique profit is taken from the nonlinearity of the tissues which where the wave energy is transferred from the fundamental frequency, in which the wave was originally transmitted to its higher harmonics.

Major improvements have been achieved by exploiting the characteristics of nonlinear fields with the utilization of harmonic frequencies, especially those of the second harmonic component which generated at two times of the transmit frequency.

Second harmonic component generation has been used to create images offering improvements over conventional B-mode images in penetration, spatial resolution and, more significantly, in the suppression of acoustic clutter and side-lobe artifacts.

Because ultrasound attenuation is more severe for higher frequencies, there is typically an implicit tradeoff between resolution and penetration depth. Moreover, artifacts due to clutter, beam defocusing due to tissue path inhomogeneities, and multiple reflections can distort the image and cause erroneous interpretation. Many methods like pulse inversion technique developed in this thesis are used in the aim to reinforce the ultrasound pressure field, and to increase the signal-to-noise ratio of second harmonic component.

In ultrasound harmonic imaging, an ongoing problem is that undesired signals are contained in the reflected waves, and that corrupt the image data which leads to the contamination of the obtained image. Harmonic received frequency band must not contain components from transmit band, and its components must sufficiently be separable from fundamental spectral component. Thus, to effectively employ the information contained in the second harmonic of the received signal, this information should be properly extracted. In this thesis, a new technique for acquiring the proper second harmonic signal is presented. An optimization of the transmitted bandwidth is recommended to receive the purely second harmonic signal for harmonic imaging. Given a certain available bandwidth for the transducer, it must be decided in what band the transmitted pulse may be sent at, and what band the second harmonic signal should be received at.

I.6 THESIS OUTLINE

Following this introductory chapter, chapter II will establish some fundamental theory background relevant to linear and nonlinear ultrasound propagation.

Chapter III will describes fundamental ultrasound imaging, and presents a numerical method used so far in modeling of linear propagation.

Harmonic ultrasound imaging and the principles of the used numerical model, and improvements achieved with the utilization of harmonic component of echo signal will be discussed in the Chapter IV.

Chapter V is dedicated to the study of bandwidths for fundamental and second harmonic spectral components and the overlap between them and how to optimize the excitation in the aim to earn more improvements in harmonic bandwidth, and consequently more details in required image.

A general conclusion will summarize this work and its main contribution, give recommendations for future works.

Chapter II

Theoretical Background

Theoretical Background

II.1 HISTORY

Robert Hooke (1635-1703), the eminent English scientist responsible for the theory of elasticity, pocket watches, compound microscopy, and the discovery of cells and fossils, foresaw the use of sound for diagnosis when he wrote: It may be possible to discover the motions of the internal parts of bodies, whether animal, vegetable, or mineral, by the sound they make [1]. Many animals in the natural world, such as bats and dolphins, use echo-location, which is the key principle of diagnostic ultrasound imaging. The connection between echo-location and the medical application of sound, however, was not made until the science of underwater exploration matured. Echo-location is the use of reflections of sound to locate objects. The discovery of piezoelectricity (the property by which electrical charge is created by the mechanical deformation of a crystal) by the Curie brothers in 1880 and the invention of the triode amplifier tube by Lee De Forest in 1907 set the stage for further advances in pulse-echo range measurement. The Curie brothers also showed that the reverse piezoelectric effect (voltages applied to certain crystals cause them to deform) could be used to transform piezoelectric materials into resonating transducers. The potential of ultrasound as an imaging modality was realized as early as the late 1940s when, utilizing sonar and radar technology developed during World War II. After this, with sonar and radar as models, a few medical practitioners saw the possibilities of using pulse-echo techniques to probe the human body for medical purposes. When commercialized versions of the reflectoscope were applied to the human body in Japan, the United States, and Sweden in the late 1940s and early 1950s (Goldberg and Kimmelman, 1988), a new world of possibility for medical diagnosis was born, and several groups of

investigators around the world started exploring diagnostic capabilities of ultrasound.

II.2 NATURE OF ULTRASOUND

Sound is the rapid oscillatory motion of atoms or molecules and is produced when a body vibrates. A wave is a disturbance whose position in space changes with time. Sound propagates in waves. Unlike electromagnetic waves, which can travel in vacuum, the propagation of sound waves requires some physical elastic medium, such as gas, liquid or solid. Sound waves are of an elastic or mechanical nature. If a particle of the medium is displaced from its equilibrium position by any external applied stress, internal forces tend to restore the system to its original equilibrium. Particles making up the medium are not propagating away from the disturbance source but are only vibrating back and forth about their equilibrium positions. Mechanical vibrations become vibrating pressure waves, transferring energy to the medium and to objects that the wave contacts by intimate contact between masses of the medium. In term of energy, sound is mechanical energy that propagates through a continuous, elastic medium by the compression and rarefaction of particles that compose it. Compression is caused by a mechanical deformation induced by an external force, with a resultant increase in the pressure of the medium. Rarefaction occurs following the compression event; as the backward motion of the piston reverses the force, the compressed particles transfer their energy to adjacent particles, with a subsequent reduction in the local pressure amplitude. The mechanical energy moves progressively from particle to particle when a sound wave propagates in a medium [2]-[3].

There exist five major modes of sound waves in terms of their particle motion in relation to the sound wave propagation direction. Longitudinal, transverse, surface, plate, and torsion waves. The longitudinal wave is a compressional wave in which the particle motion is parallel to the wave propagation direction. The transverse wave is shear wave motion in which the particle motion is perpendicular to the wave propagation direction. Surface waves have an elliptical particle motion and travel across the surface of the material, with the major axis of the ellipse perpendicular to wave propagation direction. Plate or Lamb waves propagate in thin plates or specimen of uniform thickness less than a wavelength of the ultrasound introduced into it, resulting in flexural vibration of plate. Torsion waves occur in rods or wires

when the driving source performs an oscillatory, twisting action about the rod axis. Longitudinal waves can propagate in any elastic and compressible medium (solid, liquid, or gas). However, the other wave modes barely propagate in liquids or gases [4]. The acoustic spectrum breaks down sound into three ranges of frequencies: subsonic range, audible range, and ultrasonic range. Ultrasound wave refers to the human-inaudible sound wave, whose frequency range is above 20 kHz, the upper frequency response limit of the human ear. The ultrasonic range is then further broken down into three subsections, figure (II.1). Ultrasound behaves in a similar manner to audible sound except that it has a much shorter wavelength. The frequency range normally employed in ultrasonic nondestructive evaluation or imaging is 1 MHz to 20 MHz

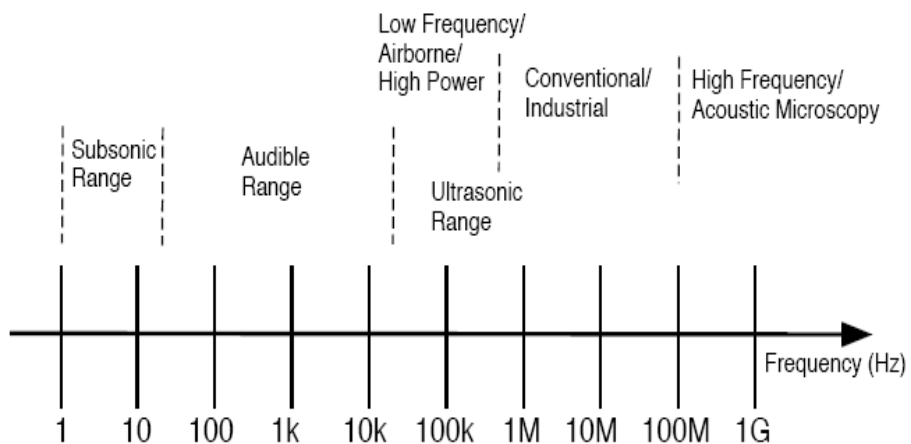


Figure II.1 : Acoustic spectrum

II.3 GENERATION AND DETECTION OF ULTRASOUND WAVES

In ultrasonic imaging, there must be a way to both generate and detect ultrasound waves. Historically, ultrasound waves were generated using whistles, sirens, and tuning forks. With these techniques, the upper limit of the frequencies that could be generated was approximately 40 kHz [5]. By exploiting the piezoelectric properties of crystals, sound waves can be generated at several tens of megahertz.

Before and after any electrical or mechanical force is applied to a piezoelectric element, the charge of the material is neutral. There is no voltage across the crystal. For generation of an ultrasound wave, an electric voltage is applied to the material. The polarity of the voltage that reaches the material determines the type of mechanical response of the element. The element either becomes thinner and longer or shorter and fatter than the material was at rest. Since the change in shape depends on the polarity of the voltage, the shape of the ultrasound wave can be controlled by controlling the voltage across the piezoelectric element. Detection of ultrasound waves is the reverse procedure of ultrasound wave generation. The polarity of the voltage across the piezoelectric element is determined by whether the piezoelectric material is pushed (made thinner and longer) or pulled (made shorter and fatter) by the reflection of the ultrasound wave. In ultrasound imaging, a piezoelectric transducer is used for both ultrasound wave generation and detection. Initially, to generate ultrasound waves, the piezoelectric element converts an applied voltage to mechanical ultrasound waves. Then, as the reflections of the ultrasound waves arrive to the transducer face, it converts that mechanical energy back into electrical energy.

II.3.1 Piezoelectric Effect

In the 1880s, the Curie brothers and Lippmann both made realizations that are the basis for the current methods of ultrasound wave generation and detection. The Curie brothers discovered that when a mechanical stress is applied to certain materials, an internal electric field is generated such that opposite charges line the opposite sides of the material. Figure (II.2a) shows the direct piezoelectric effect in which a stress induces a charge separation, and figure (II.2b) shows the reverse piezoelectric effect in which a potential difference across the electrodes induces a strain. A year later Lippmann predicted that applying an electric field to these materials would cause the material to deform. Shortly afterwards, the Curie brothers proved Lippmann's prediction experimentally [5].

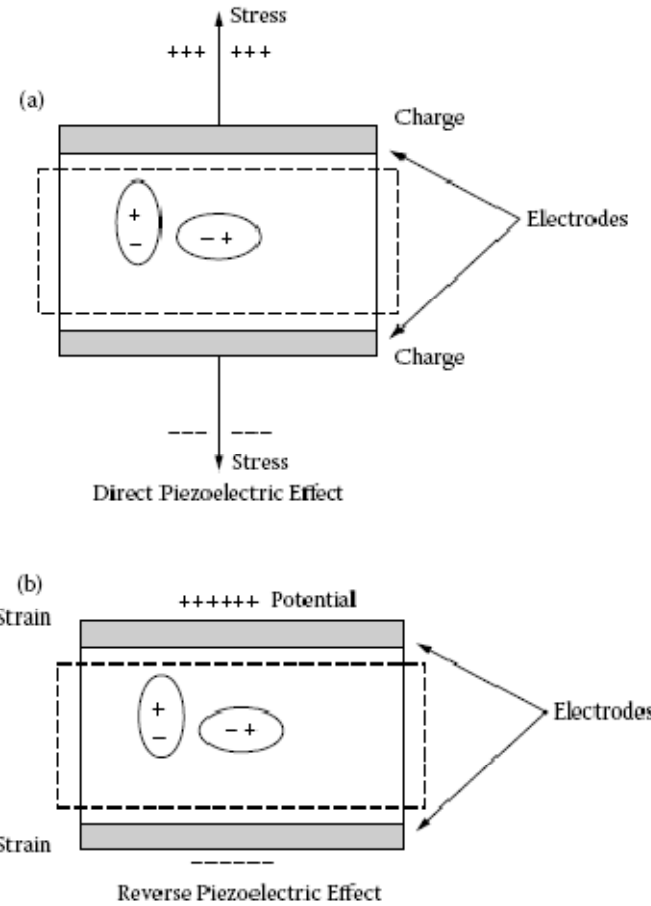


Figure II.2: Direct and reverse piezoelectric effects

II.3.2 Piezoelectric Materials

Materials that exhibit this piezoelectric behavior include the following crystals: quartz, lead zirconate, barium titanate, and lithium niobate. Typically, a slice of the material is taken so that the parallel portions of the element lie normal to an axis of non-symmetry. The cut is crucial, because a wrong cut can result in suppression of the piezoelectric activity. Furthermore, in order to obtain the piezoelectric behavior, the mechanical stress must be applied to the non-symmetrical axis. In general, ultrasound waves are then generated and detected by placing the piezoelectric element between two plates that can generate and measure an electric field [5].

II.4 ULTRASOUND WAVE PROPAGATION

II.4.1 Ultrasound Waves

Waves in diagnostic ultrasound carry the information about the body back to the imaging system. Both elastic and electromagnetic waves can be found in imaging systems. Three simple but important types of wave shapes are plane, cylindrical, and spherical, figure (I.3). A plane wave travels in one direction. Stages in the changing pattern of the wave can be marked by a periodic sequence of parallel planes that have infinite lateral extent and are all perpendicular to the direction of propagation. When a stone is thrown into water, a widening circular wave is created. In a similar way, a cylindrical wave has a cross section that is an expanding circular wave that has an infinite extent along its axial direction. A spherical wave radiates a growing ball-like wave rather than a cylindrical one. In general, however, the shape of a wave will change in a more complicated way than these simple idealized shapes, which is why the principle of superposition synthesis is needed to describe a journey of a wave.

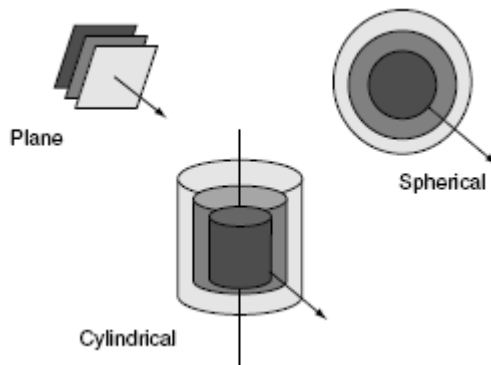


Figure II.3: *Plane, cylindrical, and spherical waves showing surfaces of constant phase*

II.4.2 Plane Wave of Small Amplitude, Equation of Propagation

Ultrasound waves can be thought of as pressure variations in a media, which propagate periodically in space and time. To a first order approximation, ultrasound

propagation is well described as a linear process, governed by a linear, second order homogeneous differential equation. The assumption of linear propagation, however, is valid only for relatively small disturbances.

The propagation of sound waves in liquids and gases is described mathematically by the equations of hydrodynamics, which connect the velocity of the particle, the density of the medium, and the pressure. The acoustic wave equation in a fluid medium can be derived from three fundamental physical laws: conservation of mass (equation of continuity), momentum equation (the equation of motion) and pressure density relation for a perfect gas (the equation of state).

$$\frac{\partial \rho}{\partial t} + \nabla \cdot (\rho v) = 0 \quad (\text{II.1})$$

$$\rho \frac{\partial v}{\partial t} + (v \nabla) \cdot (\rho v) + \nabla P = 0 \quad (\text{II.2})$$

$$P = C \rho^\gamma \quad (\text{II.3})$$

Equation (II.1) is the equation of continuity, equation (II.2) is the momentum equation, and equation (II.3) is the equation of state.

Where v is the particle velocity, P is the pressure, ρ is the mass density, C is a constant, and γ is the ratio of specific heats.

The medium is assumed to be ideal. That is, the medium has no viscosity and energy dissipation, the medium is quiescent when there is no acoustic disturbance, the sound propagation process is adiabatic and, the amplitude of acoustic disturbance is very small compared to the ambient medium condition. The linear, lossless acoustic wave equation in fluids with phase speed c_0 can be written as [4]:

$$\nabla^2 p - \frac{1}{c_0^2} \frac{\partial^2 p}{\partial t^2} = 0 \quad (\text{II.4})$$

The variable $p = P - P_0$ is the acoustic pressure, where P_0 is the quiescent pressure in the ambient medium. The plane wave solution to equation (II.4) is:

$$p(r, t) = A e^{j(\omega t - k_r r)} \quad (\text{II.5})$$

Where $\omega = 2\pi f$ is the radian frequency, r is the location of the space point field pressure with respect to the origin of the coordinate system, and k is the propagation vector perpendicular to the constant-phase surface, which points in the wave propagation direction and has magnitude $|\omega/c_0|$. The phase speed c_0 is a real number for a lossless medium. A purely imaginary phase speed corresponds to an evanescent wave whose amplitude decays as the wave propagates. Therefore, the wave vector k could be a complex vector, with its real part representing a progressive wave and its imaginary part representing a no progressive wave.

A plane wave is a certain approximation to real conditions. In reality, the perturbation is always localized in space in the form of a beam, as occurs. The propagation of real wave beams frequently differs from the behavior of rays. The reason for this difference is included in the phenomenon of diffraction.

II.4.3 Nonlinear Propagation of Sound Beams

An increase in the intensity of a sound beam brings with it the necessity of investigating processes of nonlinear propagation of a multidimensional acoustic wave.

Nonlinear propagation arises from a convective phenomenon and from a nonlinear relationship between pressure and density. Convection effects can be thought of as being like an oscillating wind travelling with the wave. Overall, the oscillation propagates with small signal speed c_0 , however, the peak of the oscillation will also have a local particle velocity above and beyond the wave velocity c_0 . Effects due to the nonlinearity of the medium can be understood as a dependence of the speed of sound with temperature and pressure. The compression phase of a wave will cause a local increase in pressure and temperature compared with the rarefaction phase. Locally, an increase in pressure and temperature causes an increase in the speed of sound, figure II.4. Thus, the compression phase of a wave travels faster than the rarefaction phase. Note that because the speed of sound is dependent on density, the plane wave impedance relation is no longer a linear relation. The slope of a graph of pressure versus density, is thus not a straight line, but is rather a curve, where the local slope is proportional to the square of the speed of sound.

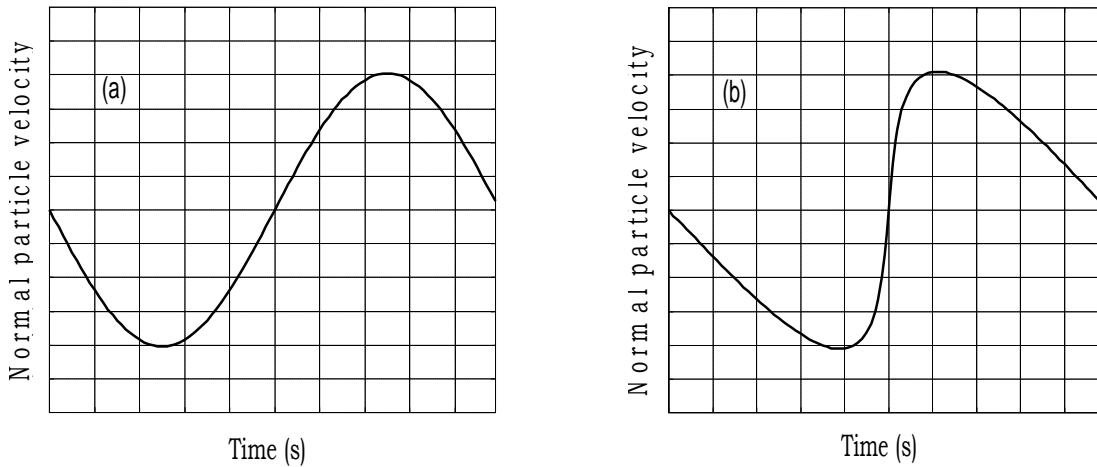


Figure II.4: Effects of nonlinear distortion of a plane sinusoidal wave: (a) Initial waveform, (b) Showing the nonlinear distortion after propagating

Thus, nonlinear propagation of the sound wave will undergo distortion, which will be more severe for higher pressure amplitudes. In the frequency domain, nonlinearity means that harmonics and sum and difference frequencies will be generated. A sinusoid distorting in the process of nonlinear propagation transforms a monofrequency source at f_0 , into an entire spectrum of harmonics, at f_0 , $2f_0$, $3f_0$, $4f_0$...

The nonlinear wave propagation process is more complicated than linear case. A sound beam travelling through a medium will involve the effects of diffraction, absorption, and nonlinearity, and the sound beam can be thought of as interacting with itself as it propagates.

II.5 PROPERTIES OF ULTRASOUND WAVES

II.5.1 Speed

Sound travels through different media at different speeds (e.g., sound travels faster through water than it does through air). The speed of a sound wave v , is given by the distance travelled by the disturbance (compression or rarefaction) during a given time and is constant in any specific material. It can be found by multiplying the frequency f by the wavelength λ and is usually measured in meters per second (m/s):

$$v = \lambda \cdot f \quad (\text{II.6})$$

The speed of sound through a material depends on both the density and the compressibility of the medium. The denser and the more compressible the medium, the slower the wave will travel through it. While media of varying properties propagate sound at different speeds, the wave's speed in a single medium remains constant as long as the temperature and the properties of the medium are held constant [6]. For medical imaging, the speed of sound is different for the various tissues in the body, Table (II.1).

Knowledge of the speed of sound is needed to determine how far an ultrasound wave has travelled. This is required in both imaging and pulsed Doppler, but ultrasound systems usually make an estimate by assuming that the speed of sound is the same in all tissues: 1540 m/s. This can lead to small errors in the estimated distance travelled because of the variations in the speed of sound in different tissues.

Medium	Speed (m/s) at 20°C to 25°C
Air	343
Water	1480
Fat	1450
Blood	1550
Liver	1570
Muscle	1585
Kidney	1561
Soft tissue	1540
Bone	3500

Table II.1: Speed of sound in different medium

Mainly two properties of a medium are considered to affect sound wave speed: elasticity and inertia of the particles within the propagating medium [7]. Elasticity is defined as the degree to which a medium resists deformation when a force is applied to it. Typically, solids have higher elasticity than liquids, which in turn have higher

elasticity than gases. Furthermore, sound waves tend to propagate faster in media with higher elasticity. Inertia, determines the responsiveness of individual particles to their neighboring particles. A greater inertia indicates a medium is composed of particles with larger mass-densities. Sound waves propagate faster in media with less particle inertia.

II.5.2 Frequency

Frequency is defined as the number of wave lengths passing through a point per second. In ultrasound, the frequency of a sound wave can be discerned by counting how many times per unit of time either a high pressure (compression) or a low pressure (rarefaction) passes a particular location. A detector can be used to record the pressure variations through the medium. When the frequency of the sound wave is not obvious from the recorded signal, a Fourier Transform can be performed on the signal in order to determine the frequencies of which the sound wave is comprised as well as the proportions of the sound wave that are at each of these frequencies [8].

II.5.3 Acoustic Impedance

The acoustic impedance of a medium is the impedance (similar to resistance) that the material offers against the passage of the sound wave through it and depends on the density and compressibility of the medium. The greater the change in the acoustic impedance, the greater the proportion of the ultrasound that is reflected. The equation for finding acoustic impedance is as follows [6]:

$$Z = \rho \cdot v \quad (\text{II.7})$$

Where Z is the acoustic impedance of the material, ρ is the density of the material, and v is the speed that sound travels in the material. Table (II.2) shows acoustic impedance of different medium.

Material	Acoustic impedance (Mrayl)
Air	0.0004
Water	1.48
Fat	1.38
Blood	1.61
Liver	1.65
Kidney	1.63
Muscle	1.64

Table II.2: Impedance of sound in different medium

II.5.4 Reflection

When a sound wave encounters the end of one medium and the beginning of another one (a boundary), a portion of the transmitted energy gets reflected. The equation used to determine the amount of energy that gets reflected is as follows [6]:

$$R = \left(\frac{Z_2 - Z_1}{Z_2 + Z_1} \right)^2 \quad (\text{II.8})$$

Where Z_1 is the acoustic impedance of the first medium, Z_2 is the acoustic impedance of the second medium, and R is the fraction of the energy that gets reflected. Clearly, this equation depends on the acoustic impedances of the two media. Therefore, measuring these acoustic impedances is necessary to evaluate the amount of reflection.

From the mathematical equation for finding a reflection, it can be concluded that a greater difference in acoustic impedances between two neighboring media results in a greater amount of reflection. Note that any energy that is reflected at a boundary is lost from the energy of the propagating sound wave.

II.5.5 Attenuation

Attenuation is the diminishing of the original sound wave's energy resulting from the combined effects of both scattering and absorption. For ultrasonic imaging,

attenuation is significant because it determines the depth of wave penetration possible and, thus, the depth of imaging that is possible. Scattering occurs when energy reflects from a very small obstacle and absorption occurs when particles in the path of the ultrasound wave retain some of the energy from the wave, possibly in the form of heat [7]. It follows that sound wave and media characteristics that are more conducive to scattering and absorption dissipate sound waves more quickly. One example is the dependency of the degree of attenuation on the sound wave frequency. Sound waves at a higher frequency tend to have greater amounts of energy absorbed by the media and, consequently, higher frequency sound waves tend to dissipate more quickly than low frequency sound waves within the same media. If we consider a pressure of a plane monochromatic wave propagating in the z-direction decreases exponentially as a function of z:

$$p(z) = p(z = 0)e^{-\alpha z} \quad (\text{II.9})$$

Where $p(z = 0)$ is the pressure at $z = 0$ and α is the pressure attenuation coefficient. Therefore,

$$\alpha = \frac{1}{z} \ln \left[\frac{p(z=0)}{p(z)} \right] \quad (\text{II.10})$$

The attenuation coefficient has a unit of nepers per centimeter (sometimes expressed in units of decibels per centimeter), like given in the table (II.3) below.

Material	Attenuation coefficient (np/cm) at 1 MHz
Air	1.38
Water	0.00025
Fat	0.06
Blood	0.02
Liver	0.11
Skull bone	1.30
Aluminum	0.0021

Table II.3: Attenuation of sound in different medium

The relative importance of absorption and scattering to attenuation of ultrasound in biological tissues is a matter that is continuously debated. Investigations have shown that scattering contributes little to attenuation in most soft tissues (Shung and Thieme, 1993). Therefore, it is safe to say that absorption is the dominant mechanism for ultrasonic attenuation in biological tissues.

II.6 ULTRASOUND TRANSDUCERS

The realizations of the Currie brothers and Lippmann are the basis for the present day use of piezoelectric transducers in ultrasonic imaging. Piezoelectric materials are dielectric materials that produce electric charge when they are subjected to strain or produce strain when the electric field distribution across them is altered. A transducer is, by definition, a device that converts one form of energy into another [9]. In the case of an ultrasound transducer, this conversion is from electrical energy to mechanical vibration. The thickness of the piezoelectric element will determine the frequency at which the element will vibrate most efficiently, this is known as the resonant frequency of the transducer.

II.6.1 Radiation and Reception

In radiation and reception, an ultrasonic transducer has dual roles by acting both as a radiation device to generate ultrasound from an electrical signal and as a reception device to convert ultrasound to an electrical signal. In contrast to the older tools that generated ultrasound waves with frequencies as high as 40 kHz, piezoelectric transducers allow for ultrasound waves in the 100s of MHz to be generated. Furthermore, the precision of detection available by measuring the voltages in the transducer that result from the ultrasound wave reflections is much greater than relying on animals and flames for ultrasound wave detection.

The main components of a transducer are the active element, backing, and wear plate, figure (II.5). The active element, which is piezoelectric or ferroelectric material, provides electric-mechanic energy transduction, and vice versa. The most commonly used piezoelectric materials are polarized ceramics. New materials such as piezo-polymers and composites are also used for their benefit to transducer and system performance. The backing is usually a highly attenuating, high-density material that absorbs the energy radiating from the back surface of the active element. It is used

to increase the bandwidth of the transducer. For immersion applications, the wear plate not only provides protection to the active element but also serves as an acoustic impedance transformer between the high acoustic impedance of the active element and the low acoustic impedance of the liquid (usually a quarter-wavelength-thick matching layer to achieve in phase output) [10].

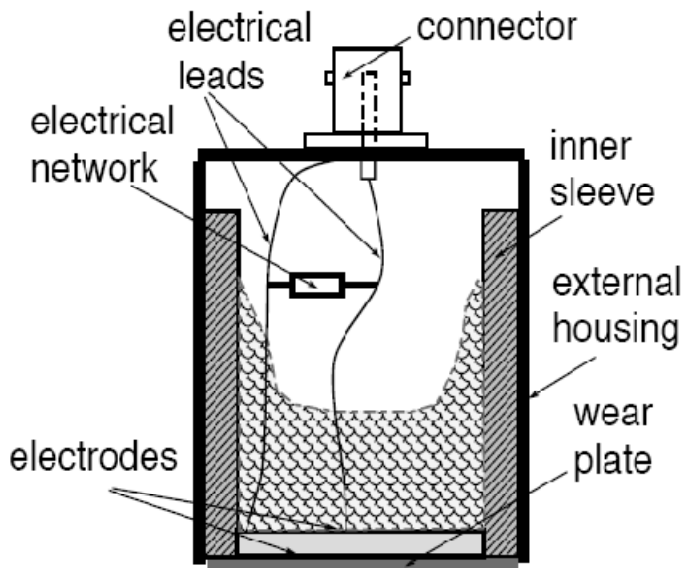


Figure II.5: Transducer components

The electrical-to-mechanical energy transduction of ultrasonic transducers can be modeled by three-port network called Mason's equivalent circuit, with two acoustic ports representing two surfaces of the active element and one electrical port. The coupling between the stress in the acoustic ports and voltage in the electrical port is modeled by an electromechanical transformer.

Unfocused transducer emits an ultrasonic beam that spreads radially due to diffraction. The beam intensity falls off and the beam diameter is too large to obtain good lateral resolution when probing an object in the farfield. Therefore, a focused acoustic beam is often employed, as in optics, to obtain good lateral resolution and high acoustic beam intensity at a point of interest [11]. The use of focused ultrasound pulse waves prompts inspection sensitivity because the ultrasound energy is concentrated in a focal region so that the response of the microstructure in

this focal region to the incident ultrasound wave could be probed with high sensitivity.

Focused ultrasound pulse waves can be generated by a single element transducer with concave surface such as spherical or cylindrical surface, which functions similarly to a focusing optical lens. There are essentially three approaches to focus an ultrasound beam: shaping the actual transducer vibrating element, attaching a concave lens to the transducer face, and inserting a biconvex lens into the ultrasound energy path which is similar to focusing the light from the sun using a magnifying glass.

The sound field of a transducer is a beam within which sound intensity varies. An unfocused beam can be divided into the nearfield and the farfield. The nearfield is the region directly in front of the transducer where the echo amplitude goes through a series of maxima and minima and ends at the last axial maximum, at distance $N = d^2/4\lambda$ from the transducer, where d is the diameter of the transducer surface. The farfield is the region at distances greater than N [12]. Attenuation is effectively a gradual loss of energy. The ultrasound beam attenuates as it progresses through a medium. Attenuation in the nearfield is associated with edge diffraction, absorption and scattering. In farfield, beam spread joins the three factors to attenuate sound intensity of the beam [12]. A spherical focusing transducer has the following important characteristics, figure (II.6):

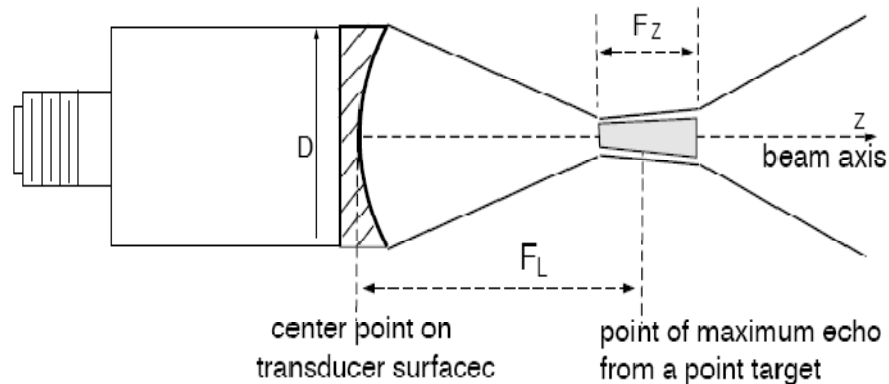


Figure II.6: The beam of a spherical focusing transducer

diameter D , focal length F_L which is the distance between the center point on transducer surface and the point of maximum echo from a point target, focal depth F_Z which is the pulse echo beam axial distance between two points whose echo amplitudes are -6 dB relative to the focal point amplitude, beam diameter BD which is the -6 dB pulse echo beam lateral diameter at F_L .

The numerical aperture of a transducer is defined as the ratio of its focal length to its diameter. The waveform of a transducer has the following parameters: center frequency, frequency bandwidth, pulse duration that is the waveform duration at the -20 dB level or 10% amplitude of peak, pulse repetition frequency that is the number of pulses produced per second. A transducer is often described by its waveform center frequency, diameter and numerical aperture.

II.6.2 Important Transducer Performance Parameters

The ultrasound transducer is one of the most important parts in any ultrasound scanner system. Electromechanical coupling coefficient, resonance frequency, bandwidth, the dimension, and the effective transducer aperture are among the major parameters that govern the performance of an ultrasound transducer [13]. Electromechanical coupling coefficient is a key parameter used to describe a transducer's effectiveness as a converter of energy. It can be defined as the ratio between the converted mechanical energy and total input energy in one cycle. It is important to note that the electromechanical coupling coefficient value is not equal to the energy conversion efficiency which determines the amount of energy that is converted, the amount that is lost as heat with respect to available input energy. A transducer that has the efficiency equal to unity but a low electromechanical coupling coefficient value will convert all input energy to output energy but it will not be able to complete it in one single cycle. It will take several cycles before all input energy is converted [14]. For piezoelectric transducers operated in the thickness mode, the resonance frequency, which approximately determines where maximum sensitivity is achieved, is determined by the thickness of the transducer layer, sound velocity and electromechanical coupling coefficient [15]-[16]. The operating frequency also affects the focusing performance of an ultrasound transducer. Higher frequency is associated with a shorter wavelength, resulting in improved lateral and axial resolution.

Bandwidth is generally defined as the frequency range over which the transducer response is greater than its half-maximum (i.e. -6 dB with respect to maximum). Higher bandwidth increases the versatility of ultrasound transducers.

The size of the transducer and each individual element plays an important role in transducer's performance. For a certain range or focal length, a larger aperture generally improves the lateral resolution. The element spacing pitch also has a significant impact and determines whether there is any grating lobe in the transducer angular response, and where the grating lobe will exist. The element width has an impact on both single element and overall array beam pattern. For an array transducer, it determines the magnitudes of the sidelobes and grating lobes. For single element beam pattern, it determines the behavior of the sidelobes. The ultrasound transducer is a complex system in the sense that every parameter has impact on net transducer performance. For every application, the transducer has to be designed carefully and has to undergo an optimization procedure to ensure the transducer performance meets the application needs [17].

II.6.3 Transducer In Medical Imaging

All ultrasonic imaging systems require a device called an ultrasonic transducer to convert electrical energy into ultrasonic or acoustic energy and vice versa. The ultrasonic field from transducers is the feature that determines the performance of a given system. The study of the spatial and temporal characteristics of the acoustical pressure field allows a greater understanding of the behavior of such devices. The medical ultrasound scanners use advanced transducer geometries for creating ultrasound fields suitable for probing the body. Ultrasound imaging is based on the transducer characterization in where pulsed ultrasound waves are directed into the human body, and echo signals from reflectors and scatterers organs are detected and used to construct an image. A first characterization of these transducers is based on computer simulation of the field. Ultrasonic transducers come in a variety of forms and sizes ranging from single-element transducers for mechanical scanning and linear arrays, to multidimensional arrays for electronic scanning. Although performance of an ultrasonic scanner is critically dependent upon transducers/arrays,

array/transducer performance has been one of the bottlenecks that prevent current ultrasonic imagers from reaching their theoretical resolution limit.

Like imaging, ultrasound transducers have also been improved over the time to meet the increasing needs demanded by new diagnostic and clinical applications. Lead Zirconium Titanate transducers (PZT) have dominated the medical ultrasound field since its beginning. Most current handheld ultrasounds probes are based on PZT technologies. In recent years, another type of transducer – Capacitive Micromachined Ultrasonic Transducer (CMUT) has gained a lot of attention and has emerged as promising transducer replacement due to its high bandwidth, low cost, and potential compatibility with tightly integrated electronics. However, both PZT and CMUT transducers have deficiencies providing opportunities for making significant improvements [17]. Figure (II.7), shows an example of a beam profile in medical ultrasound imaging field.

Harmonic imaging necessitates high transducer bandwidth. In harmonic imaging, the transducer transmits ultrasound waves at a fundamental frequency band, and receives harmonic (generally second harmonic) echoes back from the human body. Moreover, bandwidth is a critical factor determining the image axial resolution. A higher bandwidth means fewer pulse cycles in the time domain, and results in improved axial resolution (range of depth resolution) in an image. A transducer with higher electromechanical coupling effectiveness usually has wider bandwidth and shorter pulse duration.

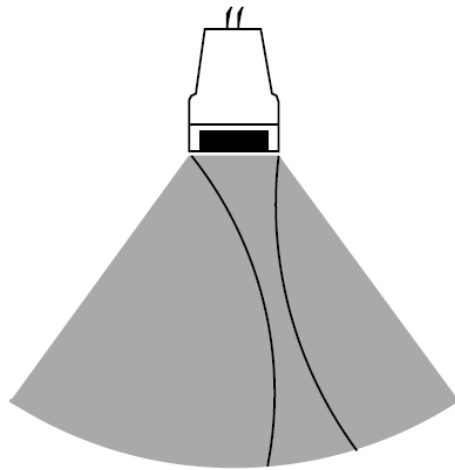


Figure II.7: Beam profile of a medical ultrasound transducer

Medical ultrasound scanners typically use high frequencies of between 1 and 20 MHz. Simple Doppler systems operate with a continuous single-frequency excitation voltage, but all imaging systems and pulsed Doppler systems use pulsed excitation signals. If ultrasound is continuously transmitted along a particular path, the energy will also be continuously reflected back from any boundary in the path of the beam, and it will not be possible to predict where the returning echoes have come from.

The pulses used in imaging ultrasound are very short and will only contain 1 to 3 cycles in order that reflections from boundaries that are close together can be easily separated. Pulsed Doppler signals are longer and contain several cycles. In fact, a pulse is made up not of a single frequency but of a range of frequencies of different amplitudes. Different shaped pulses will have different frequency contents.

II.6.3.1 Beam profile

When the vibrating surface of the transducer is in contact with the tissue which be imaged, an ultrasound beam of longitudinal waves is radiated into the tissue. According to Huygens's principle, which describes a large transducer surface as an infinite number of point sources of ultrasound energy where each point is characterized as a radial emitter, the ultrasound beam can be calculated as interference between spherical waves that originate at all points from the transducer surface. The spatial variation of the beam power is called beam profile.

The soft tissue which has inhomogeneous acoustic properties absorbs acoustic energy. This affects the ultrasound beam profile by changing the frequency content, phase aberrations, and reverberations. Exact values of the ultrasound beam profile can be obtained by numerical calculation, and in special cases we can obtain exact and approximate analytical expressions for the beam profile [18]. The ultrasound beam profile will depend on the length of the transmitted pulse, and we therefore often define a continuous wave (CW) beam pattern for a continuous vibration of the surface of the transducer, and a pulsed wave (PW) for a pulsed vibration.

II.6.3.2 Focusing

The principle of focusing an ultrasound beam is to align the pressure fields from all points of the transducer aperture to arrive at the field point at the same

time. This can be done through either a physically curved aperture, through a lens in front of the aperture, or by the use of electronic delays for multi-element arrays. The focal distance, the length from the transducer to the narrowest beam width, is shorter than the focal length of a nonfocused transducer and is fixed. The focal zone is defined as the region over which the width of the beam is less than two times the width at the focal distance; thus, the transducer frequency and dimensions should be chosen to match the depth requirements of the clinical situation.

II.7 RADIATED BEAM DESCRIPTION

II.7.1 Beam Regions

The ultrasound field that emanates from a piezoelectric transducer does not originate from a point, but instead originates from most of the surface of the piezoelectric element. Round transducers are often referred to as piston source transducers because the ultrasound field resembles a cylindrical mass in front of the transducer. Since the ultrasound field originates from a number of points along the transducer surface, the ultrasound intensity along the beam is affected by constructive and destructive wave interference. These are sometimes also referred to as diffraction effects. For a plane ultrasound transducer there are three distinct regions of the beam:

II.7.1.1 Nearfield or Fresnel region

It's the region situated between the transducer and the farfield region. The nearfield is adjacent to the transducer face and has a converging beam profile. Beam convergence in the nearfield occurs because of multiple constructive and destructive interference patterns of the ultrasound waves from the transducer surface. As individual wave patterns interact, the peaks and troughs from adjacent sources constructively and destructively interfere, causing the beam profile to be tightly collimated in the nearfield. The ultrasound beam path is thus largely confined to the dimensions of the active portion of the transducer surface, with the beam diameter converging to approximately half the transducer diameter at the end of the nearfield. The nearfield length NFL is dependent on the transducer frequency and diameter as:

$$NFL = \frac{d^2}{4\lambda} = \frac{r^2}{\lambda} \quad (\text{II.11})$$

Where d is the transducer diameter, r is the transducer radius, and λ is the wavelength of ultrasound waves in the propagation medium. Pressure amplitude characteristics in the near field are very complex, caused by the constructive and destructive interference wave patterns of the ultrasound beam. Peak ultrasound pressure occurs at the end of the nearfield, corresponding to the minimum beam diameter for a single element transducer. Pressures vary rapidly from peak compression to peak rarefaction several times during transit through the nearfield.

II.7.1.2 Farfield or Fraunhofer region

It's the region wherein the ultrasound beam spreads as a cone with a main lobe and side lobes as skirts around. The intensity falls off gradually from the axis in the main lobe, and we specify the intensity drop of the ultrasound field that defines the beam width. For a large area single element transducer, the angle of ultrasound beam divergence θ , for the farfield is given by:

$$\sin(\theta) = 1.22 \frac{\lambda}{d} \quad (\text{II.12})$$

Where d is the effective diameter of the transducer, and λ is the wavelength. Less beam divergence occurs with high frequency, large diameter transducer. Unlike the nearfield, where beam intensity varies from maximum to minimum to maximum in a converging beam, ultrasound intensity in the farfield decreases monotonically with distance.

II.7.1.3 Transition region

It's the region between the extreme nearfield and farfield regions. In the transition region, the diffraction causes a slight contraction of the central portion of the ultrasound beam before it starts to diverge in the farfield region. This phenomenon is sometimes referred to as diffraction focusing, and it causes highest intensity of the ultrasound beam for a focused transducer to be nearer the transducer than the geometric focus.

II.7.2 Energy Distribution

In the general case, the radiated transducer energy is distributed on three zones called lobes, figure (II.8):

II.7.2.1 Main lobe

The main lobe, or main beam, of a transducer radiation pattern is the lobe containing the maximum radiated power. This is the lobe that exhibits the greatest field strength.

II.7.2.2 Secondary lobes

The sidelobe is the field intensity outside the main lobe of the far field.

II.7.2.3 Grating lobes

The grating lobes are sound waves that get transmitted from the transducer at angles other than that of the ultrasound wave.

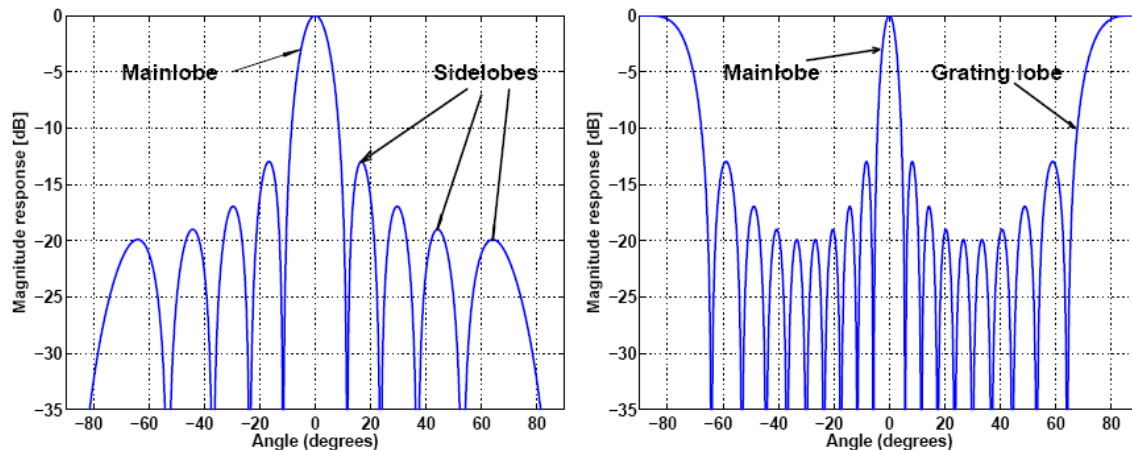


Figure II.8: Angular beam representation. Illustration of main lobe, sidelobes, and grating lobes

II.8 MEDICAL ULTRASOUND IMAGING

II.8.1 Principle

Ultrasound imaging is based on the generation, detection and processing of acoustic signals. An ultrasound transducer converts electrical voltage pulses into

mechanical pulses that propagate outwards as acoustic waves into the human body. Echo signals are produced when the ultrasound waves encounter the interfaces between human tissues with different acoustic impedances. These echo signals, which can have the same or multiple frequency of the original excitation wave, are generally detected by the same transducer. The electrical signals generated from the backscattered acoustic echoes are then beamformed and processed to form an ultrasound image. Figure (II.9), shows data processing sequences of the signal before displaying an ultrasound image.

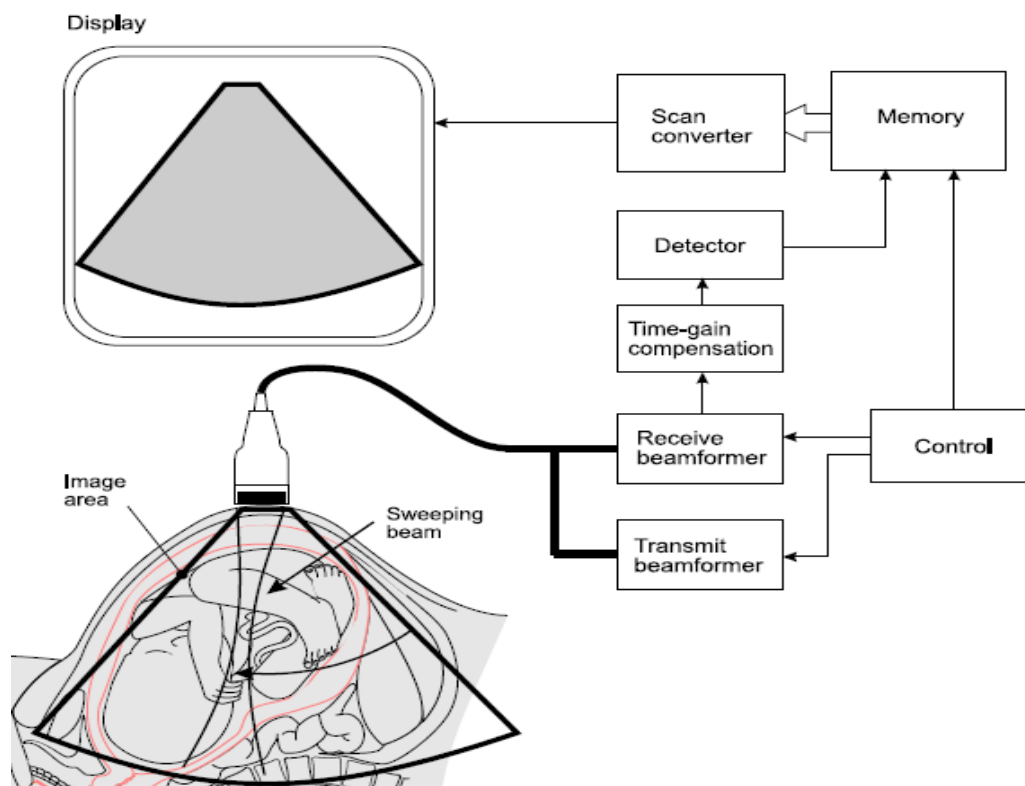


Figure II.9: Ultrasound imaging system (figure Adapted from [14])

Ultrasound imaging is one of the most popular medical imaging modalities because of several attractive features. It non-invasively forms images using reflected acoustic signals resulting from non-ionizing radiation. Ultrasound instruments for medical imaging purposes have a significantly smaller size and lower cost compared with

instruments in other medical imaging modalities such as MRI (Magnetic Resonance Imaging) and CT (Computation Tomography). One ultrasound scanner can be equipped with multiple ultrasound probes to meet various needs for imaging different regions of the human body. Another advantage of ultrasound imaging is that it can form 2D, or 3D, images in real-time.

II.8.2 Image Displaying Modes

The creation of an ultrasound image depends on the way in which ultrasound energy interacts with the tissue as it passes through the body. It uses information contained in reflected and scattered signals received by the transducer. The amplitude of the returning pulse will depend on the proportion of the ultrasound reflected or back scattered to the transducer and the amount by which the signal has been attenuated along its path. Ultrasonic pulse echo systems encompass a large number of configurations, which include both single element and multi-element ultrasonic transducers. The output of such systems can be presented in several types of display mode: A, B, and, M-mode scans. In each imaging mode, the transducer defines the limitation in terms of sensitivity and resolution of the system. Thus, there are multiple ways to interpret the echo-signals depending on different operation schemes, display, and presentation formats [19].

II.8.2.1 A-mode

The A-mode (A stands for amplitude) technology had no focusing, and simply displayed a one-dimensional signal giving the echo as function of time. It is the simplest and earliest mode of ultrasonic imaging.

II.8.2.2 B-mode

In the 1950s and 1960s the B-mode technology was developed, with the B-standing for brightness, giving the first two-dimensional views of the body. The B-mode technology forms the basis of the technology, which today permeates most modern medical facilities. In a B-mode display, the brightness in the image is proportional to the echo strength. It is the most widely used ultrasound image format, where ultrasound echoes are collected from a 2D field instead of a single beam direction. In this type of imaging, the emitted ultrasound wave is mechanically

or electronically steered to different directions. The whole image of the 2D field within a selected depth and viewing angle are formed by interpolating between the multiple scan-lines. Figure (II.10), shows an example of a B-Mode ultrasound image of a fetus (gynecology domain).



Figure II.10: Example of a *B-Mode ultrasound image of fetus*

II.8.2.3 C-mode

In C-scan mode, the reconstructed image plane is parallel to the transducer surface. C-scan captures ultrasound echoes from a fixed depth in one image and it generally requires a 2D array transducer to accomplish this.

II.8.2.4 M-mode

M-mode (or motion mode) imaging is designed to display tissue structure motion (e.g. heart chamber contractions). The echoes from moving body structures are displayed as a vertical line continuously monitored with respect to a moving time axis along the image width dimension.

According to the clinical need, and in addition of these three modes, there are : C-mode, color flow imaging mode or color flow Doppler mode, color M-mode, and other types [20].

II.9 BEAMFORMING FOR IMAGING

Beamforming can be described as the technique of using an array of transducer elements to focus or steer a wave field, and can be employed at both transmission and reception. At transmission, both the amplitude and the time of excitation are controlled at each element so that propagating waves add up constructively in the focal point, and have as much destructive interference as possible at all other locations. At reception, the received signals are weighted and added coherently so that the wave field from the desired direction is reinforced while it is suppressed as much as possible from all other directions. For conventional beamforming the question of phase control or time-delay reduces to simple geometry, translating the path length to distance travel time. The shape of the beam is usually quantified through the beampattern, which is the angular response of an array to a plane wave. Figure (II.11), shows the principle of beamforming where a wavefield impinges on an array of elements at some angle. Each element records a time-delayed version of the wavefield, and each of these recordings are then time-delayed, so that they interfere constructively when being summed.

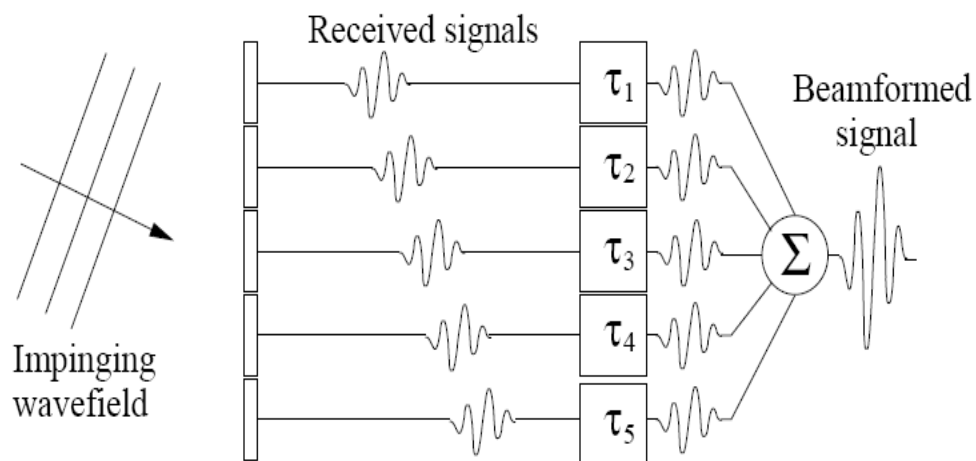


Figure II.11: Illustration of the principle of beamforming (figure Adapted from [14])

II.10 RESOLUTION AND IMAGE QUALITY

The resolution is defined as to able separate between two adjacent close points in a corresponding image. The Medical image quality relates to the subjective interpretation of visual data and does not have a simple analytical definition despite several attempts to provide one. It is the clinical information contained in the image and whether this can be goodley interpreted.

The ultrasound beam can be focused to improve the image quality within the focal zone. By using several elements, excited with a range of delays, it is possible to focus the beam. The axial resolution is determined by the length of the pulse, although this may be shorter than the actual transmitted waveform if pulse compression is used.

In fact, modern scanners use electronic transducers, which typically comprise 128 piezoelectric elements that are capable of producing many adjacent beams, or scan lines, without the need to move the transducer itself. The quality of the image will obviously depend on the distance between adjacent beam paths, known as the line density.

Chapter III

Fundamental Ultrasound Imaging

Fundamental Ultrasound Imaging

III.1 INTRODUCTION

Fundamental ultrasound imaging operates in linear mode, it transmit and receive at the same frequency. A linear theory is a simplified solution to the propagation problem, ignoring any nonlinear effects of the medium. The propagation of ultrasound waves through real media is a very complicated process involving combined effects of diffraction, nonlinearity and attenuation. A good knowledge of the properties of the linear equation may thus provide a head start when turning to the nonlinear case.

In medical imaging, it is the ultrasound field signal reflected by the constituents of the tissue that is received by the transducer. After this, a signal processing step is needed to finally show the ultrasound image. The ultrasonic field from transducers is the feature that determines the performance of a given system.

The study of the spatial and temporal characteristics of the acoustical pressure field allows a greater understanding of the behavior of such devices. The linear approximation has a wide range of validity, and it is always an important first step in the analysis of finite amplitude effects in more intense acoustic fields.

Linear and phased array are widely used in modern medical ultrasound imaging systems. They enable beams to be electronically steered and focused on both transmission and reception. Array geometry and signal processing are of key importance in improving the system resolution and contrast.

The major difficulties in developing new arrays and signal processing method are the complexities and high costs in building array and imaging system prototypes.

However, with the ever increasing computing power available to researchers, computer modeling become a more and more important tool for analyzing the resolution and contrast of an imaging system with different array designs and signal processing methods, before physically building a such system.

III.2 FUNDAMENTAL ULTRASOUND IMAGING

Ultrasound imaging is based on the generation, detection and processing of acoustic echo signals which are produced when the ultrasound waves encounter the interfaces between human tissues with different acoustic impedances.

In fundamental ultrasound imaging, the echo signal has the same frequency of the original excitation wave, and it is generally detected by the same transducer.

The medical scanners use advanced transducer geometries for creating ultrasound fields suitable for probing the body. Ultrasound imaging is based on the transducer characterization in which pulsed ultrasound waves are directed into the human body, and echo signals from reflectors and scatterers in organs are detected and used to construct the image. A first characterization of these transducers is based on computer simulation of the field.

The standard approach for linear ultrasound imaging is to use the fundamental frequency from the reflected signal to form images. Generally speaking, linear wave propagation theory is adequate for describing fundamental or conventional ultrasound imaging mode, which uses the same frequency for the excitation and reception. The linear approximation has a wide range of validity, and it is always an important first step in the analysis of finite amplitude effects in more intense acoustic fields.

Fundamental ultrasound imaging is still the primary imaging mode in clinical ultrasound scanners. It can be simulated realistically using linear acoustics.

III.3 LINEAR PROPAGATION AND SMALL SIGNAL APPROXIMATION

Ultrasound waves can be thought of as pressure variations in a medium, which propagate periodically in space and time. To a first order approximation, ultrasound propagation is well described as a linear process, governed by a linear, second order homogeneous differential equation. The assumption of linear propagation, however, is valid only for relatively small disturbances.

In considering wave propagation in fluids, one can obtain the linear wave equation from the Navier-Stokes equation by making a small signal approximation for the density and pressure [21], given by:

$$\rho = \rho_0 + \rho_1 \quad (\text{III.1})$$

$$p = p_0 + p_1 \quad (\text{III.2})$$

Where p_0 and p_1 denote the equilibrium medium density and pressure respectively. p_1 and p_1 denote changes in density and pressure, which are small. This small signal approximation leads to the equation:

$$\gamma p_0 \frac{\partial^2 p_1}{\partial t^2} = \nabla^2 p_1 + \gamma \left(\mu_b + \frac{4}{3} \mu \right) \frac{\partial}{\partial t} (\nabla^2 p_1) \quad (\text{III.3})$$

Where μ_b is the bulk viscosity, μ is the shear viscosity, and γ is the adiabatic compressibility. This is a linear equation and, can also be expressed in terms of the normal particle velocity u , or the velocity potential ϕ .

In the frequency domain, this becomes the homogeneous Helmholtz wave equation as:

$$\nabla^2 \phi + \delta^2 \phi = 0 \quad (\text{III.4})$$

Where

$$\delta^2 = \frac{k^2}{1+j\omega\gamma(\mu_b+\frac{4}{3}\mu)} \quad (\text{III.5})$$

$k = \omega/c_0$ is the wave number, ω is the radian frequency, and c_0 is ambient sound speed.

In the absence of viscous loss, the time domain equation becomes the familiar homogeneous wave equation as:

$$\nabla^2 \phi + \frac{1}{c^2} \phi = 0 \quad (\text{III.6})$$

The frequency domain equation looks the same except that $\delta = k$. The 1-D version of this equation for particle velocity is:

$$\left(\frac{\partial^2}{\partial t^2} - c^2 \frac{\partial^2}{\partial z^2} \right) u \quad (\text{III.7})$$

Equation (III.7) can be factored to obtain two uncoupled wave equations called reduced or evolution equations, one of which is:

$$\frac{\partial u(t,z)}{\partial z} = \frac{1}{c_0} \frac{\partial u(t,z)}{\partial t} \quad (\text{III.8})$$

Equation (III.8) describes linear plane waves propagating in the positive z-direction for small signal approximation.

III.4 LINEAR ULTRASOUND SYSTEM

Compared with the full nonlinear ultrasound propagation theory, the linear wave theory is much simpler to solve by numerical methods. A number of transducer field simulation methods and linear B-mode image models have been described in the literature. They roughly fall into two categories: frequency domain models and time domain models. Frequency domain simulation techniques are based on classic diffraction theory for continuous waves which can be thought of as pressure variations in a media and propagate periodically in space and time. As well known linear wave equation can be written as Helmholtz equation model [22]:

$$\nabla^2 p - \frac{1}{c^2} \frac{\partial^2 p}{\partial t^2} = 0 \quad (\text{III.9})$$

Where p is the pressure, c is the speed of sound and t is the time. When the surface of the transducer is vibrating uniformly at a single frequency with an infinite rigid baffling, the solution to the linear wave equation (III.9) is [22]:

$$p(\vec{r}, \omega) = -\frac{i\rho k c u(\omega)}{4\pi} A_0(\vec{r}, \omega) \quad (\text{III.10})$$

Where $A_0(\vec{r}, \omega)$ is the Rayleigh integral evaluated at field point \vec{r} . The latter is given by:

$$A_0(\vec{r}, \omega) = \iint_{S'} \frac{e^{ik|\vec{r}-\vec{r}'|}}{|\vec{r}-\vec{r}'|} ds \quad (\text{III.11})$$

\vec{r}' is a source point on the surface of the transducer and the integral is over the surface area s' of the transducer. If the medium is dispersive, $c(\omega)$ can be used in place of c . Attenuation is taken into account by replacing k by the complex wave number:

$$k = \frac{\omega}{c(\omega)} + i\alpha(\omega) \quad (\text{III.12})$$

Where $\alpha(\omega)$ is the attenuation coefficient.

Spectrum analysis and linear superposition have to be used to calculate the ultrasound field of a short pulse that has rich frequency content. Two dimensional integration in equation (III.11) has to be applied to calculate the diffraction in the frequency domain methods. In the time domain, the field pressure at a point in space \vec{r} from a source that is vibrating at arbitrary velocity $v(t)$ can be formulated as:

$$p(\vec{r}, t) = \rho \frac{\partial v(t)}{\partial t} \otimes h(\vec{r}, t) \quad (\text{III.13})$$

Or:

$$p(\vec{r}, t) = \rho v(t) \otimes \frac{\partial h(\vec{r}, t)}{\partial t} \quad (\text{III.14})$$

Where \otimes is the convolution operator and $h(\vec{r}, t)$ is the spatial impulse response function of the transducer at the field point. It is given by:

$$h(\vec{r}, \omega) = \iint_{S'} \frac{\delta\left(t - \frac{|\vec{r} - \vec{r}'|}{c}\right)}{2\pi|\vec{r} - \vec{r}'|} ds \quad (\text{III.15})$$

$\delta(t)$ is the Dirac delta function. Closed form expressions for the impulse response function in equation (III.14) have been derived for many geometries [23]-[24]. In linear acoustics, the emitted, scattered and received ultrasound field can be assessed by using the spatial impulse response calculated by the Rayleigh integral as developed by Tupholme and Stepanishen.

III.4.1 Field in Linear Ultrasound Systems

It is a well-known fact in electrical engineering that a linear electrical system is characterized by its impulse response. Applying a delta function $\delta(t)$ to the input of the circuit and measuring its output characterizes the system. The output $x_o(t)$ to any kind of input signal $x_i(t)$ is then given by:

$$x_o(t) = h(t) \otimes x_i(t) = \int_{-\infty}^{+\infty} h(\zeta) x_i(t - \zeta) d\zeta \quad (\text{III.16})$$

Where $h(t)$ is the impulse response of the linear system. The transfer function of the system is given by the Fourier transform of the impulse response and characterizes the systems amplification of a time-harmonic input signal.

The same approach can be taken to characterize a linear acoustic system. The basic set-up is shown in Figure (III.1), [25].

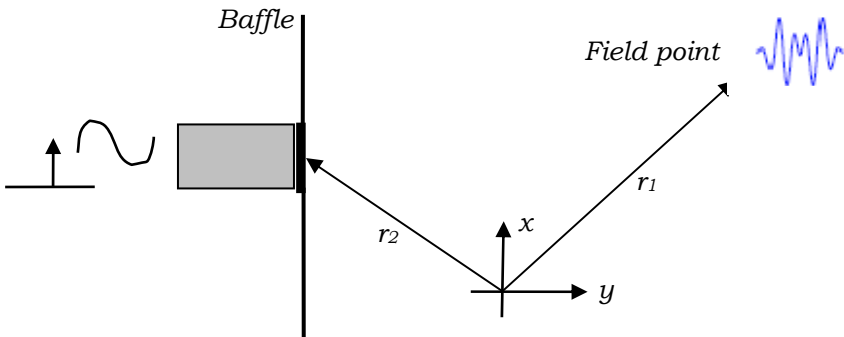


Figure III.1: Linear ultrasound system

The acoustic transducer is mounted in a infinite, rigid baffle and its position is denoted by \vec{r}_2 . It radiates into a homogeneous medium with a constant speed of sound c and density ρ_0 throughout the medium. The field point denoted by \vec{r}_1 is where the acoustic pressure from the transducer is measured by a small point hydrophone. A voltage excitation of the transducer with a delta function will give rise to a pressure field that measured by the hydrophone. The measured response is the acoustic impulse response for this particular system with the given set-up. Moving the transducer or the hydrophone to a new position will give a different response. Moving the hydrophone closer to the transducer surface will often increase the signal intensity, and moving it away from the center axis of the transducer will often diminish it. Thus, the impulse response depends on the relative position of both the transmitter and receiver ($\vec{r}_2 - \vec{r}_1$) and hence it is called a spatial impulse response.

A perception of the ultrasound field for a fixed time instance can be obtained by employing Huygens' principle in which every point on the radiating surface of the transducer is the origin of an outgoing spherical wave. Each of the outgoing spherical waves are given by:

$$p_s(\vec{r}_1, \omega) = k_p \frac{\delta(t - \frac{|\vec{r}_2 - \vec{r}_1|}{c})}{|\vec{r}_2 - \vec{r}_1|} = k_p \frac{\delta(t - \frac{|\vec{r}|}{c})}{|\vec{r}|} \quad (\text{III.17})$$

Like shown in figure (III.1), \vec{r}_1 indicates the point in space, \vec{r}_2 is the point on the transducer surface, k_p is a constant, and t is the time for the snapshot of the spatial distribution of the pressure. The spatial impulse response is then found by observing the pressure waves at a fixed position in space over time by having all the spherical waves pass the point of observation and summing them.

III.4.2 Spatial Impulse Response

The transducers excitations employed in medical ultrasound imaging are pulsed. A more accurate and general solution is, thus, needed, and this is developed in this chapter. The approach is based on the concept of spatial impulse responses developed by Tupholme and Stepanishen [26]-[28]. The spatial impulse response of a transducer is, as the name suggests the field response of a perfect impulse excitation.

III.4.3 Calculation of Spatial Impulse Response

The calculation of the spatial impulse response assumes linearity and any complex-shaped transducer can therefore be divided into smaller apertures and the response can be found by adding the responses from the sub-apertures. The integral is, as mentioned before, a statement of Huygens' principle of summing contributions from all areas of the aperture. An alternative interpretation is found by using the acoustic reciprocity theorem [29]. This states that: *If in an unchanging environment the locations of a small source and a small receiver are interchanged, the received signal will remain the same.* Thus, the source and receiver can be interchanged. Emitting a spherical wave from the field point and finding the wave's intersection with the aperture also yields the spatial impulse response.

The calculation of the impulse response is then facilitated by projecting the field point onto the plane of the aperture, and thus, determined by the relative length of the part of the arc that intersects the aperture. Thereby it is the crossing of the projected spherical waves with the edges of the aperture that determines the spatial impulse responses [18].

However, the spatial impulse response is found from the Rayleigh integral derived earlier as:

$$h(\vec{r}_1, t) = \iint_S \frac{\delta(t - \frac{|\vec{r}_1 - \vec{r}_2|}{c})}{2\pi|\vec{r}_1 - \vec{r}_2|} ds \quad (\text{III.18})$$

The solution is to project the field point onto the plane coinciding with the aperture, and then find the intersection of the projected spherical wave (the circle) with the active aperture as shown in figure (III.2).

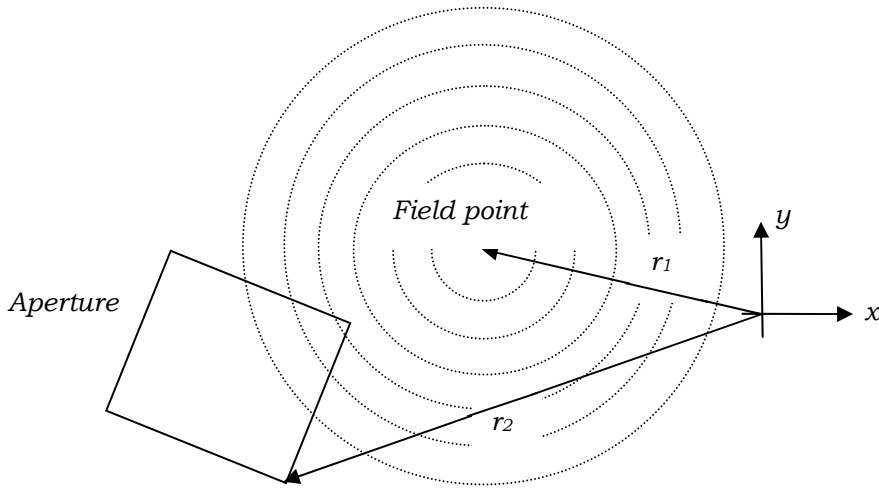


Figure III.2: Intersection of spherical waves from the field point by the aperture, when the field point is projected onto the plane of the aperture

Rewriting the integral into polar coordinates gives:

$$h(\vec{r}_1, t) = \int_{\varphi_1}^{\varphi_2} \int_{d_1}^{d_2} \frac{\delta(t - \frac{R}{c})}{2\pi R} r dr d\varphi \quad (\text{III.19})$$

Where r is the radius of the projected circle and R is the distance from the field point to the aperture given by $R = \sqrt{r^2 + z_p^2}$. Here z_p is the field point height above $z = 0$ plane of the aperture. The projected distances d_1, d_2 are determined by the aperture and are the distance closest to and furthest away from the aperture, and φ_1, φ_2 are the corresponding angles for a given time (see figure (III.3)).

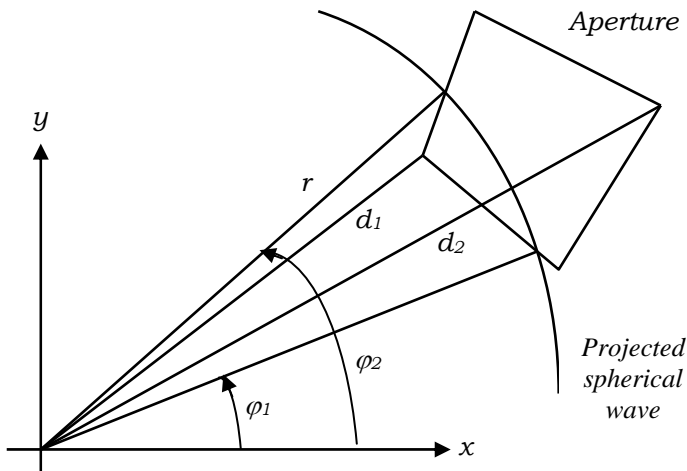


Figure III.3: Distances and angles in the aperture plan for evaluating the Rayleigh integral

Introducing the substitution $2RdR = 2rdr$ gives:

$$h(\vec{r}_1, t) = \frac{1}{2\pi} \int_{\varphi_1}^{\varphi_2} \int_{R_1}^{R_2} \delta\left(t - \frac{R}{c}\right) dR d\varphi \quad (\text{III.20})$$

The variables R_1 and R_2 denote the edges closest to end furthest away from the field point. Finally using the substitution $\tau = R/c$ gives:

$$h(\vec{r}_1, t) = \frac{c}{2\pi} \int_{\varphi_1}^{\varphi_2} \int_{t_1}^{t_2} \delta(t - \tau) d\tau d\varphi \quad (\text{III.21})$$

For a given time instance the contribution along the arc is constant and the integral gives:

$$h(\vec{r}_1, t) = \frac{\varphi_2 - \varphi_1}{2\pi} c \quad (\text{III.22})$$

When assuming the circle arc is only intersected once by the aperture. The angles φ_1 and φ_2 are determined by the intersection of the aperture and the projected spherical wave, and the spatial impulse response is, thus, determined by these intersections, when no apodization (*the apodization is the reduction of the vibration amplitude towards the edge of the aperture face*) of the aperture is used. The

response can therefore be evaluated by keeping track of the intersections as a function of time as:

$$h(\vec{r}_1, t) = \frac{c}{2\pi} \sum_{i=1}^{n(t)} [\varphi_2^i(t) - \varphi_1^i(t)] \quad (\text{III.23})$$

Where $n(t)$ is the number of arc segments that crosses the boundary of the aperture for a given time and $\varphi_2^i(t)$, $\varphi_1^i(t)$ are the associated angles of the arc. The calculation of the spatial impulse response can, thus, be formulated as finding the angles of the aperture edges intersections with the projected spherical waves, sorting the angles, and then sum the arc angles that belong to the aperture.

III.5 NUMERICAL SIMULATION

Medical ultrasound imaging can be simulated realistically using linear acoustics. One of the most powerful approaches is to employ spatial impulse response. Hereby both emitted fields and pulse echo responses from point scatterers can be determined, and the response from the transducer is found by summing the spatial impulse responses from the individual elements.

The impulse response generally exhibits discontinuities, which leads to the need for very high temporal sampling rates to obtain accurate results for the ultrasound field. However, the closed form time domain solution is exact for all field locations and is much more efficient to evaluate by numerical methods than spectrum analysis and the 2D integration in equation (III.11) that is required for calculating the pressure fields accurately in the frequency domain. To reduce the computational complexity of frequency domain methods, many approximations are used by researchers to reduce the 2D integration in equation (III.11) to 1D integration. These different approximation methods result in various degrees of accuracy and efficiency [30]-[32].

Crombie, Bascom and Cobbold surveyed many representative time domain and frequency domain simulation methods [33]. They concluded that in the frequency domain, the Fresnel approximation [34] yields the most accurate results for unsteered arrays. However, the accuracy degrades with increasing steering angle. They also showed that the frequency domain method with the Fresnel approximation is generally more efficient than the exact time domain method. Turnbull and Foster [35] did an extensive study of 2D arrays using the time domain

method. Jørgen Jensen et al. have demonstrated that realistic B-mode images can be generated by using the time domain impulse response method to calculate the transducer ultrasound field, even when approximations are used to reduce the computational complexity [36].

In this chapter, a program for the simulation of ultrasound systems called FIELD is used to calculate impulse responses and ultrasound fields [37]. It is based on the Tupholme-Stepanishen method, which uses the approach of spatial impulse responses that assumes linear propagation [26]-[28].

III.5.1 FIELD: Program Description

FIELD program is based on the Tupholme-Stepanishen method, and is fast because of the use of a far field approximation. Any kind of transducer geometry and excitation can be simulated, and both pulse-echo and continuous wave fields can be calculated for both transmit and pulse-echo. Dynamic apodization and focusing are handled through time lines, and different focusing schemes can be simulated. The versatility of the program is ensured by interfacing it to Matlab. All routines are called directly from Matlab, and all Matlab features can be used. This makes it possible to simulate all types of ultrasound imaging systems.

The prime application of the FIELD program is to simulate the image of an ultrasound scanner. This necessitates that multiple foci zones can be taken into account and that dynamic apodization can be used. The two concepts are introduced through time lines. The focus time line holds information about the dynamic behavior of the focusing. Each focal zone is characterized by a time point and a delay value for each transducer element. The time point indicates the time after pulse emission when these delay values are used. The same approach is used for the apodization time line, which assigns an apodization value for each transducer element. Multiple transducers can be handled by the program. Commands for defining linear, phased, and 2D matrix arrays are given. The commands return an identifier for the array, which can be passed to the routines for field calculation. Thereby different transducers can be used on the same scatterers and the effect of different choices can readily be evaluated. Commands are also found for setting the excitation waveform of the transducer and the electromechanical impulse response. Commands for calculating the emitted, the

pulse echo, and the scattered fields are given. Thereby the transducers can be evaluated and images for computer phantoms can be found. A simple cyst phantom with point scatterers has been defined, and can be used in imaging [37].

III.6 ARRAY TRANSDUCER

Linear and phased array are widely used in modern medical ultrasound imaging systems. They enable beams to be electronically steered and focused on both transmission and reception.

For a rectangular radiating source, figure (III.4), the Rayleigh integral in expression (III.11) becomes:

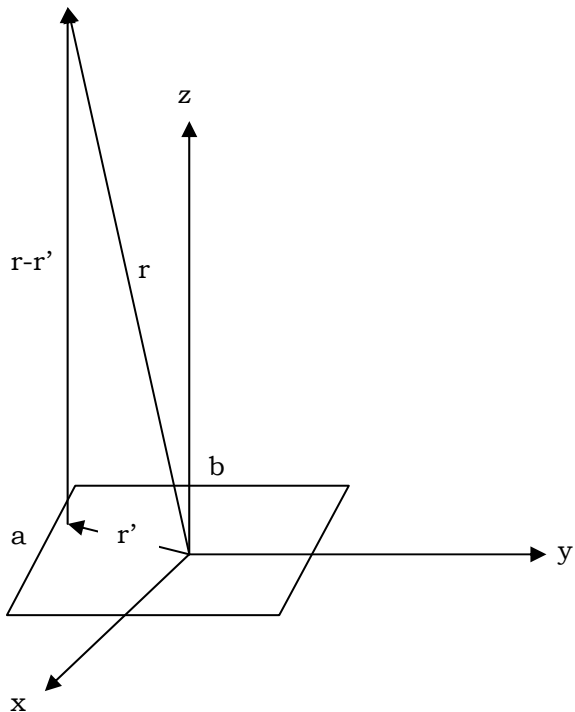


Figure III.4: Rectangular radiated source and coordinates

$$A_0(\vec{r}, \omega) = \int_{-\frac{b}{2}}^{\frac{b}{2}} \int_{-\frac{a}{2}}^{\frac{a}{2}} \frac{e^{ik|\vec{r}-\vec{r}'|}}{|\vec{r}-\vec{r}'|} dx' dy' \quad (\text{III.24})$$

For typical clinical linear or phased arrays, usually the length of the transducer element b is on the order of 1cm and the width is on the order of a half wavelength

[38], resulting in the condition $b \gg a$. Define r to be the distance from the field point to the center of the element: $r = |\vec{r}| = \sqrt{x^2 + y^2 + z^2}$. Under the assumption that $r > b \gg a$, $|\vec{r} - \vec{r}'|$ can be expanded by:

$$|\vec{r} - \vec{r}'| = \sqrt{(x - x')^2 + (y - y')^2 + z^2} \quad (\text{III.25})$$

The expression (III.25) can be approximated as:

$$|\vec{r} - \vec{r}'| \approx r + \frac{1}{2r}(x'^2 + y'^2 - 2xx' - 2yy') - \frac{1}{8r^3}(x'^2 + y'^2 - 2xx' - 2yy')^2 \quad (\text{III.26})$$

Here $\vec{r}(x, y, z)$ is the field point, and $\vec{r}'(x', y', z')$ is the source point. We can take advantage of the fact that if $a \approx \lambda/2$, terms on order of $x'^2/2r$ are negligible for the y' integration in expression (III.26). This introduces a phase error of

$(k x'^2/2r) < (k a^2/8r) \approx (\pi \lambda/16r)$ at most, which is smaller than $7 \cdot 10^{-3}$ radians in the common case when r is greater than 1 cm and the wavelength is around $300\mu\text{m}$ ($1500\text{ms}^{-1}/5\text{MHz}$). Therefore:

$$|\vec{r} - \vec{r}'| \approx r + \frac{1}{2r}(y'^2 - 2xx' - 2yy') - \frac{1}{8r^3}(x'^2 + y'^2 - 2xx' - 2yy')^2 \quad (\text{III.27})$$

In the region where $\frac{k}{8r^3}(x'^2 + y'^2 - 2xx' - 2yy')^2 \ll 1$ radian, $|\vec{r} - \vec{r}'|$ can be approximated using the first two terms. This approximation is less restrictive than the Fresnel approximation [34], the expression (III.25) is written as:

$$|\vec{r} - \vec{r}'| \approx z + \frac{1}{2z}[(x - x')^2 + (y - y')^2] - \frac{1}{8z^3}[(x - x')^2 + (y - y')^2]^2 \quad (\text{III.28})$$

The Fresnel approximation requires $\frac{k}{8z^3}[(x - x')^2 + (y - y')^2]^2 \ll 1$ radian for reasonable accuracy. The error using the Fresnel approximation is on the order of $o\left(\frac{x^4+y^4}{z^3}\right)$, while the error using the approximation in expression (III.27) is on the order of $o\left(\frac{x^2+y^2}{z^3}\right)$. When the beam is steered at a large angle, i.e., x is comparable to z , the Fresnel approximation will not hold; however the expression (III.27) is still

valid as long as r is not too small, that means: $\frac{k}{8r^3}(x'^2 + y'^2 - 2xx' - 2yy')^2 < 1$. With keeping only the first two terms in expression (III.27), $|\vec{r} - \vec{r}'| \approx r + \frac{1}{2r}(y'^2 - 2xx' - 2yy')$, and then:

$$A_0(\vec{r}, \omega) \approx \frac{a}{r} e^{ikr} \text{sinc}\left(\frac{kxa}{2\pi r}\right) \int_{-\frac{b}{2}}^{\frac{b}{2}} e^{ik\frac{y'^2 - 2yy'}{2r}} dy' \quad (\text{III.29})$$

The 2D integral in the expression (III.24) is reduced to a 1D integral. The remaining integral has to be done numerically. Note that the sinc function is a result of ignoring the term $(x'^2/2r)$. If this last cannot be ignored, i.e., the width of the array element is much larger than λ , then the integral in the x' direction must also be done numerically [38].

III.7 FOCUSING

The essence of focusing an ultrasound beam is to align the pressure fields from all parts of the aperture to arrive at the field point at the same time. This can be done through either a physically curved aperture, through a lens in front of the aperture, or by the use of electronic delays for multi-element arrays. All seek to align the arrival of the waves at a given point through delaying or advancing the fields from the individual elements. The delay (positive or negative) is determined using ray acoustics. The path length from the aperture to the point gives the propagation time and this is adjusted relative to some reference point. The propagation time t_i from the center of the aperture element to the field point is:

$$t_i = \frac{1}{c} \sqrt{(x_i - x_f)^2 + (y_i - y_f)^2 + (z_i - z_f)^2} \quad (\text{III.30})$$

Where (x_f, y_f, z_f) is the position of the focal point, (x_i, y_i, z_i) is the center for the physical element number i , and c is the speed of sound.

A point is selected on the whole aperture as a reference for the imaging process. The propagation time for this is:

$$t_c = \frac{1}{c} \sqrt{(x_c - x_f)^2 + (y_c - y_f)^2 + (z_c - z_f)^2} \quad (\text{III.31})$$

Where (x_c, y_c, z_c) is the reference center point on the aperture. The delay to use on each element of the array is then: $\Delta t_i = t_c - t_i$.

Notice that there is no limit on the selection of the different points, and the ultrasound beam can, thus, is steered in a preferred direction.

The arguments here have been given for emission from an array, but they are equally valid during reception of the ultrasound waves due to acoustic reciprocity. At reception, it is also possible to change the focus as a function of time and thereby obtain a dynamic tracking focus. For each focal zone, there is an associated focal point and the time from which this focus is used. The arrival time from the field point to the physical transducer element is used for deciding which focus is used. Another possibility is to set the focusing to be dynamic, so that the focus is changed as a function of time and thereby depth. The focusing is then set as a direction defined by two angles and a starting point on the aperture. In FIELD program, the focusing is dynamic and changes as a function of depth in tissue or corresponding time [18].

III.9 SINGLE ELEMENT CIRCULAR TRANSDUCER

Ultrasonic pulse echo systems encompass a large number of configurations which include both single element and multi-element ultrasonic transducers. In ultrasound imaging, the output of such systems can be represented in several types of display mode, and in each mode the transducer defines the limitation in terms of sensitivity and resolution [39]. In the case of a single element circular transducer, the integral in equation (III.11) becomes:

$$A(\rho, z) = \int_0^a \int_0^{2\pi} \frac{e^{ik|\vec{r}-\vec{r}'|}}{|\vec{r}-\vec{r}'|} \rho' d\theta' d\rho' \quad (\text{III.32})$$

The cylindrical coordinate system is used in this situation. $\vec{r}(\rho, \theta, z)$ is the field point, and $\vec{r}'(\rho', \theta', z')$ is the source point.

Equation (III.32) describes the ultrasound pressure field from a flat unfocused transducer. To approximate a focused transducer with a focal distance d , a phase factor $e^{-ik\sqrt{d^2+\rho'^2-d}} \approx e^{-ik\rho'^2/2d}$ can be added to the integral. Therefore, for a focused transducer, the Rayleigh integral becomes:

$$A(\rho, z) = \int_0^a \int_0^{2\pi} \frac{e^{ik|\vec{r}-\vec{r}'|}}{|\vec{r}-\vec{r}'|} e^{-i\frac{k\rho'}{2d}} \rho' d\theta' d\rho' \quad (\text{III.33})$$

Moreover, this can be further simplified by a parabolic approximation:

$$|\vec{r} - \vec{r}'| = \sqrt{r^2 + \rho'^2 - 2\rho\rho' \cos(\theta - \theta')} \approx r + \frac{\rho'^2}{2r} - \frac{\rho\rho' \cos(\theta - \theta')}{r} \quad (\text{III.34})$$

Where $r = |\vec{r}| = \sqrt{\rho^2 + z^2}$.

With the help of equation (III.34), equation (III.33) reduces to a 1D integral as:

$$A(\rho, z) = 2\pi \frac{e^{ikr}}{r} \int_0^a J_0\left(\frac{k\rho\rho'}{r}\right) e^{ik\left(\frac{1}{2r} - \frac{1}{2d}\right)\rho'^2} \rho' d\rho' \quad (\text{III.35})$$

Where J_0 is the zero degree Bessel function and, expression (III.35) can be evaluated using numerical methods [40].

III.10 APODIZATION

Often ultrasound transducers do not vibrate as a piston over the aperture. This can be due to the clamping of the active surface at its edges [18]. The apodization term designates the reduction of the vibration amplitude towards the edge of the transducer face. It is used for reducing sidelobe levels and thereby increases the dynamic range of the image. The apodization can be dynamic and changes as a function of depth in tissue or corresponding time. Applying a Gaussian apodization will significantly lower sidelobes and generate a field with a more uniform point spread function as a function of depth. Apodization can be found by writing [41]:

$$h(\vec{r}_1, t) = \int_{\varphi_1}^{\varphi_2} \int_{d_1}^{d_2} a_p(r, \varphi) \frac{\delta(t - \frac{R}{c})}{2\pi R} r dr d\varphi \quad (\text{III.36})$$

Where $a_p(r, \varphi)$ is the apodization function over the aperture. Using the same substitutions as above yields:

$$h(\vec{r}_1, t) = \frac{c}{2\pi} \int_{\varphi_1}^{\varphi_2} \int_{t_1}^{t_2} a_{p_1}(\tau, \varphi) \delta(t - \tau) d\tau d\varphi \quad (\text{III.37})$$

In which, $a_{p_1}(\tau, \varphi) = a_p \left(\sqrt{(c\tau)^2 - z_p^2}, \varphi \right)$. The inner integral is a convolution of the apodization function with a Dirac function and readily yields:

$$h(\vec{r}_1, t) = \frac{c}{2\pi} \int_{\varphi_1}^{\varphi_2} a_{p_1}(t, \varphi) d\varphi \quad (\text{III.38})$$

The response for a given time point can be found by integrating the apodization function along the arc with a radius of $r = \sqrt{(ct)^2 - z_p^2}$ for the angles for the active aperture [41]-[43]. Any apodization function can therefore be incorporated into the calculation by employing numerical integration [18].

III.11 SIMULATION RESULTS

Simulation results are realized for a single element of diameter 14mm, an excitation frequency of 2.5MHz.

III.11.1 Unfocused Circular Transducer

In figure (III.5) is shown the excitation waveform (Gaussian waveform), and figure (III.6) shows the variation of the ultrasound field pressure along the propagation axis (axis of the transducer).

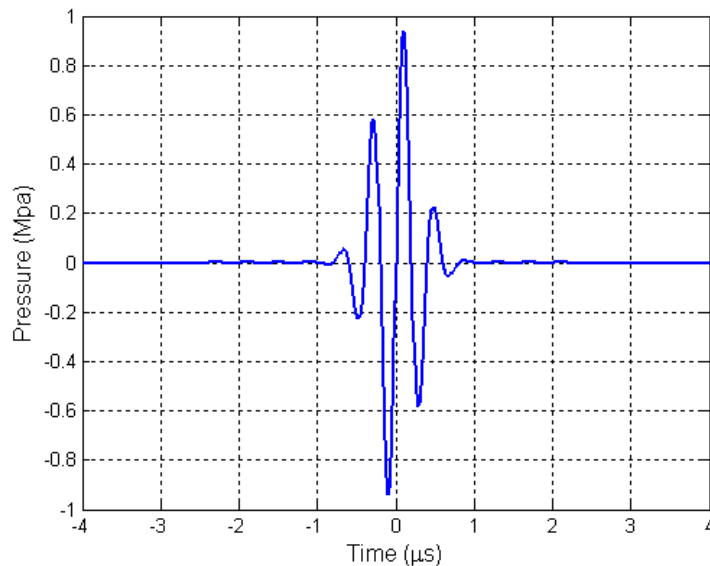


Figure III.5: Excitation waveform

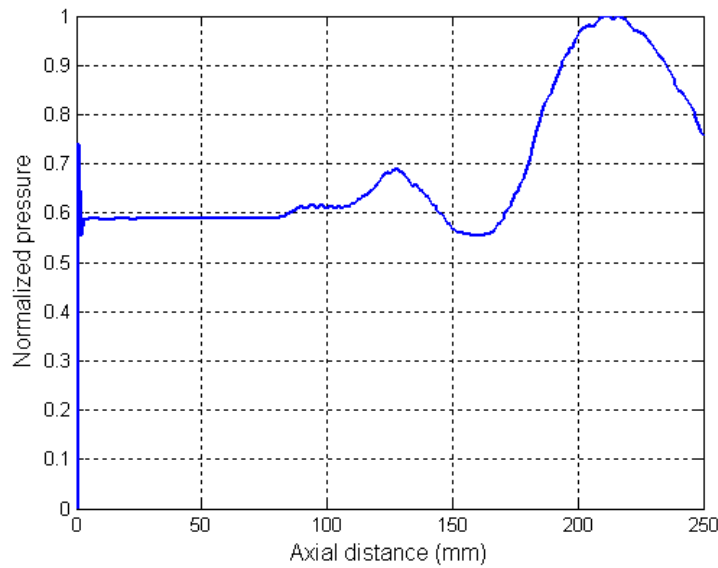


Figure III.6: Piston ultrasound field pressure variation

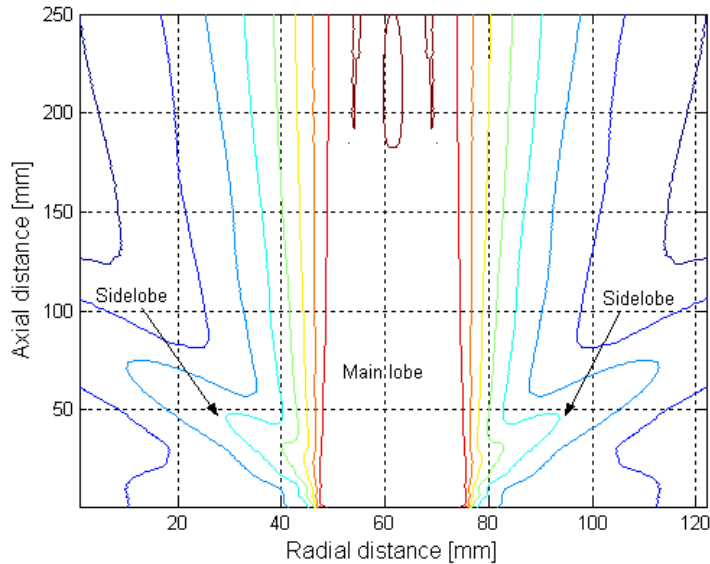


Figure III.7: Diagram pattern in x - z plane

Figures (III.7, 8) show how the ultrasound field intensity is distributed, the main lobe and the sidelobes.

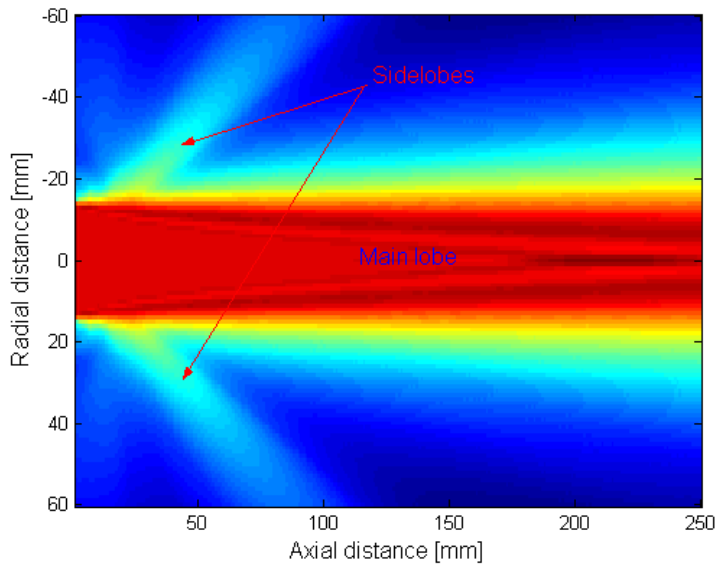


Figure III.8: Beam energy distribution

III.11.2 Focused Circular Transducer

For the focused transducer example case, we have chosen the case of the echocardiography. The heart is located at 60mm in-depth of the thoracic cage. To construct echocardiographic images, the ultrasonic field from the transducer must be focused at the heart depth. Figure (III.9) shows a focused ultrasound field at heart depth. Figures (III.10, 11) show the field diagram pattern in x-z plane, and the concentration of the emitted energy at the focalized point.

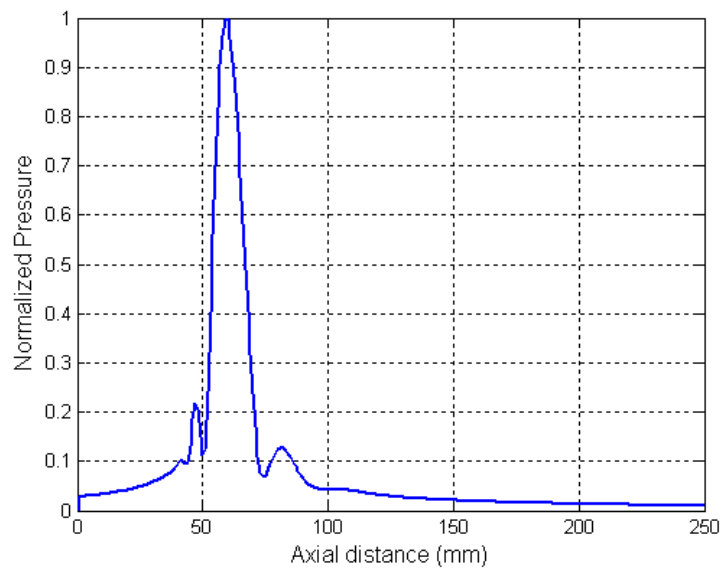


Figure III.9: Focused ultrasound field at 60mm (heart depth)

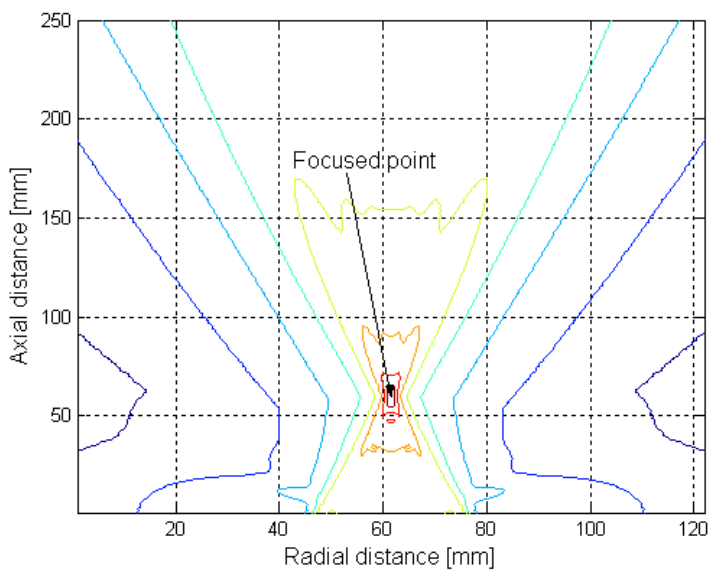


Figure III.10: Diagram pattern in *x-z* plane

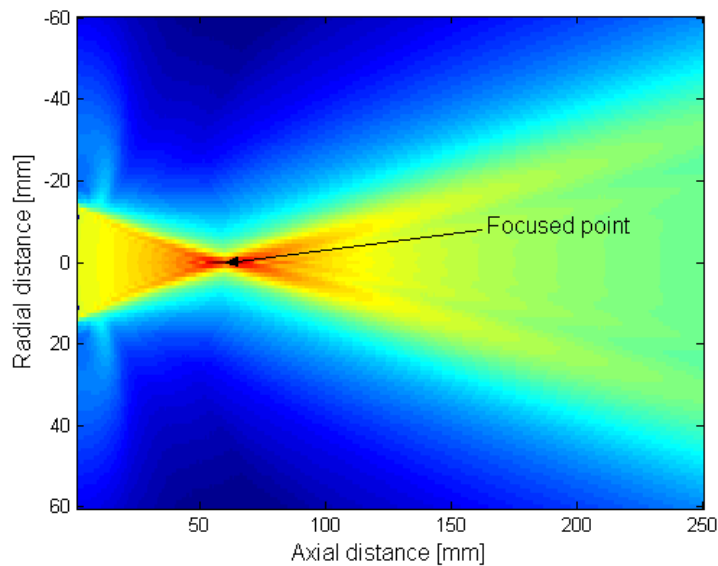


Figure III.11: Beam energy distribution for 60mm focused transducer

III.12 EXAMPLE OF B-MODE IMAGE



Figure III.12: Example of B-mode image (fetus of 22 week)

Chapter IV

Harmonic Ultrasound Imaging

Harmonic Ultrasound Imaging

IV.1 INTRODUCTION

An ultrasound imaging system includes transmitting ultrasound waves into a human body, collecting the reflections, manipulating the reflections, and then displaying them on computer screen as images. Traditionally ultrasound imaging operates in a linear mode. The standard approach is to use the fundamental frequency from the reflected signal to form images. However, it has been shown that images generated using the harmonic content have improved resolution as well as reduced noise, resulting in clearer images.

Until recently, the development of medical ultrasound operated under the implicit and convenient assumptions of infinitesimal acoustics where ultrasound waves were assumed to propagate in a linear fashion. Unfortunately, these assumptions became invalid at biomedical frequencies and intensities used nowadays. Today, it has been proven that ultrasound waves undergo gradual distortion in almost every medical use. The distortion is due to slight nonlinearities in sound propagation that gradually deform the shape of the wave, and results in development of harmonic frequencies, which were not present at the source. Selective imaging of these harmonic frequencies turned out to considerably improve ultrasound images. This technology called tissue harmonic imaging, which has emerged as a major imaging modality over the past years, exploits the generation of harmonic frequencies, called native harmonic signals, as ultrasound waves propagate through tissue. These nonlinear propagation effects have become of major interest in diagnostic ultrasound, by reducing unwanted artifacts in ultrasound images and, thus, enabling physicians to make more precise diagnoses than was possible before. Thus, the choice to use harmonic imaging to image tissue began as a result of recent experimentation in which it was unexpectedly seen that harmonics are generated when ultrasound waves travel through tissue.

Harmonic ultrasound imaging takes advantage of the fact that a finite amplitude acoustic waveform propagating through a medium gradually distorts. Among other effects, this results in greater attenuation losses, particularly in a tissue-like medium. In the past, the presence of harmonic signals was essentially ignored in the simple envelope detection schemes utilized in clinical scanner signal processing. Current harmonic image signal processing captures and displays as images the harmonic echo signals produced by these nonlinearly distorted pressure waveforms. Major recent improvements have been achieved in medical ultrasound imaging by exploiting the characteristics of nonlinear fields with the utilization of harmonic frequencies. Harmonic generation has been used to create images offering improvements over conventional B-mode images in spatial resolution, great penetration, and more significantly, in the suppression of acoustic clutter and side-lobe artifacts [44], [45].

IV.2 HARMONIC ULTRASOUND IMAGING

Harmonic ultrasound imaging is based on nonlinear acoustics, and is more difficult to model than conventional linear ultrasound imaging. Nonlinear phenomena were first described for biological tissues in the early 1980's [46]-[48]. Although there were several early attempts to measure and display nonlinear parameters of tissue, most of the early work in this area involved effects of nonlinear propagation on measurements of the output level of scanners.

Many diagnostic and therapeutic ultrasound systems employ excitations for which the small signal approximation is not valid. Although linear analysis of propagation is a good first order approximation, nonlinear effects are often non-negligible. Disturbances which are large enough to invalidate the small signal approximation are often referred to as finite amplitude waves. Finite amplitude wave propagation is a nonlinear process, and is a good deal more complicated than linear wave motion. A sound beam travelling through a medium will involve the effects of diffraction, absorption, and nonlinearity, and the sound beam can be thought of as interacting with itself as it propagates.

High amplitude sound waves often exhibit nonlinear effects, which linear acoustic theory cannot predict. In addition to the diffraction and attenuation effects

considered in linear acoustic theory, the nonlinearity of the media has to be taken into account.

Because sound waves behave nonlinearly, it is clear that frequencies other than the transmitted frequency are produced within a propagating sound wave. Thus, reflections from the sound wave at boundaries are also at harmonic frequencies, which are multiples of the fundamental frequency. Imaging that extracts the harmonic frequencies from a reflected signal and uses those for imaging is called harmonic imaging. Harmonic imaging is advantageous over the standard mode of imaging because images tend to have less noise and higher resolution, and consequently improved image clarity.

IV.3 BENEFITS OF HARMONIC IMAGING

Ultrasound imaging plays a vital role in modern medicine. Its applications are constantly expanding, with breakthroughs in ultrasound science and technology occurring every year. Linear and phased array are widely used in modern medical ultrasound imaging systems. They enable beams to be electronically steered and focused on both transmission and reception.

Harmonic imaging takes advantage of the fact that a finite amplitude acoustic waveform propagating through a medium gradually distorts. In medical ultrasound, the waveform distortion is encountered where intense sound beams are employed.

In the past, the presence of harmonic signals was essentially ignored in the simple envelope detection schemes utilized in clinical scanner signal processing. In contrast, current harmonic image signal processing captures and displays as images the harmonic echo signals produced by these nonlinearly distorted pressure waveforms.

A demonstrated advantage of harmonic imaging is a substantial reduction in acoustic noise resulting from reverberations and phase aberrations when the incident sound pulse penetrates the patient's body wall and tissue structure. Harmonic imaging results in cleaner images with greater contrast, particularly for large, overweight patients [38] [49].

IV.4 NONLINEARITY IN WAVE PROPAGATION

Effects due to the nonlinearity of the medium can be understood as a dependence of the speed of sound with temperature and pressure. The medium (water, tissue) is not a completely incompressible medium; the compression phase of acoustic wave will cause a local increase in pressure and temperature compared with the rarefaction phase (expansion) in where the temperature decreases. Locally, an increase in pressure and temperature causes an increase in the speed of sound. Thus, the compression phase of a wave travels faster than the rarefaction phase. Thus, this change in the temperature of the medium influences the propagation speed of sound. Indeed, the positive cycle of the wave propagates a bit faster than the negative cycle, leading to a slight deformation in the shape of the wave. This deformation accumulates with propagation distance and is more significant for high acoustic pressure. The waveform distortion is encountered in medical ultrasound where intense sound beams are employed.

The slope of a graph of pressure versus density, is thus not a straight line, but is rather a curve, where the local slope is proportional to the square of the speed of sound. The general propagation speed of sound can thus be written as [50]:

$$\frac{\partial p}{\partial z} = c_0 + \beta u \quad (\text{IV.1})$$

β is the parameter of nonlinearity. We will show in section (IV.5.2) that:

$$\beta = 1 + \frac{B}{2A} \quad (\text{IV.2})$$

Where first term (unity) is due to convection and the second term ($B/2A$) is a parameter related to the nonlinear relationship between pressure and density. In the case where u is very low, the speed of sound reduces to c_0 , the small signal speed. Convective and nonlinear effects can collectively be referred to as nonlinear effects, as both these effects will contribute a nonlinear term in the differential equations describing nonlinear propagation. These nonlinear effects can contribute to distortion of a given initial waveform. The compression phase of a sinusoid, for example, will have a propagation speed greater than that of the rarefaction phase, see figure (IV.2).

The sinusoid distorting in the process of nonlinear propagation transforms a monofrequency source at f_o , into an entire spectrum of harmonics, at f_o , $2f_o$, $3f_o$, $4f_o$... as shown in Figure (IV.1).

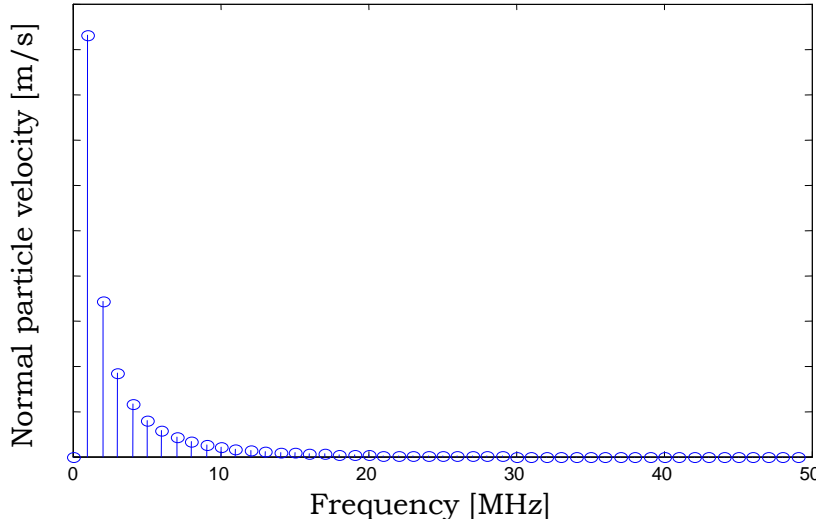


Figure IV.1: Spectrum of harmonics of a 1 MHz monofrequency source resulting from nonlinear propagation

IV.5 THEORY OF HARMONIC GENERATION

Harmonic generation results from the physics of sound waves and their interactions with the media through which they travel. As sound waves propagate through a medium, they compress and expand the medium. Sound waves travel at a faster speed in compressed regions than in expanded regions. Consequently, as an ultrasound wave propagates through a medium, the shape of the sinusoidal wave that was initially pulsed into the medium transforms. This transformation indicates that there is an introduction of harmonic information into the propagating ultrasound wave.

Thus, when treating sound waves as having finite amplitudes, the explanation for the nonlinear behavior of sound waves is quite simple. Ultrasound waves behave as pressure waves compressing and expanding the medium that they pass through with the compressed regions having increased density and the expanded regions having decreased density. The speed at which a wave propagates through a medium depends partly on the medium's density with waves traveling faster in denser media.

Consequently, the compressed regions of a medium propagate sound waves faster, and the expanded regions propagate sound waves slower. As a result, sound waves experience a gradual physical change of the shape of a sound wave similar to the one that is shown in Figure (IV.2), [51]:

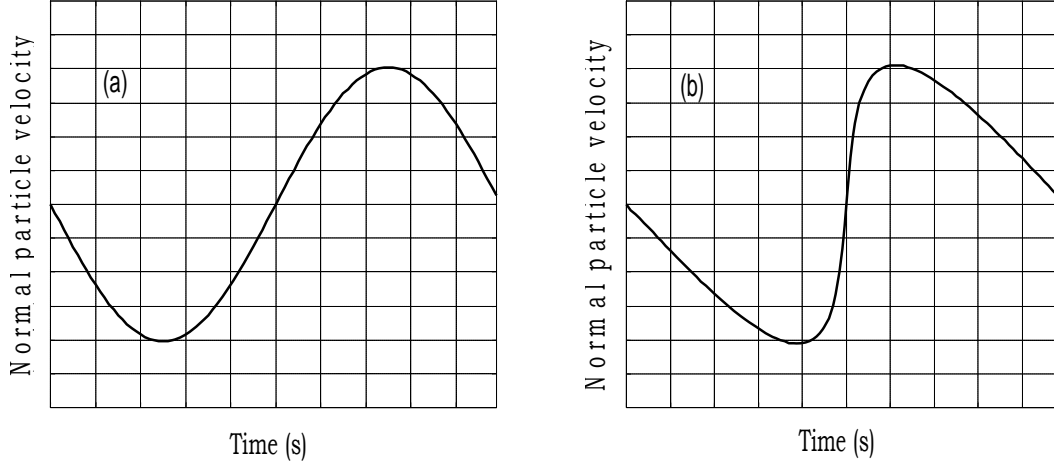


Figure IV.2: Effect of nonlinear distortion of a plane sinusoidal wave. (a) Initial waveform. (b) Showing the distortion of the initial wave after propagation

A linear propagation of the sound wave would mean that the transmitting wave would propagate in the physical shape shown in figure (IV.2.a). Thus, the physical change seen in figure (IV.2.b) indicates that there is a growing addition of harmonics to the propagating sound waves. In conclusion, we can say that all finite amplitude ultrasonic waves undergo a degree of nonlinear distortion when travelling through real media. This manifests itself in the frequency domain by the appearance of additional harmonic signals at integer multiples of the original excitation frequency, figure (IV.1).

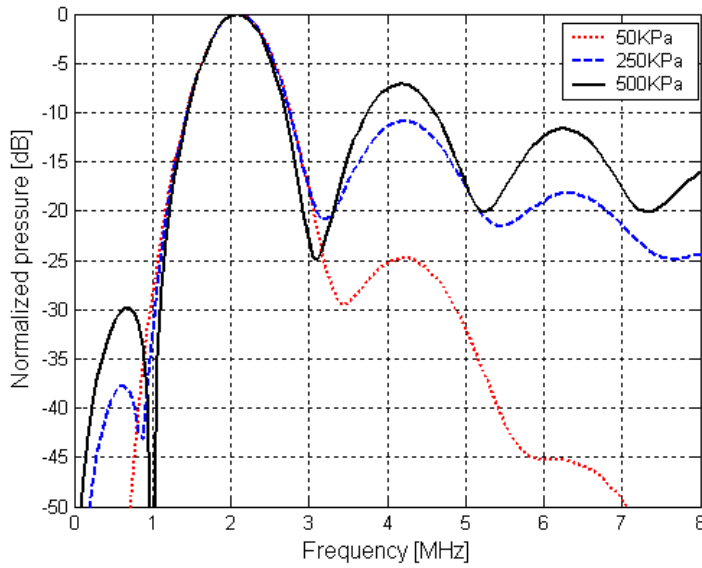


Figure IV.3: Effect of the excitation intensity over the harmonic generation

Figure (IV.3) shows the effect of the excitation intensity over the generation of the additional harmonics. The excitation frequency is of 2MHz, and the additional harmonics have amplitudes proportional to the excitation intensity.

IV.5.1 Variation of Wave Speed in a Wave

In linear sound theory, the speed of sound is assumed to be independent of the sound intensity. This assumption is valid only for low intensity sound waves. In Figure (IV.2), it is clear that the wavelength of the sound waves remains constant regardless of the degree of distortion occurring from point to point within the wave form. Thus, assuming a linear sound wave where the frequency of the sound wave remains constant during propagation, it makes sense that the speed of the sound wave should be the value determined by $v = \lambda \cdot f$. This speed is called c_0 . However, it is clear that the wave speed varies for different phases of the sound wave and this indicates that there is an addition of harmonics to the sound wave. Two non-linear factors contribute to the speed variation within the waveform. Firstly, convection affects individual particle behavior introducing the particle velocity u into the phase speed, and secondly, the relationship between pressure variation and density variation in a medium is nonlinear introducing a speed that depends on the

properties of the medium into the phase speed [51]. A shock wave is a very abrupt change in the pressure and particle velocity. For a plane wave travelling in a non-attenuating medium, a shock wave forms when the maximal slope of the wave becomes infinite.

The material nonlinearity results from nonlinearity in the equation of state, the relationship between pressure and density of the material. When compressed, the bulk compressibility of most materials decreases, making it progressively harder to compress them further. This effect causes the speed of sound to increase with increasing sound intensity. The rate of development of the second harmonic component is proportional to the square of the pressure amplitude of the propagating wave [52]. In a propagating sound wave, regions of high pressure correspond to regions of high particle velocity, so that:

$$c = c_0 + u + \frac{B}{2A}u = c_0 + \beta u \quad (\text{IV.3})$$

Where β is the coefficient of nonlinearity of the medium is, u is the particle velocity of a point in tissue, and (B/A) is a material constant.

As an initial step to development of the full 3-D nonlinear wave equations, consider the simple case of a finite amplitude plane wave of normal particle velocity u in a dissipationless medium. One peculiarity of nonlinear acoustics is that the propagation speed of a wave depends on the amplitude of excitation. While it is true that the beginning and end of a pulse propagate with the small signal speed c_0 , within the pulse, the propagation speed varies. The variation of propagation speed with initial amplitude is actually due to two separate effects: convection, and nonlinearity of the medium.

Convection effects can be thought of as being like an oscillating wind travelling with the wave. Overall, the oscillation propagates with small signal speed c_0 , however, the peak of the oscillation will also have a local particle velocity u above and beyond the wave velocity c_0 .

IV.5.2 Parameter B/A

The ratio B/A has its origin in the Taylor series expansion of the variations of the pressure in a medium in terms of variations of the density [53]. The

thermodynamic relationship between pressure and density is in general not a linear one. The pressure-density relation can be written as in equations (III.1) and (III.2). A Taylor series expansion can be done:

$$P_1 = \left. \frac{\partial p}{\partial \rho} \right|_0 \rho_1 + \left. \frac{1}{2!} \frac{\partial^2 p}{\partial \rho^2} \right|_0 \rho_1^2 + \dots = A \frac{\rho_1}{\rho_0} + \frac{B}{2!} \left(\frac{\rho_1}{\rho_0} \right)^2 + \frac{C}{3!} \left(\frac{\rho_1}{\rho_0} \right)^3 + \dots \quad (\text{IV.4})$$

$$A = \rho_0 \left. \frac{\partial p}{\partial \rho} \right|_0 = \rho_0 c_0^2, \quad B = \rho_0^2 \left. \frac{\partial^2 p}{\partial \rho^2} \right|_0, \quad C = \rho_0^3 \left. \frac{\partial^3 p}{\partial \rho^3} \right|_0 \quad (\text{IV.5})$$

The first order measure of nonlinearity, B/A , is the parameter of nonlinearity [50]. The coefficient of nonlinearity is defined as:

$$\beta = 1 + \frac{B}{2A} \quad (\text{IV.6})$$

Table (IV.1) shows some biomedical media and their corresponding (B/A) values. It should be noted that for a linear medium $\beta = 0$.

Biomedical medium	B/A value
Water	4.96
Whole blood	6.1
Nonfat soft tissues	6.3-8.0
Fatty soft tissues	9.6-11.3

Table IV.1: Media and their B/A values

Although a larger value of (B/A) indicates that a greater amount of harmonics are generated by a medium, it will be seen that this value is not sufficient in itself to indicate how effective harmonic imaging will be in a particular medium.

IV.5.3 Amount of Wave Distortion

Something further that can be seen in Figure (IV.2) is that sound wave distortion increases with time. This is because the effects of convection and the

nonlinearity of the pressure-density relation accumulate with propagation distance. More specifically, the distortion occurring at any location merely adds to any distortion that was already present [54]. The equation (IV.7) is a computation that allows for the amount of sound wave distortion to be discerned [51]:

$$\sigma = \beta \varepsilon k z \quad (\text{IV.7})$$

Where z is the distance the wave has traveled, ε is the Mach's number at the source, and k is the wave number. Thus, the amount of harmonics generated is linearly dependent on the distance the sound wave travels, the coefficient of nonlinearity, the pressure intensity at the source, and the excitation frequency. Furthermore, a medium with a higher (B/A) value results in richer amounts of harmonics. Since harmonic generation requires that the amplitude of the propagating wave be large enough, a larger acoustic pressure at the source contributes to larger amounts of harmonic generation.

IV.5.4 Goldberg's Number

The amount of harmonics generated can be viewed as a battle between two forces: harmonic generation arising from the nonlinear nature of sound waves and attenuation. Both of these values can be input into an equation from which the amount of harmonics can be estimated [51], [55]:

$$\Gamma = \frac{\ell_a}{\ell_d} \quad (\text{IV.8})$$

Γ is the Goldberg's number, ℓ_a is the absorption length, and ℓ_d is the distance at which a shock first forms in the absence of dissipation. The Goldberg's number indicates the importance of nonlinear effects relative to dissipative effects. It is used to characterize the relative influence of absorption and nonlinear effects. Values of the Goldberg number less than one signify that attenuation effects dominate the propagation of the wave form, equaling one signify that the contributions from the nonlinearity and attenuation are about equal, and exceeding one signify that the nonlinear effects dominate. This last case is desirable for harmonic imaging.

IV.5.5 Mechanical Index

The mechanical index (MI) is defined as the peak rarefactional (that is, negative) pressure, divided by the square root of the ultrasound frequency as:

$$MI = \frac{P_-}{\sqrt{f}} \quad (\text{IV.9})$$

Ultrasound scanners marketed in the USA are required by the Food and Drugs Administration (FDA) to carry an on-screen label of the estimated peak negative pressure to which tissue is exposed. In clinical ultrasound systems, this index usually lies somewhere between 0.1 and 2.0. Although a single value is displayed for each image, in practice the actual MI varies throughout the image. In absence of attenuation, the MI is maximal at the focus of the ultrasound beam [56]. The mechanical index is one of the most important machine parameters, it is usually controlled by means of the output power control of the scanner. Ultrasound scanners are required to carry an on-screen label of the estimated peak negative pressure to which tissue is exposed.

IV.6 EQUATION OF PROPAGATION

To identify limitations and domains of applicability associated with model equations of nonlinear acoustics, it is very important to understand the assumptions and ordering procedures on which the equations are based, and the need to understand the physical processes involved in the propagation of finite amplitude sound beams.

For nonlinear acoustics many developments and considerations were carried out on the basic equation of propagation before arriving to the Burgers model. The Burgers equation is the simplest model that describes the combined effects of nonlinearity and losses on the propagation of plane progressive sound waves. This derivation begins with high amplitude sound waves often exhibit nonlinear effects, which linear acoustic theory cannot predict. In addition to the diffraction and attenuation effects considered in linear acoustic theory, the nonlinearity of the media has to be taken into account. To understand nonlinear wave propagation, many analytical and numerical methods have been developed [38].

IV.6.1 Lossless Burgers Equation

Lossless Burgers equation is an equation which describes the propagation of a finite amplitude plane wave in a lossless fluid. The propagation of the plane wave in the positive z direction can be obtained by discarding the diffraction and absorption terms in the KZK equation as:

$$\frac{\partial P}{\partial z} = \frac{\beta}{2\rho_0 c_0^3} \frac{\partial P^2}{\partial t'} \quad (\text{IV.10})$$

Equation (IV.10) is often referred to as the lossless Burgers equation. The exact solution of equation (IV.10) for waves without shocks is [57]:

$$P = P_0 f(\varphi), \quad \varphi = t' + \frac{\beta P z}{\rho_0 c_0^3} \quad (\text{IV.11})$$

Where f is an arbitrary function. Equation (IV.11) which is referred to as Poisson solution indicates that wavelets with larger pressure amplitudes propagate faster than those with lower amplitudes. The differences in propagation speed result in distortion of the profile of the wave. The source waveform, however smooth initially, eventually steepens into a shock even if the source pressure amplitudes are very small excluding the case of pure expansion waves. The formation of shocks in the waveform is inevitable since viscosity and heat conduction, which exist in a real medium, are not taken into consideration in equation (IV.10). Figure (IV.2) above shows a distorting waveform.

IV.6.2 Burgers Equation

In the early 18th century, Poisson [58] predicted the shock and multi-valued wave formation from a plane wave in a lossless medium. Experimental development of the shock and multi-valued wave predicted by that theory is physically impossible, however, due to the effects of absorption in any real medium [38]. Later, the Burgers equation was developed for describing finite amplitude plane waves in a lossy thermoviscous fluid [59].

A real fluid exhibits thermoviscous absorption. This absorption, however small, prevents a waveform from becoming discontinuous. The equation which describes

the propagation of nonlinear progressive plane waves in a thermoviscous medium in the positive z direction is obtained by neglecting the diffraction term in the KZK equation as:

$$\frac{\partial P}{\partial z} = \frac{D}{2c_0^3} \frac{\partial^2 P}{\partial t'^2} + \frac{\beta}{2\rho_0 c_0^3} \frac{\partial P^2}{\partial t'} \quad (\text{IV.12})$$

Equation (IV.12) is the Burgers equation [59]. An integral solution of the Burgers equation is also obtained by transforming the nonlinear equation into a linear diffusion equation. Burgers equation can be solved by applying the spectral method as the case of many problems in nonlinear acoustics. The spectral methods for solving the Burgers equation are based on solutions of the Fourier series form as:

$$P = \sum_{n=-M}^M p_n(z) e^{jn\omega_0 t'} \quad (\text{IV.13})$$

Where p_n are the complex spectral amplitudes, and M is the number of harmonics retained in the expansion.

IV.6.3 Sound Beams and KZK Equation

The waveform distortion is encountered in medical ultrasound where intense sound beams are employed. When an acoustic source of finite size radiates into free space, the effects of diffraction must be considered. The KZK (Khokhlov, Zabolotskaya, and Kuznetsov) nonlinear parabolic wave equation is known to describe very accurately the propagation of a finite amplitude sound beam by including, to the lowest order, the combined effects of diffraction, absorption, and nonlinearity. Zabolotskaya and Khokhlov derived the lossless of the KZK equation (sometimes called KZ equation), and Kuznetsov subsequently included the effect of thermoviscous absorption [60]-[62].

The KZK equation which models the ultrasound propagation in the z direction for a finite source in the x - y plane is given by:

$$\frac{\partial^2 P}{\partial z \partial \tau} = \frac{c_0}{2} \nabla_T^2 P + \frac{\delta}{2c_0^3} \frac{\partial^3 P}{\partial \tau^3} + \frac{\beta}{2\rho_0 c_0^3} \frac{\partial^2 P^2}{\partial \tau^2} \quad (\text{IV.14})$$

∇_T^2 is the Laplacian in the plane perpendicular to the axis of the beam and it is given by:

$$\nabla_T^2 = \frac{\partial^2}{\partial x^2} + \frac{\partial^2}{\partial y^2} \quad (\text{IV.15})$$

P is the sound pressure, z is the axis of propagation, $\tau = t - z/c_0$ is the retarded time, c_0 is the speed of sound, δ is the diffusivity of sound corresponding to thermoviscous absorption, ρ_0 is the ambient density of the medium, and β is the coefficient of nonlinearity. For circular sources (axisymmetric beams), the operator ∇_T^2 is given by:

$$\nabla_T^2 = \frac{\partial^2}{\partial r^2} + \frac{1}{r} \frac{\partial}{\partial r} \quad (\text{IV.16})$$

The first term on the right side of equation (IV.14) represents diffraction, the second term accounts for thermoviscous attenuation (absorption) and the third term accounts for nonlinearity.

The KZK equation describes accurately the propagation of sound fields produced by directive sound sources. However, since this equation is based on a parabolic approximation, its accuracy is limited to distances beyond a few source radii and in a region close to the axis of the transducer [63].

IV.7 MODELING OF NONLINEAR MEDICAL ULTRASOUND

All finite amplitude ultrasonic waves undergo a degree of nonlinear distortion during propagation through real media [64]. This manifests itself in the frequency domain by the appearance of new harmonic signals at integer multiples of the transmitted frequency. Since the medium (water, tissue) is not completely incompressible medium,

Nonlinear effects have many applications and implications for medical ultrasound imaging. Harmonic imaging quickly became routine practice in the ultrasound clinic because of its improved image quality compared to conventional imaging [65]. For the design and engineering of new technologies and techniques that exploit the nonlinear properties of the ultrasound field, it is primordial to be able to model the physical process with sufficient accuracy. Doing this, we can predict the

consequences of certain design choices before we try to implement them and therefore the cost of design of new instrumentation can be reduced significantly.

For the design and engineering of new technologies and techniques that exploit the nonlinear properties of the ultrasound field it is primordial to be able to model the physical process with sufficient accuracy. This can predict the consequences of certain design choices before their implementation. Many attempts have been undertaken in literature to obtain an accurate model of the acoustic beam of medical transducers and the nonlinear effects playing a role in it. Up to now, most of the models are based on the KZK equation. This is a parabolic approximation of the Westervelt equation, which describes the ultrasound field in a thermoviscous fluid, thereby including the largest loss and nonlinear terms [3].

IV.7.1 Medium Under Consideration

For medical ultrasound applications, the acoustic field propagates through the human body, and therefore it would be appropriate to use the human tissue as the medium when modeling the ultrasound propagation. We should account for the different layers in the tissue, like the skin, fat layers and muscle layers. In the development of echographic instrumentation it is common use to start with water as the medium. The use of these measurements in water to predict the fields in tissue is called derating, and there have been proposed several tissue models for this purpose [3]. These models work well for situations where linear theory applies. However, for the investigation of nonlinear effects, extrapolation of water data to tissues becomes much more complex. Using water, the medium can be considered homogeneous and isotropic. We can still use it as a first approach for the development of a good model for nonlinear acoustic effects, but the step from tissue to water cannot be made without some caution. Table (IV.2) shows some constants for water ($T = 20^\circ\text{C}$, $P = 1 \text{ Bar}$) [66]-[68].

Parameter	Symbol	Value
density	ρ_0	$0.9982 \times 10^3 \text{ Kg/m}^3$
Parameter of nonlinearity	B/A	5
Small-signal sound speed	c_0	$1.482 \times 10^3 \text{ m/s}$
Shear viscosity	η	$1.002 \times 10^{-3} \text{ Kg/ms}$
Dilatational viscosity	η'	$2.815 \times 10^{-3} \text{ Kg/ms}$
Adiabatic compressibility	κ_s	$5.559 \times 10^{-10} \text{ Pa}^{-1}$
Isothermal compressibility	κ_T	$4.591 \times 10^{-10} \text{ Pa}^{-1}$
Thermal conductivity	σ_T	0.5984 J/Kms
Heat capacity at constant pressure	c_p	$4.182 \times 10^3 \text{ J/Kg K}$
Heat capacity at constant volume	c_v	$4.153 \times 10^3 \text{ J/Kg K}$

Table IV.2: List of constants for water

IV.7.2 Nonlinear Numerical Methods

Harmonic imaging is based on nonlinear acoustics, and is more difficult to model than conventional linear ultrasound imaging. Nonlinear phenomena were first described for biological tissues in the early 1980's [38], [46]-[48]. Although there were several early attempts to measure and display nonlinear parameters of tissue, most of the early work in this axis involved effects of nonlinear propagation on measurements of the output level of probes.

Pressure waveforms from diagnostic ultrasound devices undergo substantial distortion during propagation. High amplitude ultrasound waves often exhibit nonlinear effects, which linear acoustics theory cannot predict. In addition to the diffraction and attenuation effects considered in linear acoustic theory, the nonlinearity of the medium of propagation must be taking into account [69], [70]. Many numerical methods have been developed in the literature to solve the generalized nonlinear process in both frequency and time domain [71]-[74]. Hybrid methods were also used when an inefficiency of one method or another is noticed [75], [76]. Quasilinear analytical solutions have been developed for cases in which

the nonlinearity is weak. Quasilinear solutions assume the pressure field consists of a fundamental pressure field describes by linear theory along with the second harmonic added as a small correction. The second harmonics are assumed to be weak, and thus, do not generate further higher order harmonics. Thus, quasi-linear theory does not describe the higher order harmonics that are produced by an intense acoustic source [38]. Quasilinear theory is not suitable when the nonlinearity is strong or the higher order harmonics are of interest. Therefore, numerical methods must be developed to solve the full nonlinear models for these cases.

IV.7.3 Finite difference Analysis for Ultrasound Modeling

In many engineering problems, either the structure geometry is complicated or some critical material properties and behaviors are not uniform. Thus, an analytical solution can not be found, or involves too many simplifying assumptions, which degrade the accuracy of the resulting solutions. In these situations, numerical analysis provides an alternative solution for many engineering problems.

Finite difference is a numerical analysis technique that obtains piecewise approximate solutions for many engineering problems. It divides the structure in problem into a large number of small regions. Finite difference Analysis provides an approximation solution of the general governing equations at all the nodes. It has higher accuracy as the density of grid points increases. Finite difference is capable to handle extraordinary complex three dimension device geometries.

It was widely accepted by engineering from structural analysis of airplanes or bridges to heat conduction, fluid mechanics, and even transient, highly nonlinear investigations of weapons. It has been many years since the finite difference analysis method was introduced into acoustic engineering areas. Finite difference was frequently used for ultrasound transducer designing, modeling, optimization, as well as ultrasound energy propagation and acoustic field investigations.

IV.8 NUMERICAL SOLUTION OF KZK EQUATION

The KZK equation can be solved like several problems in nonlinear acoustics by applying the spectral method which based on solutions of the Fourier series. Aanonsen and Coworkers [73] sought a solution of the KZK equation in terms of sine and cosine series as:

$$P = p_0 \sum_{n=1}^M g_n(r, z) \sin n\omega_0 t' + h_n(r, z) \cos n\omega_0 t' \quad (\text{IV.17})$$

The resulting coupled sets of partial differential equations are solved by finite difference methods or others. The KZK equation can be solved in a number of ways using time domain, frequency domain, or combined time-frequency domain algorithms. All of the approaches are based on the time-integral of the KZK equation in retarded time [80].

In the present thesis, a time-domain numerical algorithm for solving the KZK (Khokhlov-Zabolotskaya-Kuznetsov) nonlinear parabolic wave equation is used for pulsed, finite amplitude sound beams in thermoviscous fluids. The time domain algorithm is used to investigate waveform distortion and shock formation in directive sound beams radiated by pulsed circular piston sources. The algorithm is developed mainly for sound beams radiated by unfocused sound sources, and it is modified to facilitate calculation for focused sources. For unfocused beams, a coordinate transformation is applied to the KZK equation to improve the computational efficiency in the farfield. The transformed coordinate system provides a geometry that follows the eventual spherical spreading of the beam [81]. With or without the transformation, the KZK equation has three individual terms, which account for diffraction, absorption, and nonlinearity. The equation is solved sequentially, at each range step, as follows: first the diffraction term, then the absorption term, and finally the nonlinear term. The diffraction term is integrated with a finite difference method in space and a trapezoidal rule in time. Energy dissipation that accompanies propagation over the same distance is then included by integrating the absorption term with a finite difference method in time. Finally, nonlinearity is included. The simulation is able to determinate the ultrasound field at any point in space and gives information about localized maximum and minimum energy produced by the transducer. Figure (IV.4) shows these computational

procedures in terms of the axial coordinate z . Although the three effects are included independently over each increment in space, the use of sufficiently small steps preserves the mutual interactions.

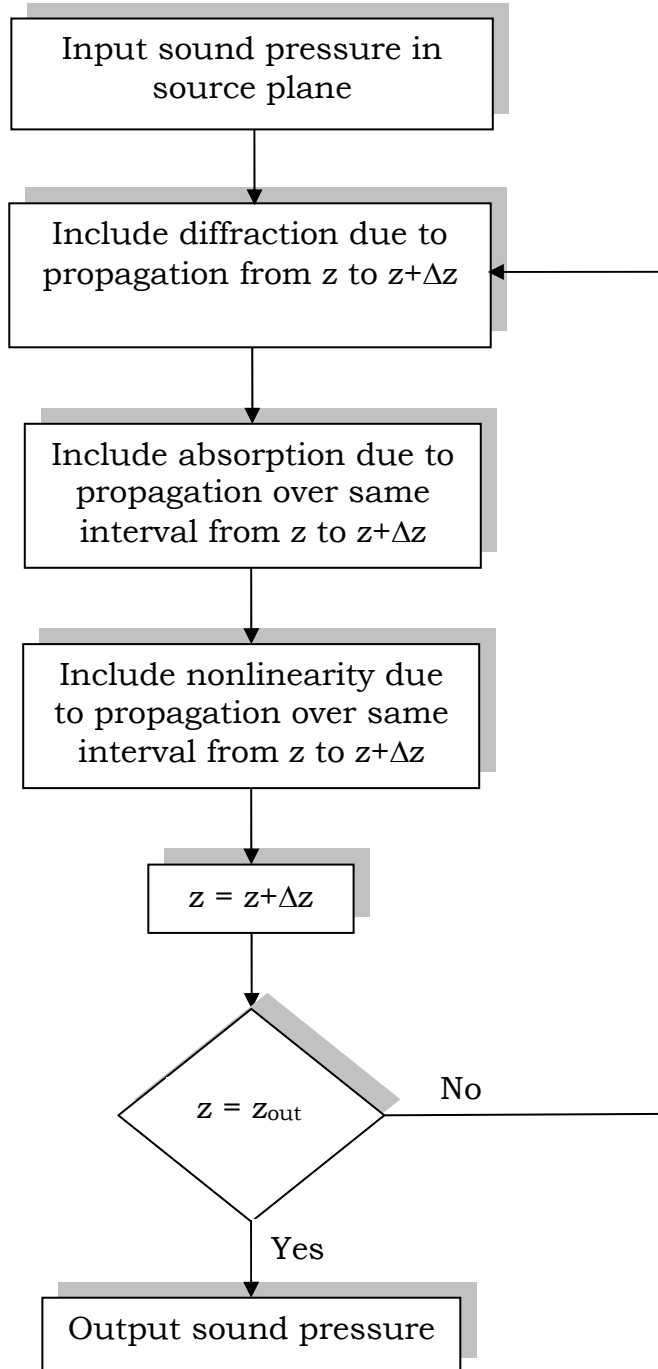


Figure IV.4: Computational procedure in terms of axial coordinates z

IV.8.1 Boundary Conditions

We begin with the transformation with the following variables:

$$\sigma = \frac{z}{z_0} \quad (\text{IV.18})$$

$$\rho = \frac{r/a}{1+\sigma} \quad (\text{IV.19})$$

$$\tau = \omega_0 t - \frac{(r/a)^2}{1+\sigma} \quad (\text{IV.20})$$

$$P = \frac{(1+\sigma)p}{p_0} \quad (\text{IV.21})$$

Here a the characteristic radius of the source, σ is a dimensionless range coordinate in terms of the Rayleigh distance $z_0 = \omega_0 a^2 / 2c_0$ at the characteristic angular frequency ω_0 , ρ is the dimensionless transverse coordinate, τ is a dimensionless retarded time, and p_0 is a characteristic source pressure amplitude.

For $\sigma \gg 1$, ρ is proportional to $\tan \theta = r/z$, where θ is the angle with respect to the axis of the beam, i.e.,

$$\tan \theta = \frac{2}{ka} (1 + \sigma^{-1}) \rho \sim \frac{2\rho}{ka} , \quad \sigma \gg 1 \quad (\text{IV.22})$$

The transverse coordinate ρ thus provides the proper geometry for the spherically radially spreading sound in the farfield. For $\sigma \gg 1$, τ reduces to $\omega_0(t - z/c_0 - r^2/2c_0 z)$, for which a surface of constant phase describes, within the parabolic approximation, a sphere centered at the origin $(r, z) = (0, 0)$.

The time coordinate τ is therefore convenient for tracking pulses that are localized in time, so that time windows of reasonable length can be used to encompass pulses at off-axis points in the numerical computations. The transformed dimensionless pressure P has the spherical spreading factor $1/z$ factored out.

Figure (IV.5) shows the finite difference grids in the (a) transformed and (b) untransformed coordinate systems. A rectangular region in the transformed coordinate system corresponds to an expanding region in the original, untransformed coordinate system. Note that the axial step sizes increases with

distance from the source. Smaller axial step sizes are required in the nearfield of piston sources, where the sound pressure exhibits a highly oscillatory behavior, and therefore high spatial resolution is needed. In the farfield, where the nearfield oscillations have disappeared and the sound exhibits properties of spherical wavefields, larger step sizes can be used in order to reduce computation time. Note also that a constant transverse step size $\Delta\rho$ in the transformed coordinate system corresponds to a transverse step size Δr that increases with z in the untransformed coordinate system. Less transverse resolution is needed in the farfield, where the sound beam has a nominally constant angular distribution.

The KZK equation for an axisymmetric sound beam that propagates in the positive z direction can be written in terms of the acoustic pressure P as following [60]:

$$\frac{\partial^2 P}{\partial z \partial t'} = \frac{c_0}{2} \left(\frac{\partial^2 P}{\partial r^2} + \frac{1}{r} \frac{\partial P}{\partial r} \right) + \frac{D}{2c_0^3} \frac{\partial^3 P}{\partial t'^3} + \frac{\beta}{2\rho_0 c_0^3} \frac{\partial^2 P^2}{\partial t'^2} \quad (\text{IV.23})$$

Here $t' = t - z/c_0$ is the retarded time variable, t is the time, c_0 is the small signal sound speed, $r = \sqrt{x^2 + y^2}$ is the radial distance from the z axis, $\partial^2/\partial r^2 + (1/r)\partial/\partial r$ is the transverse Laplacian operator, and ρ_0 is the ambient density of the medium. Furthermore, $D = \rho_0^{-1}[(\zeta + 4\eta/3) + \kappa(1/c_v - 1/c_p)]$ is the sound diffusivity of a thermoviscous medium, where ζ is the bulk viscosity, η the shear viscosity, κ the thermal conductivity, and c_v and c_p the specific heats at constant volume and pressure, respectively [83]. The coefficient of nonlinearity is defined by $\beta = 1 + B/2A$, where B/A is the parameter of nonlinearity of the medium [50]. In the derivation of the equation (IV.23), the sound waves are assumed to be collimated about the z axis, and local nonlinear effects due to finite source displacement are ignored. The first term on the right-hand side of equation (IV.23) accounts for diffraction, the second term for absorption, and the third term for nonlinearity [71].

The time-domain numerical algorithm is developed on the basis of the following equation:

$$\frac{\partial P}{\partial z} = \frac{c_0}{2} \int_{-\infty}^{t'} \left(\frac{\partial^2 P}{\partial r^2} + \frac{1}{r} \frac{\partial P}{\partial r} \right) dt'' + \frac{D}{2c_0^3} \frac{\partial^2 P}{\partial t'^2} + \frac{\beta}{2\rho_0 c_0^3} \frac{\partial P^2}{\partial t'} \quad (\text{IV.24})$$

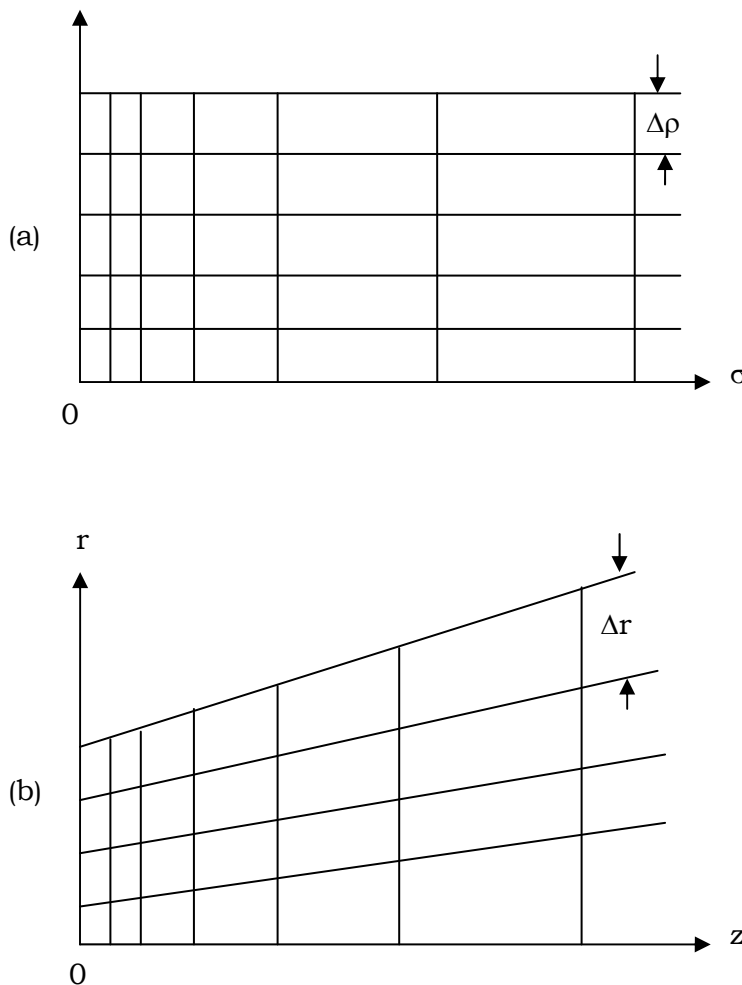


Figure IV.5: Finite difference grids in (a) transformed and (b) untransformed coordinate systems

For unfocused sound beams, it is advantageous to use transformed coordinates that follow the eventual spherical spreading of the beam when computing the farfield of the diffracting sound beam.

IV.9 SIMULATION RESULTS USING CIRCULAR TRANSDUCER

The simulations are realized for both the two cases: low excitation pressure intensity, and high excitation pressure intensity in the aim to show the effect of this last. The simulations are realized for a focalized piston.

IV.9.1 Low Excitation Intensity

Figure (IV.6) shows an excitation of ($P=50$ Kpa, $f=2$ MHz, length=3 cycle), and its corresponding spectra. However, the distortion of the excitation waveform due to nonlinear propagation is no consequent, and only one additional harmonic, which appears at double of the excitation frequency is created, see figure (IV.7).

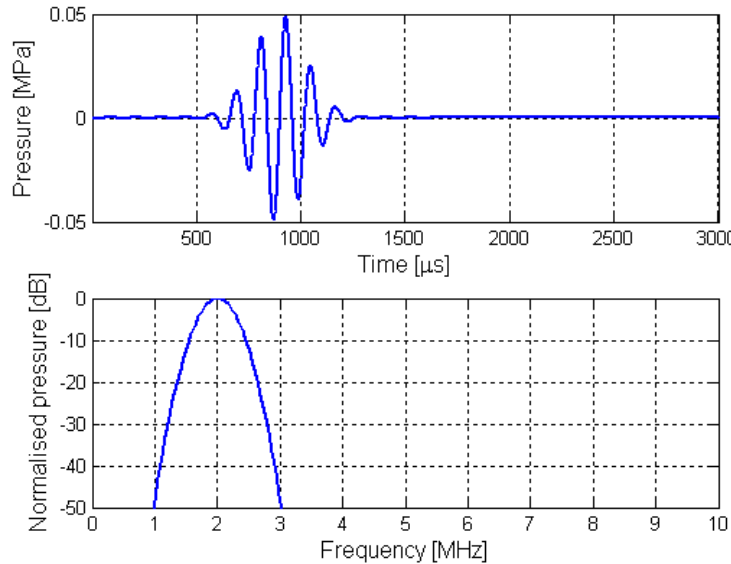


Figure IV.6: Waveform at transducer plane (top), and corresponding spectra (bottom)

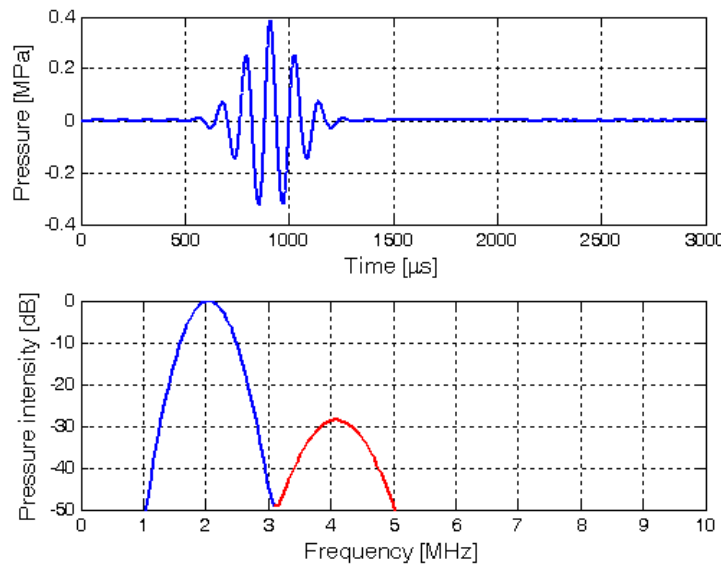


Figure IV.7: Waveform at focal depth distance (top), and corresponding spectra (bottom)

Figure (IV.8) shows a low axial pressure level of the created second harmonic, whereas in harmonic imaging application, a high second harmonic level is highly recommended.

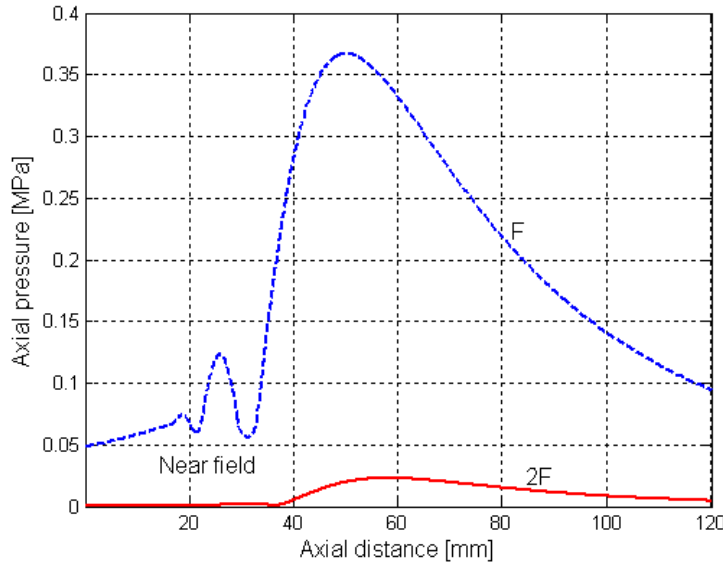


Figure IV.8: Axial pressure: fundamental component (dashed), and second harmonic component (solid)

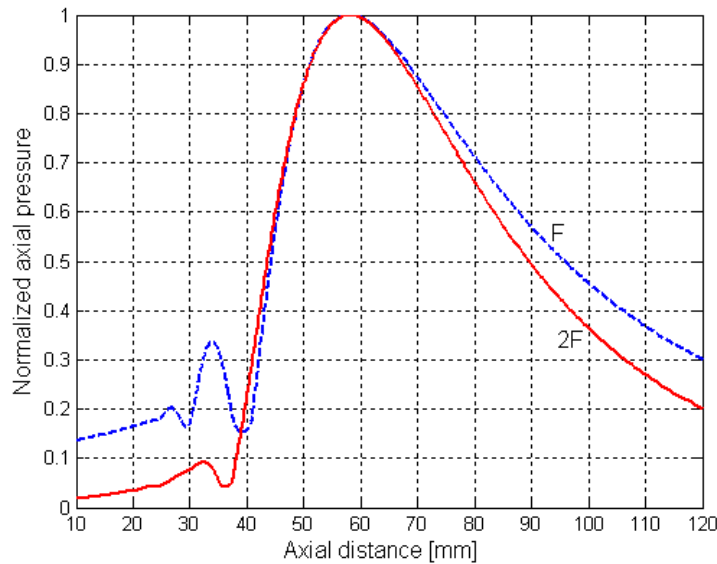


Figure IV.9: Normalized axial pressure: fundamental component (dashed), and second harmonic component (solid)

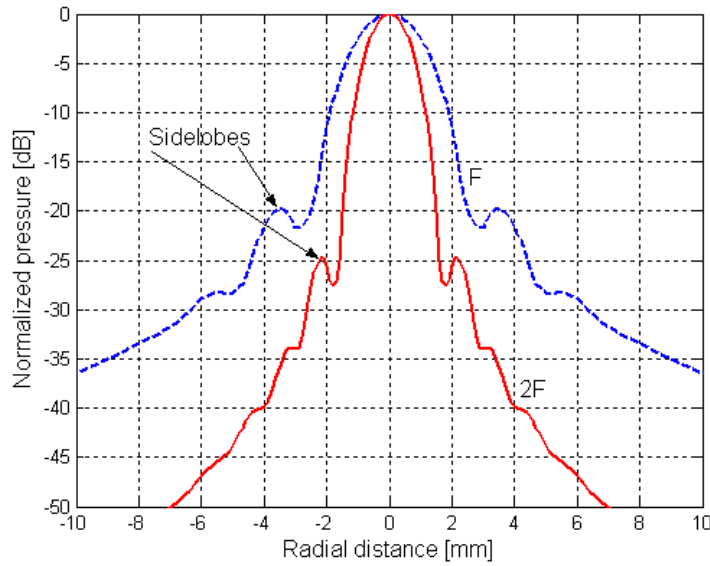


Figure IV.10: Radial pressure: fundamental component (dashed), and second harmonic component (solid)

The radial second harmonic field is presented in figure (IV.10) as solid line. The figure shows that the second harmonic component is narrower than the fundamental. This means that the second harmonic image has a good lateral resolution than the fundamental one. In addition, second harmonic component presents lower level of sidelobes, and consequently the second harmonic image presents fewer artifacts.

IV.9.2 High Excitation Intensity

The use of high intensity ultrasound in medical applications has considerably increased in recent years in addition of harmonic imaging. Nonlinear effects have become especially important at the acoustic intensity employed in lithotripsy, ultrasonic hyperthermia, or cavitation-induced tissue destruction [84]. Figure (IV.11) shows an excitation of ($P=500$ Kpa, $f=2$ MHz, length=3 cycle), and its corresponding spectra. In this case, the distortion of the excitation waveform due to nonlinear propagation is consequent, and a succession of additional harmonic appeared at integer multiples of the original excitation frequency, see figure (IV.12). Thus, the appearance of additional harmonic signals depends not only on nonlinear

propagation, which depends on medium characteristics, but also on the excitation pressure intensity.

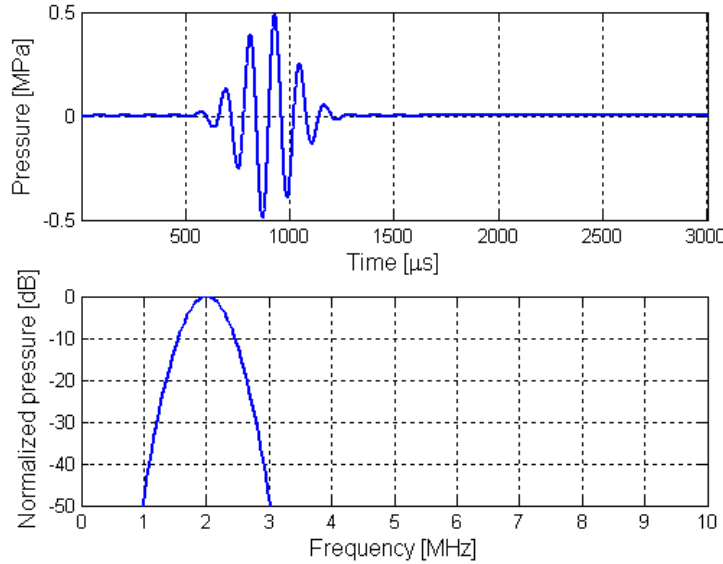


Figure IV.11: Waveform at transducer plane (top), and corresponding spectra (bottom)

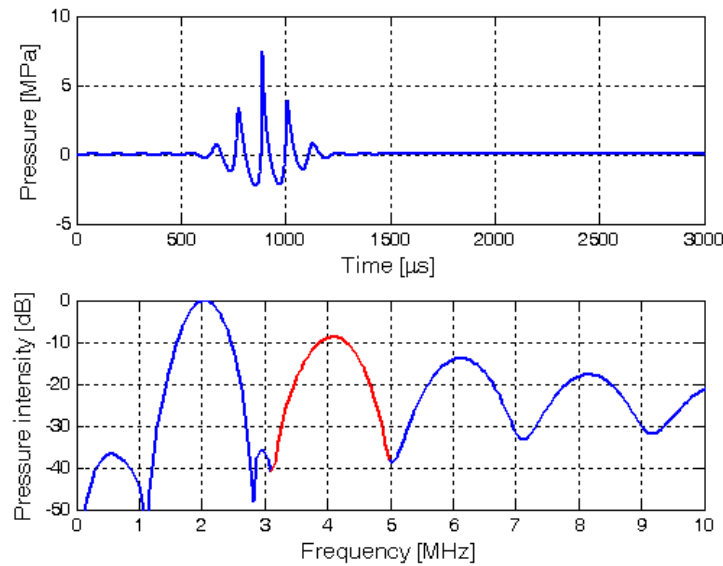


Figure IV.12: Waveform distortion at focal depth distance (top), and corresponding spectra (bottom)

Consequent excitation pressure intensity implies a consequent axial pressure level of the created second harmonic, figure (IV.13).

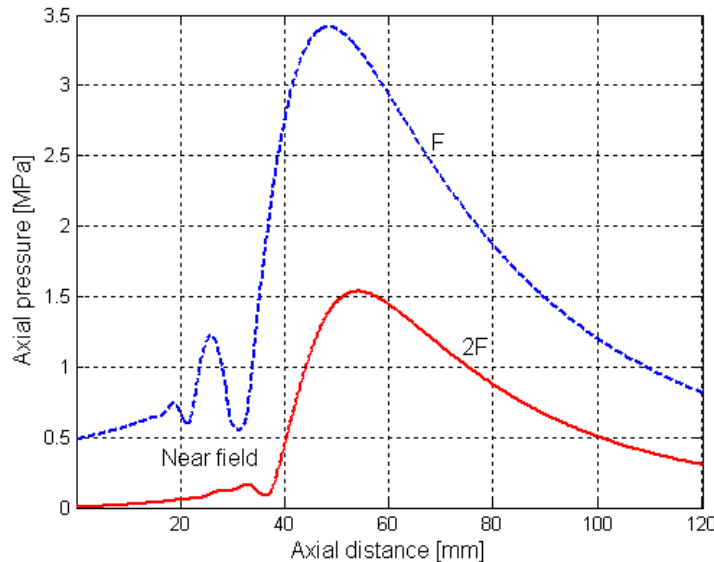


Figure IV.13: Axial pressure: fundamental component (dashed), and second harmonic component (solid)

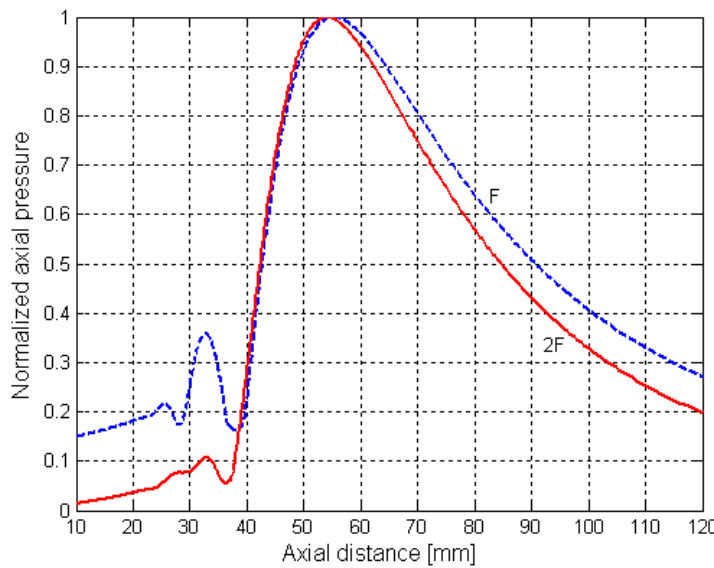


Figure IV.14: Normalized axial pressure: fundamental component (dashed), and second harmonic component (solid)

Second harmonic signal presents a relatively narrower beamwidth, and lower level at nearfield than the fundamental component, figures (IV.14, 9). This, led respectively to an improvement in axial resolution, and less in artifacts and reverberations of the resulting ultrasound image, see also figure (IV.16). Figure (IV.15) shows narrower second harmonic component with lower sidelobes levels in high intensity excitation, this explains a better lateral resolution and fewer artifacts in second harmonic resulting image.

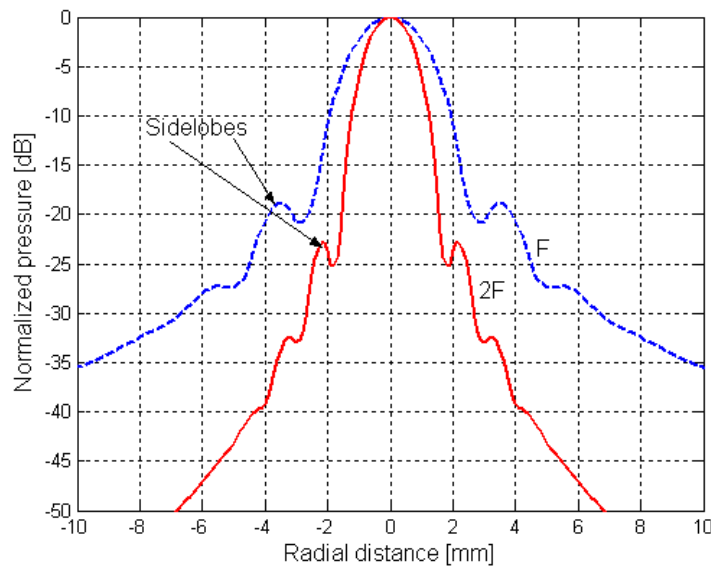


Figure IV.15: Radial pressure: fundamental component (dashed), and second harmonic component (solid)

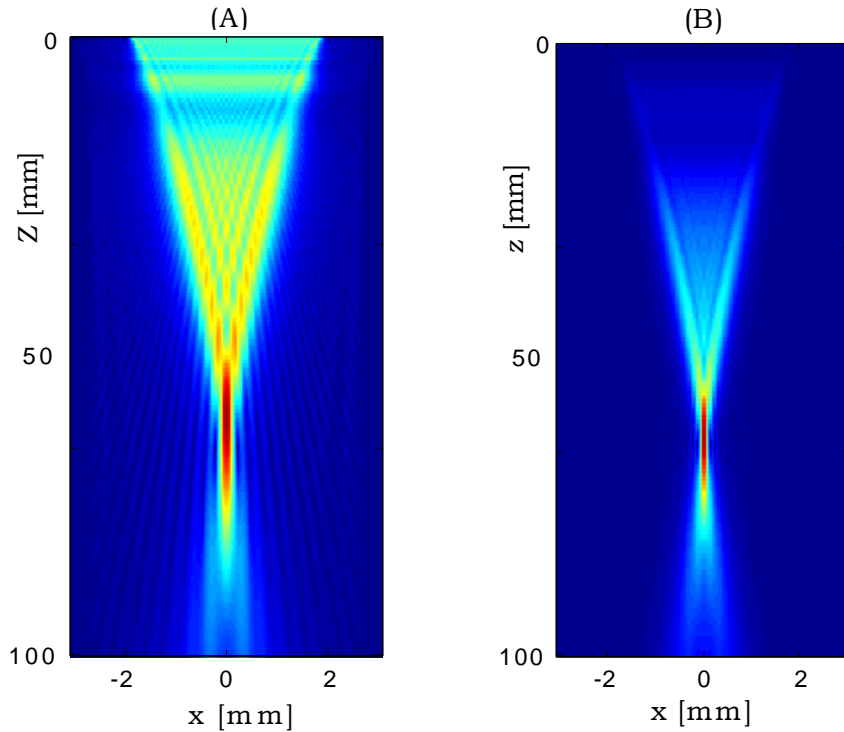


Figure IV.16: Focalized axial pressure field pattern: fundamental component (A), and second harmonic component (B).

IV.10 GRATING LOBES

Grating lobes, which are sound waves that get transmitted from the transducer at angles other than that of the ultrasound wave, are also source of reverberations and artifacts in ultrasound image. Figure (IV.17) shows grating lobes pattern of fundamental and second harmonic components in which, and another time, the second harmonic ultrasound imaging proves better quality than the conventional imaging.

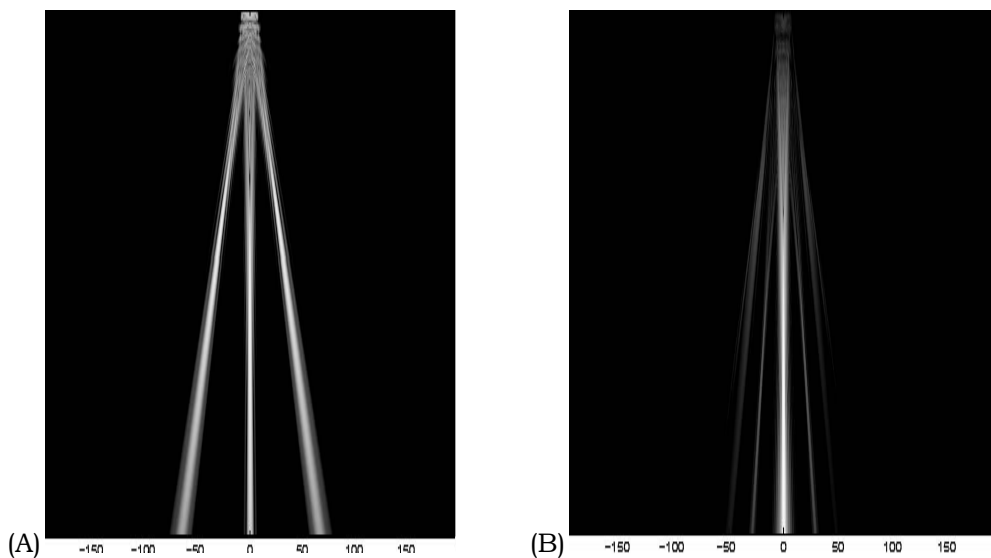
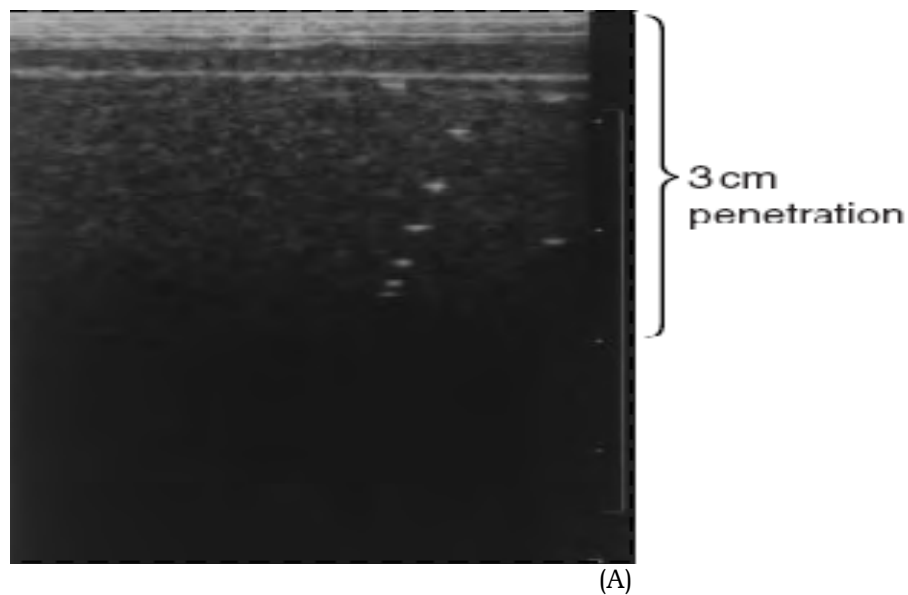


Figure IV.17: Grating lobes pattern: Fundamental component (A) and second harmonic component (B) [84_2]

IV.11 PENETRATION

The ultrasound second harmonic pressure field presents the advantage of greater depth of penetration than the fundamental component, see figure (IV.18).



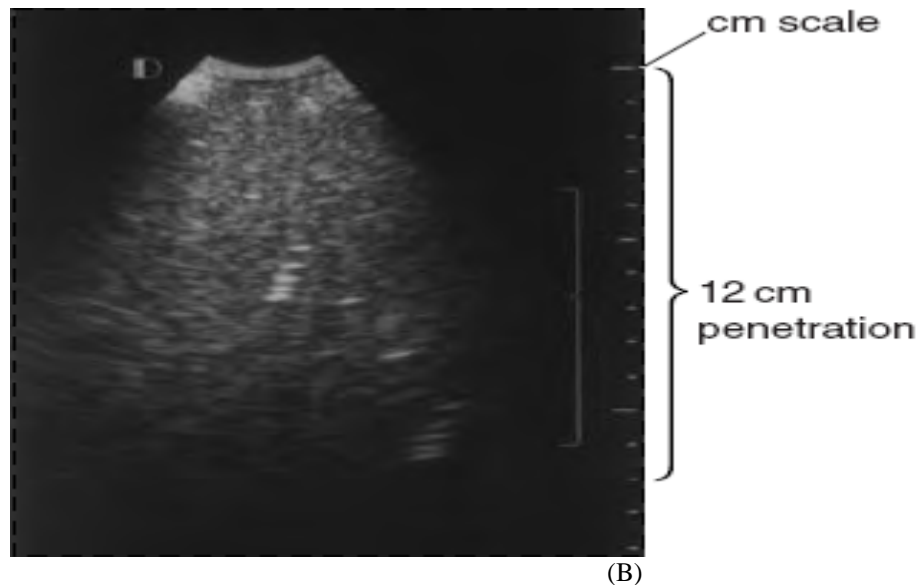


Figure IV.18: Illustration of difference in penetration between fundamental (A) and second harmonic (B) ultrasound pressure fields

IV.12 EXAMPLE OF COMPARATIVE IMAGES

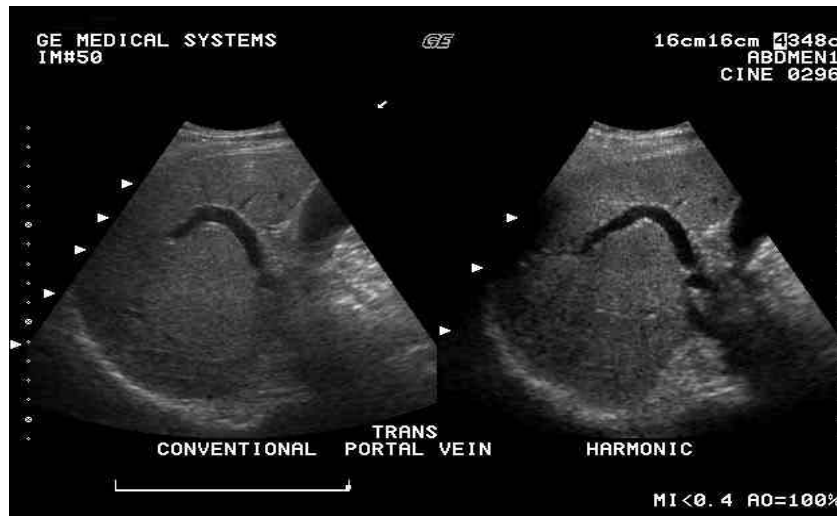


Figure IV.19: Clinic images Liver and Portal vein: note the improvement in penetration and contrast resolution with second harmonic imaging (*)

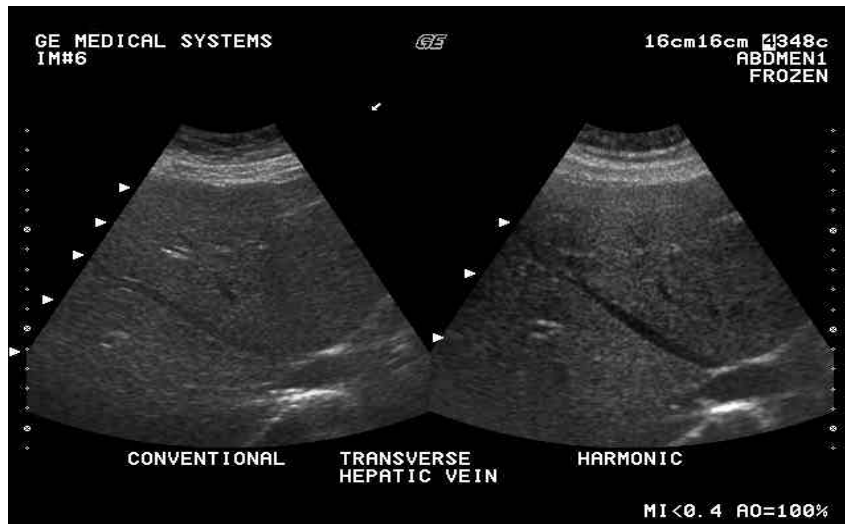


Figure IV.20: Clinic images Liver and hepatic veins: note the improvement in cystic clearing in this vessel with second harmonic imaging (*)

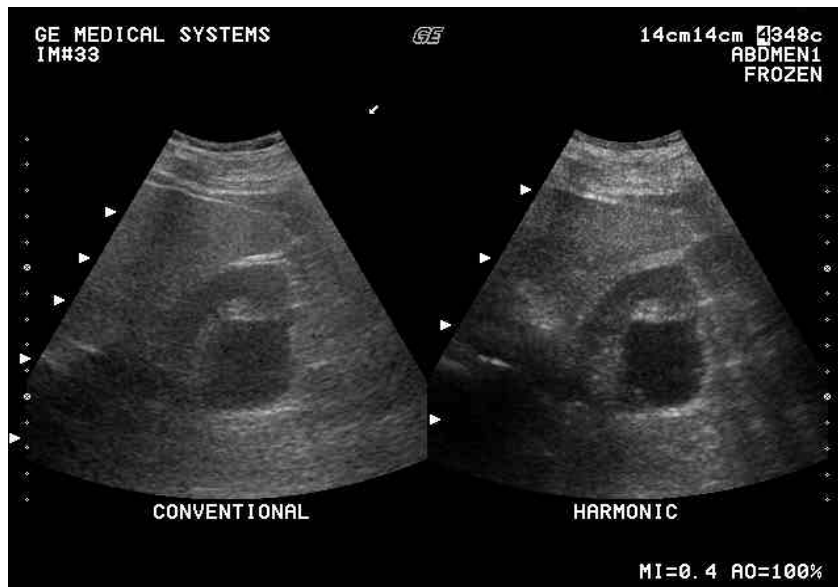


Figure IV.21: Large renal cyst: note the improvement in contrast resolution that is achieved with the improved slice thickness available with second harmonic imaging (*)

(*) images from GE medical systems, **ultrasound technology update** review

Chapter V

Optimization of Harmonic Imaging

Optimization of Harmonic Imaging

V. 1 INTRODUCTION

Major improvements have been achieved recently in medical ultrasound imaging by exploiting the characteristics of nonlinear fields with the utilization of harmonic frequencies. Harmonic generation has been used to create images offering improvements over conventional B-mode images in spatial resolution, and more significantly, in the suppression of acoustic clutter and side-lobe artifacts. The second harmonic beam generated at two times of the transmit frequency provide greater depth of penetration, greater resolution, and information content in the images. When these harmonics are not present in the transmitted pulse, they are mostly caused either by nonlinear propagation of the sound wave in the tissue or by the presence of a medium that is capable of reflecting the transmitted energy in nonlinear manner. In ultrasound imaging, an ongoing problem is that undesired signals are contained in the reflected waves, and that corrupt the image data.

When evaluating the performances of an ultrasound imaging system, knowledge of the bandwidth is essential. Knowledge of the system bandwidth (transmitted bandwidth, received bandwidth, their variation, and overlap between them) is the subject of the present chapter which leads to such system quality.

Harmonic received frequency band must not contain components from transmit frequency band, and its components must sufficiently be separable from fundamental spectral component. Thus, in harmonic imaging the corresponding band must be clearly received. Spectral overlapping in transmission between the fundamental and the second harmonic components must be minimal even null to avoid the transmission of the frequential component with $2f_0$ (f_0 is the transmitted frequency), and consequently the contamination of the harmonic component, and the obtained image.

In second harmonic imaging it is essential to avoid receiving any spectral component around transmitted frequency (f_0) which can contaminate the harmonic band around the received frequency ($2f_0$), and consequently the contamination of the obtained image. Therefore, to effectively employ the information contained in the second harmonic of the received signal, this information should be properly extracted. As a consequence, several imaging modalities and techniques have been developed during the last decade, which are intended to acquire and process the harmonic information, or even to separate one kind of such information from another [55], [85]-[90]. In this chapter, a new technique for acquiring the proper second harmonic signal is presented. An optimization of the transmitted bandwidth is recommended to receive the purely second harmonic signal for harmonic imaging [91].

V.2 IMAGE FORMATION IN TISSUE HARMONICS

Tissue harmonic imaging operates by transmitting a fundamental beam that has a lower frequency. This fundamental pulse, as it propagates through tissue inside the body, generates the higher frequency harmonic sound. The key to understanding tissue harmonic imaging is that the image is formed only from the higher frequency harmonic sound. Echoes from the fundamental frequency are rejected and thus, are not used in making the image. Indeed, if the higher amplitude fundamental echoes are not eliminated, they degrade the image to the point that there is no benefit from tissue harmonic imaging. The stronger fundamental echoes, if not eliminated, will mask the harmonics. Obviously, sophisticated transmit beam formation and signal detection is required to produce good quality harmonic images. It is possible that the ability to produce high quality harmonic images may be an interesting test of an ultrasound system's overall capabilities. Ultrasound image quality has experienced a significant improvement with the utilization of harmonic frequencies. Several techniques are currently employed to detect harmonics and eliminate the unwanted fundamental echoes [87]-[89]. Filtration techniques remove the echoes from the fundamental frequency and allow the harmonic frequencies to pass, so that the harmonic image can be formed. Other techniques cancel the fundamental echoes. Some of these include pulse inversion [85], amplitude or power modulation, side-by-side phase cancellation, and

transmit pulse encoding [86]. All of these techniques require excellent transmit beamformer performance.

V.3 SECOND HARMONIC EXTRACTION TECHNIQUES

Tissue harmonic imaging is a new grayscale imaging technique. It creates images that are derived solely from the higher frequency, second harmonic sound produced when the ultrasound pulse passes through tissue within the body. Tissue harmonics uses various techniques to eliminate the echoes arising from the main transmitted ultrasound beam (the fundamental frequency), from which conventional images are made. Once the fundamental frequencies are eliminated, only the harmonic frequencies are left for image formation. Tissue harmonic imaging offers several advantages over conventional pulse-echo imaging, including improved contrast resolution, reduced noise and clutter, improved lateral resolution, reduced slice thickness, reduced artifacts (side lobes, reverberations) and, in many instances, improved signal-to-noise ratio. Indeed, the quality of the harmonic image is primarily dependent on the complete elimination of all echoes derived from the transmitted frequencies. To effectively employ the information contained in the second harmonic of the received signal, this information should be properly extracted.

V.3.1 Filtration Technique

Filtration to remove the fundamental frequency is the technique currently used most commonly to produce tissue harmonic images. Filtration uses sophisticated transmit beam formers to produce a narrower bandwidth and signal processing techniques to filter out the spectrum of frequencies that are likely to arise from the fundamental beam. The fundamental ultrasound pulse is not a single frequency, but is really a range of many frequencies that are distributed around the mean transmitting frequency (for example, a band of frequencies from 1.2 to 2.8 MHZ for a 2 MHZ transducer centre frequency), see figure (V.1). Because of this, there are frequencies at which the information from both the fundamental signal and the harmonic signal overlaps.

If a system produces a broader bandwidth, then the overlap between the received harmonic signal and the fundamental signal is greater. In this setting, filtration will

then result in the removal of significant harmonic information along with the unwanted fundamental echoes. However, use of a narrower bandwidth will result in less overlap. With narrow bandwidth beams, filtration can provide a much cleaner separation of the harmonic-related information from the fundamental signal. A high-pass or band-pass filter must be designed to filter the spectrum of the received echo and pass the second harmonic. The ability of the filter to reject the fundamental is critical since its presence will contribute to a loss of contrast resolution.

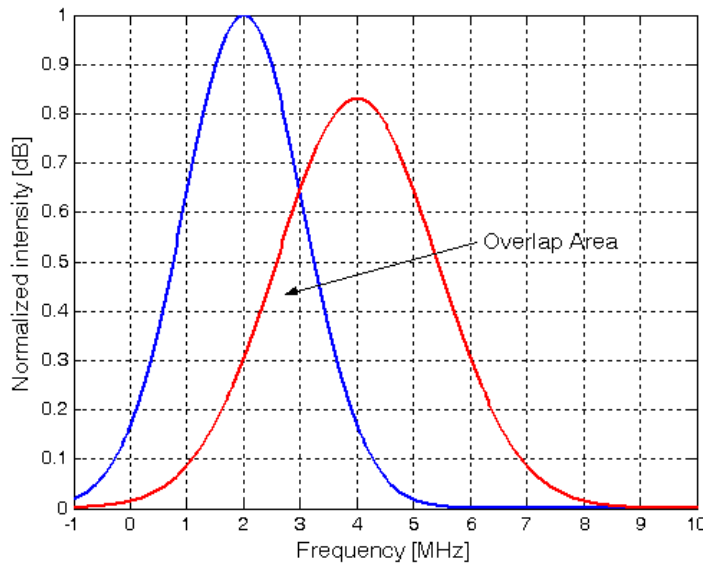


Figure V.1: Illustration of the overlap between the fundamental (dashed), and second harmonic (solid) components

Note that the second harmonic has reduced amplitude; this is due to the attenuation that higher frequencies experience during propagation within a medium. The overlap of the fundamental and the second harmonic frequencies means that any filtering will inevitably cut part of the second harmonic signal out while retaining part of the fundamental signal. Therefore, high-pass filtering provides a flawed means for extracting the harmonic signal from the reflected ultrasound data.

V.3.2 Pulse Encoding Technique

Pulse encoding of the transmitted ultrasound beam is another technique to cancel the fundamental echoes and enhance harmonic detection [86]. Transmit pulse encoding uses relatively complex waveform sequences to give each a unique, recognizable signature or code. This complex, coded pulse is sent into the body. The unique code is then recognized in the return waveform by a special decoder that is part of the equipment. Because the linear, fundamental echoes have a specific code, they can be identified and canceled. The remaining nonlinear harmonic signal is then processed to form the image. This technique has proved especially useful in the near field.

V.3.3 Pulse Inversion Technique

Pulse inversion is a technique that adds the echoes from two opposite polarity pulses to cancel the fundamental (linear) echoes, leaving only the harmonic (nonlinear) information, see figure (V.2).

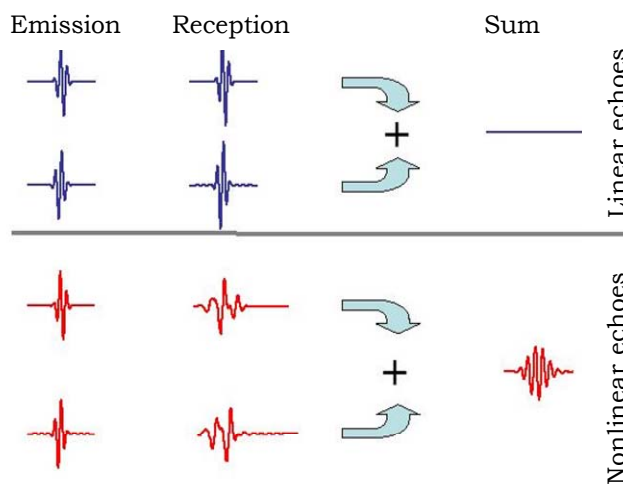


Figure V.2: Pulse inversion technique principle

An initial pulse is sent into the body and the returning echoes are recorded. This first pulse-echo cycle results in both fundamental and harmonic frequencies returning from the tissue and the data received are stored. A second inverted pulse (opposite in phase) is then transmitted. Fundamental and harmonic frequencies of the second cycle are received and added to the data received from the first cycle. Adding the data will then cancel the linear, fundamental echoes. The nonlinear harmonic information remains, resulting in an unfiltered harmonic signal over the entire frequency bandwidth of the transducer. Simulation results have been realized with a circular transducer of 15mm of radius. The corresponding ultrasound beam is focalized at 60mm depth of axial distance, and excited with a 400KPa Gaussian waveform of three cycles at a centered frequency of 2MHz. Figure (V.3) shows the first excitation pulse (a) and its corresponding spectra (c). The inverted pulse and its corresponding spectra are shown in figures (b) and (d) respectively.

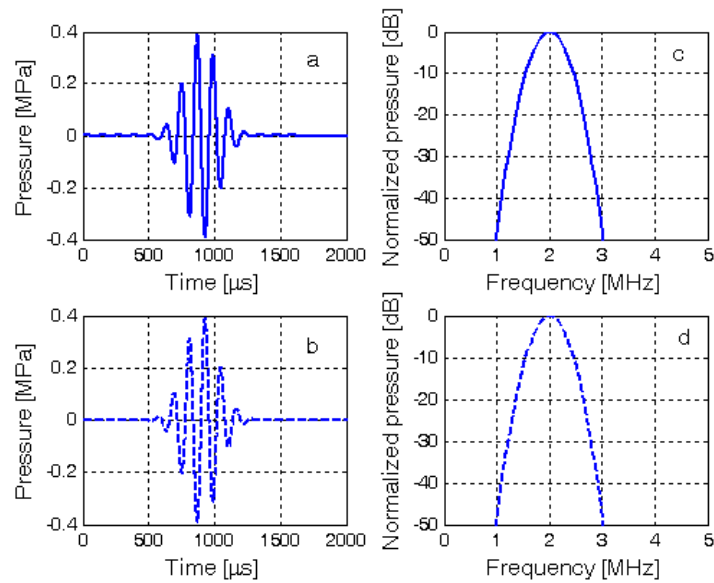


Figure V.3: The two inverted pulses (solid & dashed) and their corresponding spectra in the pulse-inversion technique

Pulse inversion scheme has been proposed for rejection of the fundamental signal component in contrast harmonic imaging. In the pulse-inversion technique, and due to the nonlinear nature of harmonic frequencies, adding two echo signals that are generated by transmitting pulses out of phase by 180 degrees causes the linear portions as well as the odd harmonics to zero out while the even harmonics double, see figure (V.4).

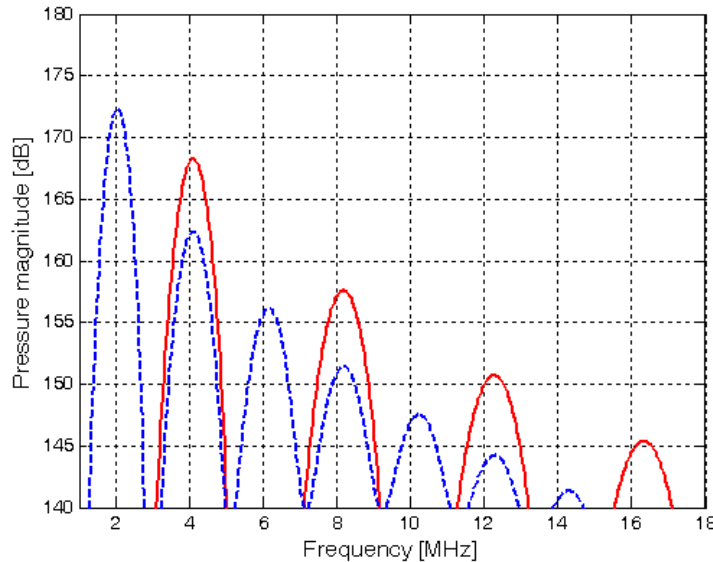


Figure V.4: Spectra of received signals: before (dashed), and after (solid) using the pulse-inversion technique

Because the second harmonic component has less energy than the fundamental component, high sensitivity and wide dynamic range are needed in the receiving system to achieve an acceptable signal-to-noise ratio. The pulse inversion technique is used to reinforce the ultrasound pressure and increase the signal-to-noise of the second harmonic component in harmonic imaging. Figures (V.5) and (V.6), show respectively an increased intensity in axial and radial second harmonic signals of the ultrasound field after the use of the pulse-inversion technique.

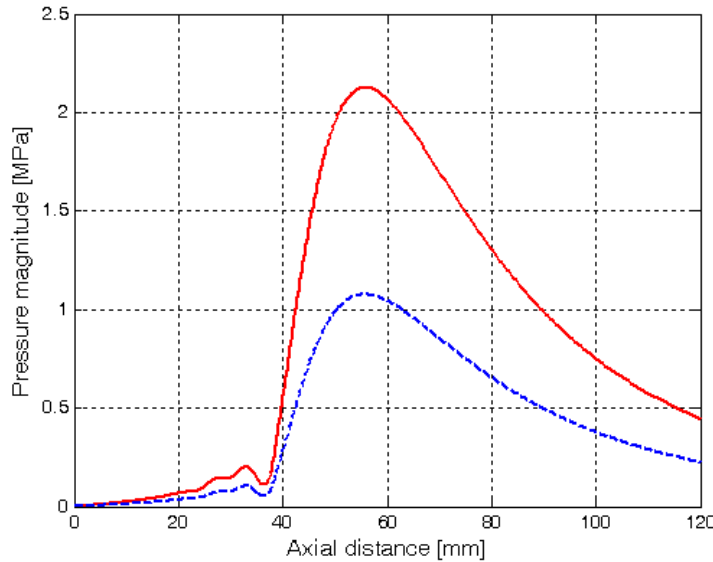


Figure V.5: Axial second harmonic pressure: before (dashed), and after (solid) the pulse-inversion technique

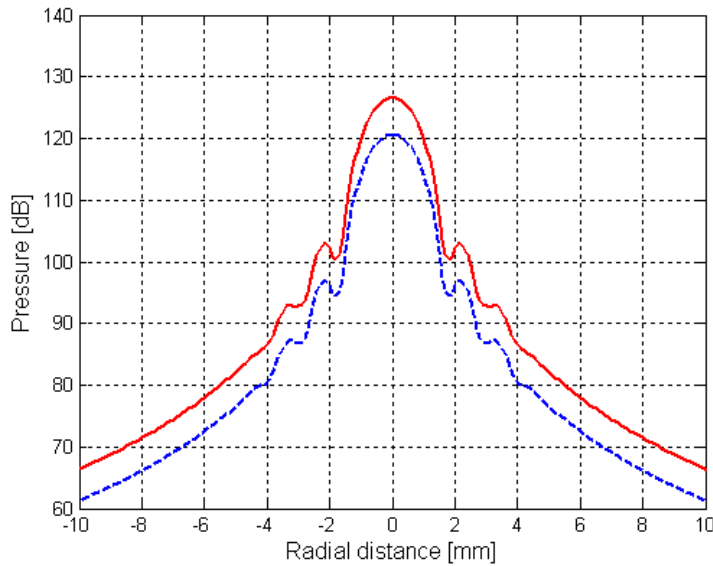


Figure V.6: Radial second harmonic pressure: before (dashed), and after (solid) the pulse-inversion technique

V.3.4 Side-by-side Phase Cancellation Technique

Side-by-side phase cancellation technique is similar to pulse-inversion technique cited above. Instead of two firings of opposite phase ultrasound beams along the same line, this method sends both signals together at the same time with opposite phases. These adjacent lines are then added. The resulting cancellation of the fundamental opposite phase lines leaves the harmonics, from which images can be made. Like pulse inversion, this technique preserves the bandwidth of the harmonic sound. This technique is a spatial cancellation technique, while pulse inversion is a temporal cancellation technique.

V.3.5 Power Modulation Technique

Power-modulation is a harmonic imaging method in which the amplitude (and hence power) of every other pulse is transmitted into the body is changed (for example, doubled), see figure (V.7). The received echoes from each low amplitude pulses are then amplified more (doubled in this case) so that all linear echoes are equal. Sequential pairs of pulses are then subtracted. Linear echoes cancel, but nonlinear echoes do not, see figure (V.9).

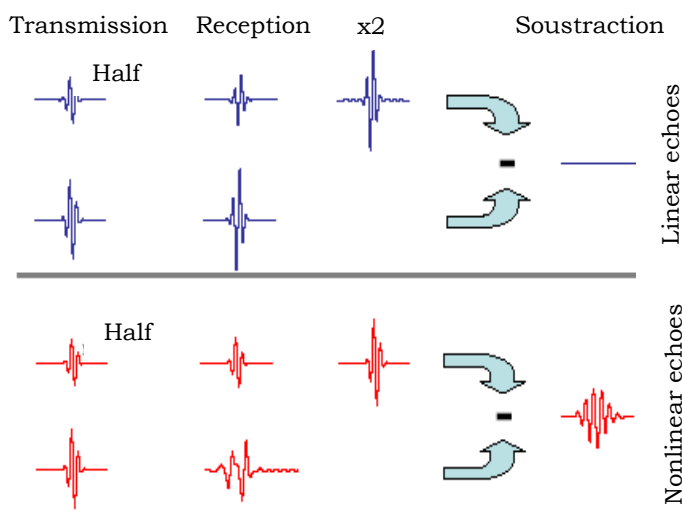


Figure V.7: Power-modulation technique principle

Figure (V.8) shows a full excitation pulse of a 400KPa (a) and its corresponding spectra centered at 2MHz (c). The half excitation pulse (200KPa) and its corresponding spectra are shown in figures (b) and (d) respectively.

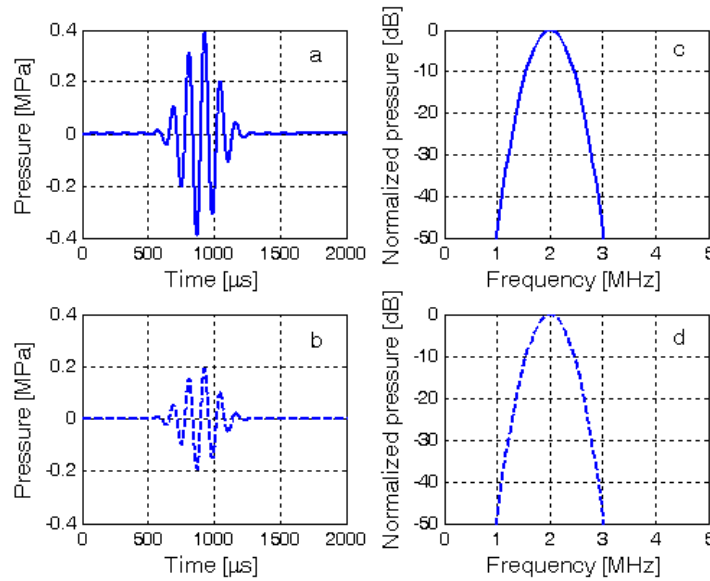


Figure V.8: The two pulses (full & half) and their corresponding spectra in the power-modulation technique

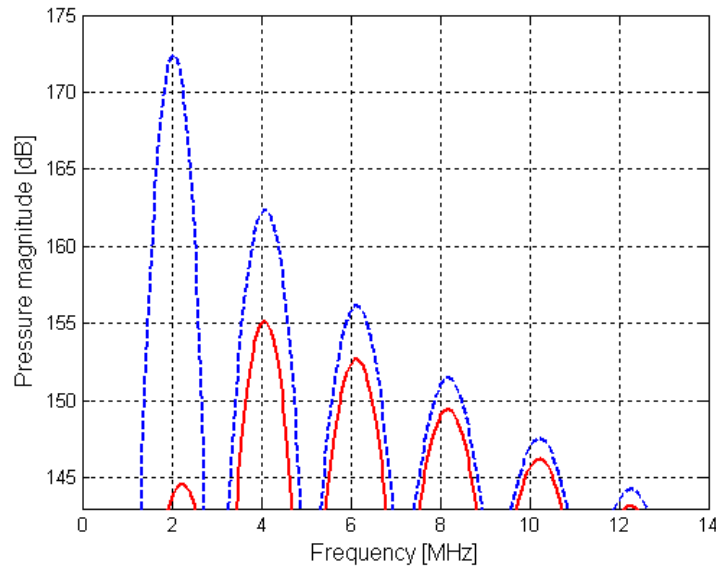


Figure V.9: Spectra of received signals: before (dashed), and after (solid) using the power-modulation technique

Unlike the pulse-inversion technique, the power-modulation technique preserves all nonlinear harmonics but without increasing in their corresponding signal levels. Figure (V.9) shows a less signal levels of the nonlinear harmonics, and especially the second harmonic component in comparison with the pulse-inversion technique.

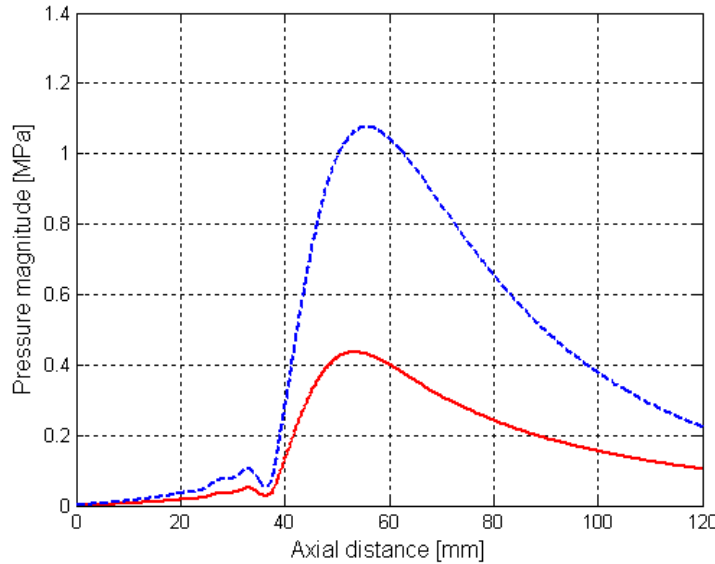


Figure V.10: Axial second harmonic pressure focalized at depth of 60mm: before (dashed), and after (solid) the power-modulation technique

Figures (V.10) and (V.11), show respectively a decreased intensity in axial and radial second harmonic signals of the ultrasound field after the use of the power-modulation technique in comparison with the pulse-inversion technique.

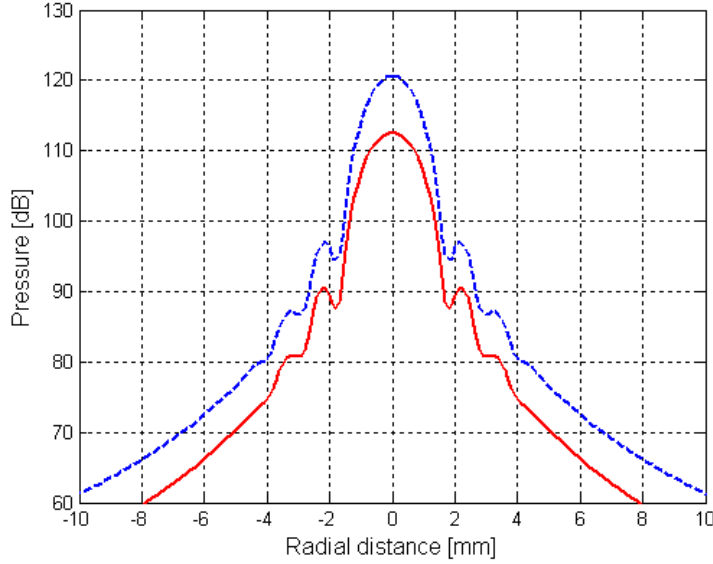


Figure V.11: Radial second harmonic pressure: before (dashed), and after (solid) the power-modulation technique

V.4 OPTIMIZATION OF HARMONIC IMAGING

Harmonic imaging creates images that are derived solely from the higher frequency, second harmonic ultrasound signal produced when the ultrasound pulse passes through tissue within the body.

Tissue harmonics uses various techniques to eliminate the echoes arising from the main transmitted ultrasound beam, from which conventional images are made. Once the fundamental frequencies are eliminated, only the harmonic frequencies are left for image formation. Indeed, the quality of the harmonic image is primarily dependent on the complete elimination of all echoes derived from the transmitted frequencies

In second harmonic imaging, an ongoing problem is that undesired signals are contained in the reflected waves, and that corrupt the image data, which leads to the contamination of the obtained image.

An optimization of the transmitted bandwidth is recommended to receive the purely second harmonic signal for harmonic imaging [91]. Given a certain available bandwidth for the transducer, it must be decided in what band the transmitted

pulse may be sent at, and what band the second harmonic signal should be received at.

Example (200KPa, 2MHz): Figure (V.12) shows an overlap of 275 KHz (bandwidths at -10dB) between the excitation and the received second harmonic bandwidths. The transmitted bandwidth is at 100%. Receive a purely harmonic signal component imply a transmission of only 72.5% of bandwidth. In this case, the second harmonic signal is purely nonlinear.

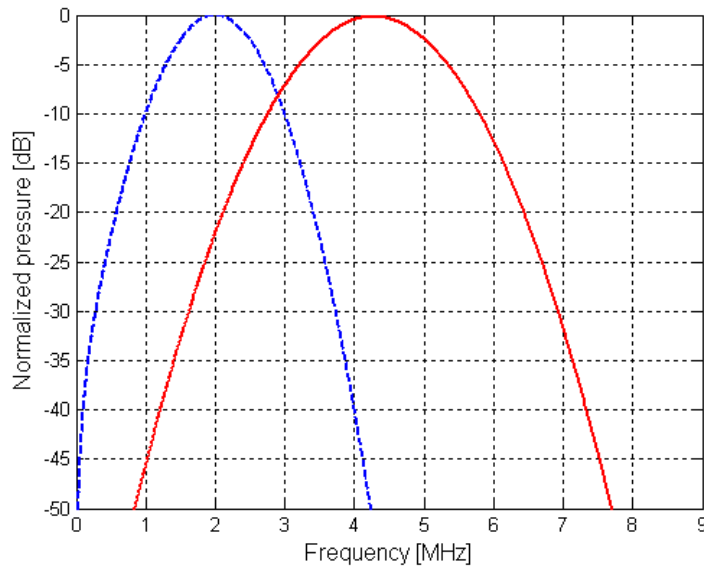


Figure V.12: 100% transmitted bandwidth (dashed), and received second harmonic signal component (solid)

V.4.1 Bandwidth

The bandwidth is the range of frequencies present in a signal. It is defined as that portion of the signal's frequency spectrum between upper and lower frequency bounds. When evaluating the performances of an ultrasound imaging system, knowledge of the bandwidth is essential. Transmitted and received bandwidths are two factors, which can define an ultrasound imaging system, and consequently the image quality.

Figure (V.13) shows the excitation waveform (a) and its distortion after propagation (b). In this section, only the fundamental and second harmonic bandwidths are for

interesting. Figures (V.13c, d) show respectively the spectra of an excitation of 2MHz and the second harmonic signals.

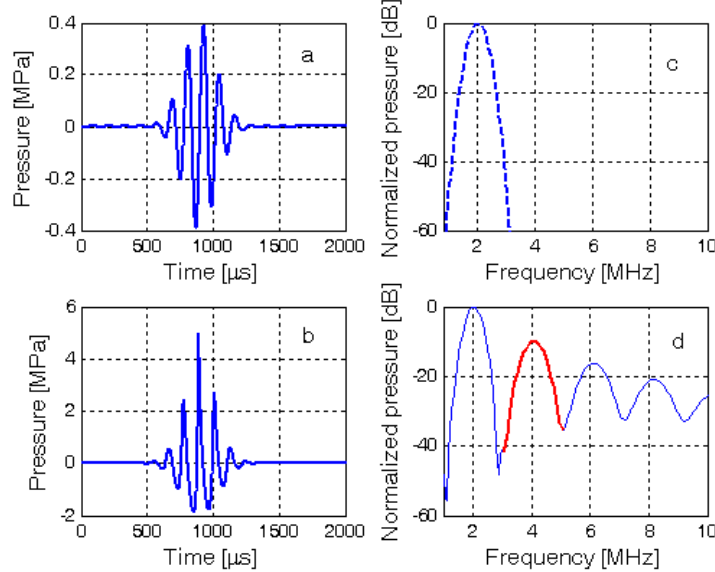


Figure V.13: Excitation waveform, its distorted waveform after propagation, and their corresponding spectra

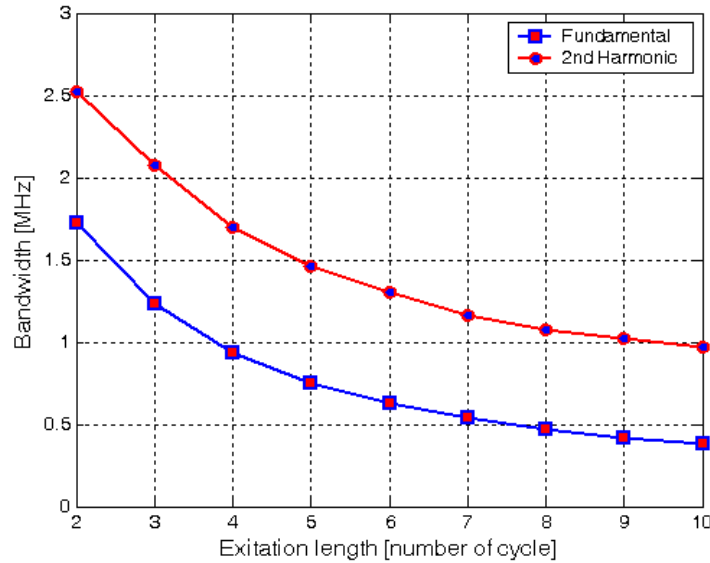


Figure V.14: Fundamental & second harmonic bandwidth as a function of excitation length

In figure (V.14) are represented the fundamental and the second harmonic bandwidths as a function of the excitation (case of 200KPa, 2MHz) length (number of cycle in excitation). It confirms that the bandwidth decreases with the temporal signal length.

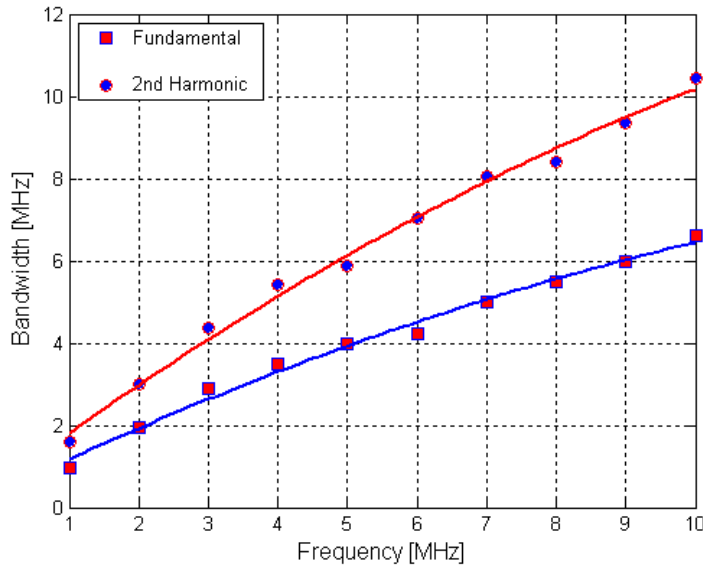


Figure V.15: Fundamental and second harmonic bandwidths in function of the excitation frequency

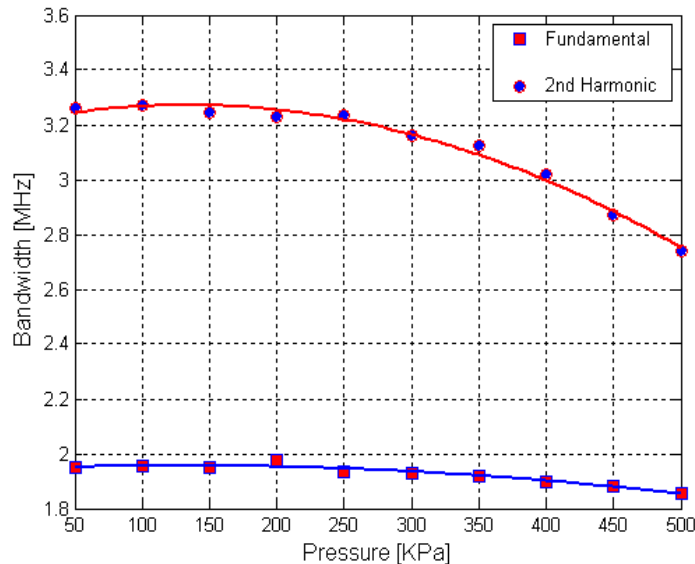


Figure V.16: Fundamental and second harmonic bandwidths in function of the excitation pressure intensity

Figures (V.15, 16) show respectively the variation of the fundamental and the second harmonic components bandwidths as a function of the excitation frequency and pressure intensity.

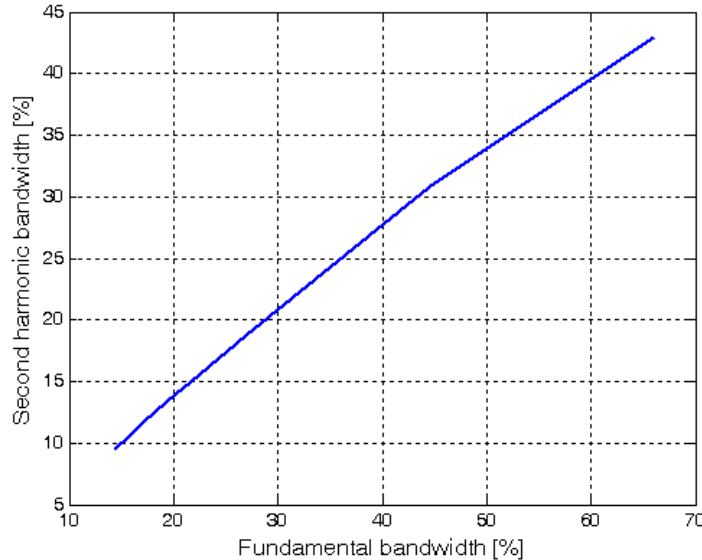


Figure V.17: Fundamental and second harmonic bandwidths in percentage

Figure (V.17) shows the fundamental and the second harmonic in percentage. 60% of fundamental bandwidth engenders 40% of second harmonic bandwidth, i. e: transmit bandwidth, $BW=[1.4 — 2.6]$ MHz, and second harmonic bandwidth, $BW=[3.2 — 4.8]$ MHz, this means that the second harmonic component is purely nonlinear.

V.4.2 Overlap

Spectral overlapping in transmission between the fundamental and the second harmonic bands must be minimal even null to avoid the transmission of frequential component with $2f_0$ (f_0 is the transmitted frequency), and consequently the contamination of the harmonic band, and thereafter the obtained image. In this section, the overlap between the fundamental and second harmonic bands is computed for optimizing the transmitted bandwidth.

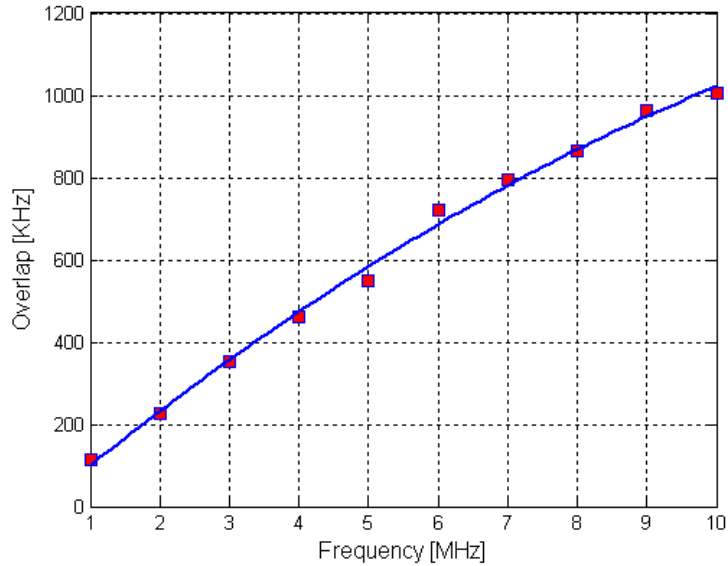


Figure V.17: Overlap between fundamental and second harmonic Bandwidths in function of the excitation frequency

The overlap between the fundamental and the second harmonic components increases with the excitation frequency, figure (V.17). Overlap is very significant for high excitation frequencies.

In figure (V.18), this same overlap decreases in function of the excitation pressure intensity, the overlap is not very significant for high excitation pressures.

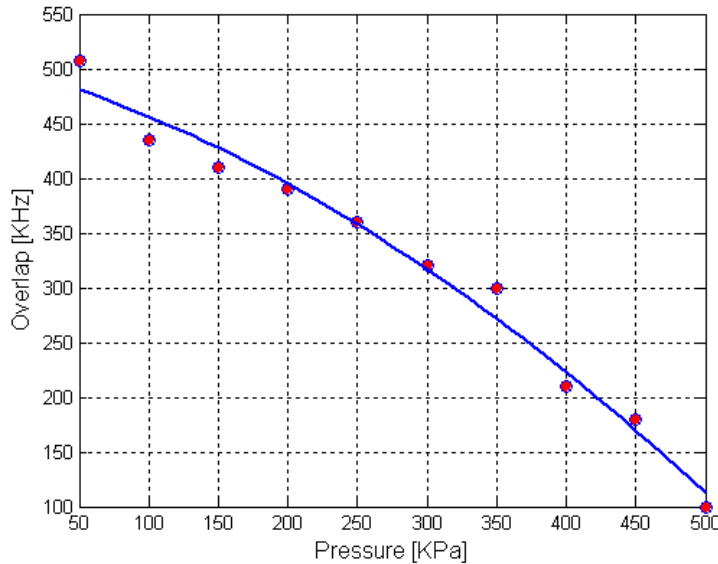


Figure V.18: Overlap between fundamental and second harmonic Bandwidths in function of the excitation pressure intensity

Due to the limited transducers bandwidths, the transmitted ultrasound waves must have narrow bandwidths for not overlap between fundamental and second harmonic bands. Therefore, the excitation bandwidth should be large enough to ensure resolution while overlapping with harmonic frequencies should be minimized. An optimization of the transmitted bandwidth is a compromise for each desired situation.

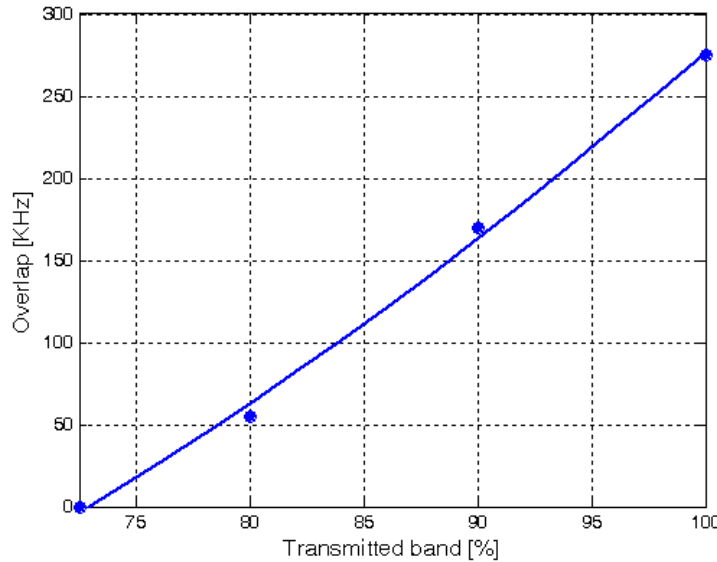


Figure V.19: Overlap between fundamental and second harmonic Bandwidths in function of the transmitted bandwidth

Figure (V.19) shows the variation of the overlap between fundamental and second harmonic bandwidths as a function of the percentage of the transmitted bandwidth, case of an excitation of 200KPa, 2MHz. to receive a purely harmonic signal component, we must transmit only 72.5% of bandwidth. In this case, the second harmonic signal is purely nonlinear.

Chapter VI

Conclusion & Future Works

Conclusion & Future Works

VI.1 CONCLUSION

Until recently, the development of medical ultrasound operated under the implicit and convenient assumptions of infinitesimal acoustics where ultrasound waves were assumed to propagate in a linear fashion like studied in chapter III. Unfortunately, these assumptions became invalid at biomedical frequencies and intensities used nowadays. However, it has been proven that ultrasound waves undergo gradual distortion in almost every medical use. The distortion is due to slight nonlinearities in sound propagation that gradually deform the shape of the wave, and results in development of additional harmonic frequencies which were not present at the source.

Selective imaging of these harmonic frequencies turned out to considerably improve ultrasound images. This technology called tissue harmonic imaging has emerged as a major imaging modality over the past years.

Ultrasound harmonic imaging, which exploits nonlinear tissues properties, has the advantage in reduced reverberations and artifacts due to reduced sidelobes and grating lobes levels, greater depth of penetration at high frequencies, and better resolution of the resulting image due to narrower beams. Decreased noise from sidelobes improves signal-to-noise ratios and consequently reduces artifacts as shown in chapter IV. Deleterious effects of the body wall are also reduced. It was seen that a clearer image could be synthesized by processing the second harmonic frequency instead of the frequency of the emitted pulse.

Due to nonlinear tissues properties, these nonlinear propagation effects have become of major interest in diagnostic ultrasound, by reducing unwanted artifacts in ultrasound images and, thus, enabling physicians to make more precise diagnoses than was possible before. The advantages of native tissue harmonic imaging were recently demonstrated in various clinical applications, and a long list of literature is already available on that subject. In Radiology for example, it has showed that selective imaging at harmonic frequencies enhances the liver-lesion.

They also demonstrated the usefulness of harmonic imaging in obstetrics where clear depiction of fetal anatomy is obtained. In cardiology, it has proved that noise and clutter artifacts are reduced and endocardial borders are enhanced when imaging is made in harmonic mode. These observations clearly confirmed that tissues nonlinearities have a significant effect on acoustic beams used in medical ultrasound, and therefore bring the need to predict the influence of such nonlinear effects in the medical use.

In this thesis, numerical simulation of the ultrasound propagation applied to medical imaging is carried out by a finite difference model of the nonlinear wave equation. In order to characterize the harmonic beam, a time domain solution of the parabolic nonlinear wave equation is used. KZK equation is traditionally applied in a propagation direction along the central transducer axis, and has been shown to model the pulse propagation satisfactorily.

In chapter IV, the characteristics and performances of the second harmonic acoustic beam from a focused piston aperture are described and the physical principles behind tissue harmonic imaging are computed. The field properties are then discussed regarding image quality.

For the full three-dimensional model, the time domain algorithm for the KZK equation developed by YS-Lee is used. The KZK equation is known to accurately describe the propagation of a finite amplitude ultrasound wave including the effects of nonlinearity, absorption and diffraction. The time domain algorithm has been shown as an accurately model of the solution of the KZK equation for the pulsed source. The solution is an efficient computer model for simulating nonlinear ultrasound propagation in tissue. This model shall enable accurate modeling of finite amplitude effects in modern clinical ultrasound scanners, and in particular, may be useful as a tool for optimizing the design of tissue harmonic imaging systems.

In ultrasound harmonic imaging, an ongoing problem is that undesired signals are contained in the reflected waves, and that corrupt the image data which leads to the contamination of the obtained image. Harmonic received frequency band must not contain components from transmit band, and its components must sufficiently be separable from fundamental spectral component. Thus, to effectively employ the information contained in the second harmonic of the received signal, this

information should be properly extracted. As a consequence, several imaging modalities and techniques have been developed, which are intended to acquire and process the harmonic information, or even to separate one kind of such information from another. In chapter V, five techniques are presented in where two of them, pulse inversion and power modulation techniques, are developed. In this chapter, a new technique for acquiring the proper second harmonic signal is presented. An optimization of the transmitted bandwidth is recommended to receive the purely second harmonic signal for harmonic imaging. Given a certain available bandwidth for the transducer, it must be decided in what band the transmitted pulse may be sent at, and what band the second harmonic signal should be received at.

Spectral overlapping in transmission between the fundamental and the second harmonic bands must be minimal even null to avoid the transmission of frequential component with $2f_0$ (f_0 is the transmitted frequency), and consequently the contamination of the harmonic band, and thereafter the obtained image.

VI. FUTURE WORKS

1. Modern medical ultrasound systems have a very high relative bandwidth, so that the emitted pulse can be just a few wavelengths long, giving high range resolution. In addition, the development of promising technologies such as capacitive micromachined ultrasonic transducers (cMUT) as an alternative to the currently used piezoelectric materials will most likely bring great changes to medical ultrasound imaging systems. In this way, a future work can be envisaged.

2. Emboli classification is of high clinical importance for selecting appropriate patient treatment. Several ultrasonic methods using Doppler signal processing have been used for emboli detection and classification as solid or gaseous matter.

The ultrasound radio-frequency signal backscattered by the emboli contains more information about the embolus than the Doppler signal, especially, the nonlinear components. Future research can be oriented to the analysis of the radio-frequency signals using artificial neural networks methods and Support Vectors Machines (SVM) in order to classify microemboli as gaseous or particulate matter.

References

References

- [1] Thomas L. Szabo, *Diagnostic ultrasound imaging*, Elsvier academic press, 2004.
- [2] L. E. Kinsler, A. R. Frey, A. B. Coppens, and J. V. Sanders, *Fundamentals of acoustics*, 4th ed. New York: John Wiley & Sons, 2000.
- [3] B. Carlin, *Physical acoustics-Principles and methods*, Vol. I, part B. New York: Academic Press, 1964.
- [4] A. D. Pierce, *Acoustics: An introduction to its physical principles and applications*, Woodbury, NY: The Acoustical Society of America, 1989.
- [5] A. P. Cracknel, *Ultrasonics*, Great Britain: Wykeham Publication (London) Ltd., 1980.
- [6] Rossing, D. Thomas, *The science of sound*, Reading: Addison Wesley Publishing Company Inc., 1982.
- [7] Stephens, R. W. B., and A. E. Bate, *Acoustics and vibrational physics*, Great Britain: William Clowes and Sons, 1966.
- [8] Hamilton, F. Mark and, T. David Blackstock, eds, *Nonlinear acoustics*, San Diego: Academic Press, 1998.
- [9] Lempriere, M. Brian, *Ultrasound and Elastic Waves*, New York: Academic Press, 2002.
- [10] Xiangtao Yin, *The study of ultrasonic pulse-echo subwavelength defect detection mechanism*, Thesis submitted in partial fulfillment of the requirements for the degree of Doctor of philosophy in electrical engineering in the graduate college of the university of Illinois at Urbana-Champaign, 2003.
- [11] G. S. Kino, *Acoustic waves: devices, imaging, and analog signal processing*, Englewood Cliffs, NJ: Prentice-Hall, Inc., 1987.
- [12] NCRP, *Biological effects of ultrasound: mechanism and clinical implications*, National Council on Radiation Protection and Measurements, Bethesda, MD, Tech. Rep. 74, 1983.
- [13] K. K. Shung, and M. Zippardo, *Ultrasonic transducer and arrays*, IEEE Engineering in medicine and biology, vol. 15, pp. 20-30, 1996.
- [14] G. Kino, *Acoustic waves: Devices, imaging, and analog signal processing*, Englewood Cliffs: Prentice-Hall, NJ, 1987.
- [15] G. S. Kino, and C. S. DeSilets, Designs of slotted transducer arrays with matched backing, *Ultrasound imaging*, vol. 1, pp. 189-209, 1979.
- [16] A. R. Selfridge, G. S. Kino, and B. T. Khuri-Yakub, *Fundamental concepts in acoustic transducer array design*, IEEE Ultrasonics Symposium, pp. 989-993, 1980.
- [17] Shiwei Zhou, *Improving ultrasound transducer performance using assisted designs and digitized waveform compensation techniques*, Thesis submitted in partial fulfillment of the requirements for the degree of Doctor of philosophy in biomedical engineering in the faculty of the school of engineering and applied science, University of Virginia, 2006.
- [18] J. A. Jensen, *Ultrasound imaging and its modeling*, Chapter in. Fink et al. (EDS): *Imaging of complex media with acoustic and seismic waves, topics in applied physics*, vol. 84, pp. 135-165, Springer Verlag, 2002.
- [19] J. A. Zagzebski, *Essentials of ultrasound physics*, St. Louis, MO: Mosby-Year book Inc., 1996.
- [20] Thomas L. Szabo, *Diagnostic ultrasound imaging*, Elsevier Academic press, 2004.

- [21] Roger James Zemp, *Modeling nonlinear ultrasound propagation in tissue*, thesis submitted in conformity with the requirements for the degree of Masters of Applied Science. Graduate Department of Electrical and Computer Engineering and Institute of Biomaterials and Biomedical Engineering. University of Toronto, 2000.
- [22] P. M. Morse and K. U. Ingard, *Theoretical Acoustics*, Princeton, NJ: Princeton Univ. Press, 1986.
- [23] J. L. Emeterio and L. G. Ullate, *Diffraction impulse response of rectangular transducers*, J. Acoust. Soc. Amer., vol. 92, no. 2, pp. 651-662, 1992.
- [24] J. A. Jensen, *Ultrasound field from triangular apertures*, Chapter in. Fink et al. (EDS): Imaging of complex media with acoustic and seismic waves, J. Acoust. Soc. Amer., vol. 100, pp. 2049-2056, Oct. 1996.
- [25] J. A. Jensen, *Linear description of ultrasound imaging systems*, Notes for the international summer school on advanced ultrasound imaging, technical university of Denmark, 1999.
- [26] G. E. Tupholme, *Generation of acoustic pulses by baffled plane pistons*, Mathematika, 16: 209:224 1969.
- [27] P. R. Stepanishen, *The time-dependent force and radiation impedance on a piston in a rigid infinite planar baffle*, J. Acoust. Soc. Amer., 49:841-849, 1971.
- [28] P. R. Stepanishen, *Transient radiation from pistons in an infinite planar baffle*, J. Acoust. Soc. Amer., 49:1629-1638, 1971.
- [29] L. E. Kinsler, A. R. Frey, A. B. Coppens, and J. V. Sanders, *Fundamentals of acoustics*, John Wiley & Sons, New York, third edition, 1982.
- [30] J. Y. Lu and J. F. Greenleaf, *A study of two-dimentional array transducers for limited diffraction beams*, IEEE Trans. Ultrason., Ferroelect., Freq Contr., vol. 41, pp. 821-827, 1994.
- [31] G. Jacovitti, A. Neri, and G. Scarano, *Pulsed response of focused arrays in echographic b-mode systems*, IEEE Trans. Ultrason., Ferroelect., Freq Contr., vol. SU-32, pp. 850-860, 1985.
- [32] B. G. Bardsley and D. A. Christensen, *Beam patterns from pulsed ultrasonic transducers using linear system theory*, J. Acoust. Soc. Amer., vol. 69, pp. 25-30, 1981.
- [33] P. Crombie, A. J. Bascom, and S. C. Cobbold, *Calculating the pulsed response of linear arrays: Accuracy vs. computational efficiency*, IEEE Trans. Ultrason., Ferroelect., Freq Contr., vol. 44, no. 5, pp. 997-1009, 1997.
- [34] J. W. Goodman, *Introduction to Fourier optics*, New York, NY: McGraw-Hill, 1968.
- [35] D. H. Turnbull and F. S. Foster, *Beam steering with pulsed two-dimensional transducers arrays*, IEEE Trans. Ultrason., Ferroelect., Freq Contr., vol. 38, pp. 320-333, 1991.
- [36] J. A. Jensen and N. B. Svendsen, *Calculation of pressure fields from arbitrarily shaped, apodized and excited ultrasound transducers*, IEEE Trans. Ultrason., Ferroelect., Freq Contr., vol. 39, no. 2 pp. 262-267, 1992.
- [37] J. A. Jensen, *FIELD: A program for simulating ultrasound systems*, Medical & Biological Engineering & Computing, pp. 351-353, Vol. 34, supplement 1, Part 1, 1996.
- [38] Yadong Li, *Computer simulation of linear and harmonic ultrasound imaging*, A dissertation submitted to the university of Wisconsin-Madison in partial fulfillment of the requirements for the degree of Doctor of philosophy, 2001.
- [39] M. Bahaz, K. Benmohammed, N. Benoudjitt, and A. Bouakaz, *Piston ultrasound field properties applied to echographic imaging*, 1st international conference on electronic systems, Batna, Algeria, proceeding pp. 73-77, 2005.
- [40] W. H. Press, S. A. Teukolsky, W. T. Vetterling, and B. P. Flannery, *Numerical recipes in C*, Cambridge, United Kingdom: Cambridge University Press, 1992.
- [41] G. R Harris, *Transient field of a baffled planar piston having an arbitrary vibration amplitude distribution*, J. Acoust. Soc. Am., 70:186-204, 1981.
- [42] P. R. Stepanishen, *Acoustic transients from planar axisymmetric vibrators using the impulse response approach*, J. Acoust. Soc. Am., 70:1176-1181, 1981.
- [43] J. Nase Tjøtta and S. Tjøtta , *Nearfield and farfield of pulsed acoustic radiators*, J. Acoust. Soc. Am., 71:824-834, 1982.

- [44] M. Bahaz, K. Benmohammed, N. Benoudjit, and A. Bouakaz, Characterization and performance of harmonic pulsed pressure field from focused circular transducer applied to medical ultrasound imaging, International conference on electronic systems, Tunisia, 2007.
- [45] M. Bahaz, K. Benmohammed, N. Benoudjit, and A. Bouakaz, *Characterization of harmonic pressure field: Application to medical ultrasound imaging*, IJCISIM, vol. 1, pp. 118-124, 2009.
- [46] E. L. Carstensen, W. K. Law, and T. G. Muir, *Demonstration of nonlinear acoustical effects at biomedical frequencies and intensities*, Ultrason. Med. Biol., vol. 6, pp. 359-368, 1980.
- [47] T. G. Muir and E. L. Carstensen, *Prediction of nonlinear acoustic effects at biomedical frequencies and intensities*, Ultrason. Med. Biol., vol. 6, pp. 345-357, 1980.
- [48] H. C. Starritt, F. A. Duck, and V. F. Humphrey, *The development of harmonic distortion in pulsed finite-amplitude ultrasound passing through liver*, Phys. Med. Biol., vol. 31, pp. 1401-1409, 1986.
- [49] B. Waad, A. C. Baker, and V. F. Humphrey, *Nonlinear propagation applied to the improvement of resolution in diagnostic medical ultrasound*, J. Acoust. Soc. Am., vol. 101, pp. 143-154, 1997.
- [50] R. T. Beyer, *Nonlinear Acoustics*, Naval Sea Systems Commands, Washington, D.C., 1974 (reprinted, with a new appendix containing more recent references and published by: Acoustical Society of America, Woodbury, N.Y., 1997).
- [51] Hamilton, Mark F. and David T. Blackstock, *Nonlinear Acoustics*, San Diego: Academic Press, eds, 1998.
- [52] Fry, W. J. and Dunn. F, *Physical techniques in biological research*, Chap. 6 Ultrasound: Analysis and Experimental Methods in Biological Research: Academic Press, 1962.
- [53] M. F. Hamilton and D. T. Blackstock, Nonlinear acoustics, Academic press, the University of Texas at Austin, 1998.
- [54] Frinking, Petar J. A., Ayache Bouakaz, Johan Kirkhorn, Folkert J. Ten Cate, and Nico de Jong, *Ultrasound contrast imaging: Current and new potential methods*, Ultrasound in Medicine & Biology, 29: 965-975, 2000.
- [55] Danna Gurari, *Harmonic imaging using a mechanical sector B-mode*, A thesis presented to the Henry Edwin Sever Graduate School of Washington University in partial fulfillment of the requirement for the degree of Master of Science, Washington University in St. Louis, School of engineering & applied science, 2005.
- [56] L. Solbiati, A. Martegani, E. Leen, J. M. Correas, P. N. Burns, and D. Becher, *Contrast-Enhanced Ultrasound of Liver Diseases*, Springer Science, Italia, 2003.
- [57] D. T. Blackstock, *Propagation of plane sound waves of finite amplitude in nondissipative fluids*, J. Acoust. Soc. Am. 34, 9-30, 1962.
- [58] S. D. Poisson, *Memoir on the theory of sound*, J. L'Ecole Polytech., 1808.
- [59] J. S. Mendousse, *Nonlinear dissipative distortion of progressive sound waves at moderate amplitudes*, J. Acoust. Soc. Am. Vol. 25, pp. 51-54, 1954.
- [60] N. S. Bakhvalov, Ya. M. Zhileikin, and E. A. Zabolotskaya, *Nonlinear theory of sound beams*, American Institute of Physics, New Work, 1987.
- [61] E. A. Zabolotskaya and R. V Khokhlov, *Quasi-plane waves in the nonlinear acoustics of confined beams*, Sov. Phys. Acoust. 15, 35-40, 1969.
- [62] V. P. Kuznetsov, Equation of nonlinear acoustics, Sov. Phys. Acoust., 16, 467-470, 1970.
- [63] Froysa, K.E., Naze Tjotta, J., and Berntsen, J., *Finite amplitude effects in sound beams, Pure tone and pulse excitation*, In *Advances in Nonlinear Acoustics*, H. Hobaek, ed., World Scientific, Singapore, pp.233-238, 1993.
- [64] Bakhvalov, N.S., Zhileikin, Y.M., Zabolotskaya, E.A., Khokhlov, R.V., *Nonlinear propagation of a sound beam in a nondissipative medium*, Sov. Phys. Acoust., 22, 272-274, 1987.
- [65] F. Tranquart, N. Grenier, V. Eder, and L. Pourcelot, *Clinical use of ultrasound tissue harmonic imaging*, Ultrason. Med. Bio., vol. 25, pp. 889-894, 1999.

- [66] Gray, D. E. (ed.), American Institute of Physics Handbook, third edition, McGraw-Hill, New York, 1972.
- [67] Litovitz, T. A. and C. M. *Structural and shear relaxation in liquids*, in Mason, W. P. (ed), Physical Acoustics, vol. IIa, Academic Press, New York, 1965.
- [68] Lide, D. R. (ed.), Handbook of Chemistry and physics, 82nd edition, CRC Press, Boca Raton, 2001.
- [69] D. H. Trivett and A. L. V. Buren, *Propagation of plane, cylindrical and spherical finite amplitude waves*, J. Acoust Soc. Am., vol. 69, pp. 943-949, 1981.
- [70] A. Korpel, *Frequency approach to nonlinear dispersive waves*, J. Acoust Soc. Am., vol. 67, pp. 1954-1958, 1980.
- [71] Y. S. Lee, *Numerical solution of the KZK equation for pulsed finite amplitude sound beams in thermoviscous fluids*, A dissertation presented to the Faculty of the graduate school of the University of Texas at Austin in partial fulfillment of the requirement for the degree of Doctor of Philosophy, 1993.
- [72] F. H. Fenlon, *A recursive procedure for computing the nonlinear spectral interactions of progressive finite-amplitude waves in nondispersive fluids*, J. Acoust Soc. Am., vol. 50, pp. 1299-1312, 1971.
- [73] S. I. Aanonsen, *Numerical computation of the nearfield of a finite amplitude sound beam*, Technical Report No. 73, Department of Mathematics, University of Bergen, Bergen, Norway, 1983.
- [74] S. I. Aanonsen, T. Barkve, J. N. Tjotta, and S. Tjotta, *Distortion and harmonic generation in the nearfield of a finite amplitude sound beam*, J. Acoust Soc. Am., vol. 75, pp. 749-768, 1984.
- [75] F. S. McKendree, *A numerical solution of the second-order-nonlinear acoustic wave equation in one and in three dimensions*, PhD thesis, the Pennsylvania State University, 1981.
- [76] K. E. Froyza, J. N. Tjotta, and J. Berntsen, *Finite amplitude effects in sound beams, pure tone and pulsed excitation*, in H. Hobaek, in Advances in nonlinear acoustics: 13th ISNA, Singapore Word Scientific, 1992.
- [77] K. H. Huebner, D. L. Dewhirst, D. E. Smith, and T. G. Byrom, *The Finite Element Method for Engineers*, Toronto: John Wiley & Sons, Inc., 2001.
- [78] S. Moaveni, *Finite Element Analysis – Theory and application with ANSYS*, Upper Saddle River, NJ: Prentice-Hall, Inc., 1999.
- [79] A. Macovski, *Medical Imaging Systems*, Englewood Cliffs: Prentice-Hall, Inc., 1983.
- [80] A. Bouakaz, C. Lancee, C. Frinking and, N. de Jong, *Simulations and measurements of nonlinear pressure field generated by linear array transducers*, IEEE International Ultrasonic Symposium, Lake Tahoe, 1999.
- [81] François Vignon, *Focalisation d'ultrasons par filtre inverse et retournement temporel, application à l'échographie transcrânienne*, Thèse de Doctorat de l'université de Paris 7, Denis Diderot, 2005.
- [82] A. Bouakaz, C. T. Lancee, and N. de Jong, *Harmonic ultrasonic field of medical phased arrays: simulations and measurements*, IEEE Trans. Ultrason., Ferroelect., Freq. Contr., vol. 50, no. 6, pp. 730-735, 2003.
- [83] M. J. Lighthill, *Surveys in Mechanics*, edited by G. K. Batchelor and R. M. Davies (Cambridge University Press), Cambridge, England, pp. 250-351, 1956.
- [84] J. P. Remenieras, O. Bou Matar, V. Labat, and F. Patat, *Time-domain modeling of nonlinear distortion of pulsed finite amplitude sound beams*, Elsevier ultrasonics, 38, pp. 305-311, 2000.
- [84_2] Helge Fjellestad and Sverre Holm, *Simulation of nonlinear fields from 2D ultrasound transducers and a new secondary grating lobes phenomenon*.
- [85] Qingyu Ma, Yong Ma, Xiufen Gong, and Dong Zhang, *Improvement of tissue harmonic imaging using the pulse-inversion technique*, Ultrason. Med. & Biol., vol. 31, No. 7, pp. 889-894, 2005.
- [86] Borsboom JMB, Chin CT, de Jong N., *Nonlinear coded excitation method for ultrasound contrast imaging*, Ultrason. Med. & Biol., 29: 277-284, 2003.

- [87] Oleg Michailovich, *A high-resolution technique for ultrasound harmonic imaging using sparse representations in Gabor frames*, IEEE Trans. Medical Imaging, vol. 21, No. 12, pp. 1490-1503, 2002.
- [88] Bouakaz A, de Jong N, *Native tissue imaging at super-harmonic frequencies*, IEEE Trans. Ultrason. Ferroelec Freq Contr, 44:125-139, 2003.
- [89] Bouakaz A, Krenning BJ, Vletter WB, Ten Cate FJ, de Jong N, *Contrast superharmonic imaging: A feasibility study*, Ultrasound Med. & Biol., 29:547-553, 2003.
- [90] Hohl C, Schmidt T, Haage P, et al., *Phase-inversion tissue harmonic imaging compared with conventional B-mode ultrasound in the evaluation of pancreatic lesions*, Eur. Radiol; 14(6): 1109-1117, 2004.
- [91] M. Bahaz, K. Benmohammed, N. Benoudjit, and A. Bouakaz, *Optimization of ultrasound excitation for improved harmonic imaging*, International conference on electrical engineering design and technologies, Tunisia, 2008.